

## **Appendix E: Water Quality**

**E-1 INTRODUCTION**

This appendix presents a summary of modeling activities and pollutant loading calculations conducted in support of the analysis of the potential impacts to water resources of the Hudson River from the construction of the Replacement Bridge Alternative. It describes the two public domain models employed in the hydrodynamic modeling, inputs to the models and includes documentation of the analyses used to develop some of these inputs as attachments in addition to other studies conducted in support of the water resources assessment. The attachments to this appendix include:

- Attachment 1—Lamont-Doherty Earth Observatory's (LDEO's) 20th century sediment deposition study.
- Attachment 2—Memorandum from Donald F. Hayes, Ph.D., P.E., BCEE, University of Nevada, Las Vegas, dated June 9, 2012, presenting the SedFlume testing and results.
- Attachment 3—Memorandum from Donald F. Hayes, Ph.D., P.E., BCEE, University of Nevada, Las Vegas, dated June 18, 2012, on estimating water quality impacts from construction vessel traffic.
- Attachment 4—Memorandum from Donald F. Hayes, Ph.D., P.E., BCEE, University of Nevada, Las Vegas, dated June 9, 2012, presenting an overview of Tappan Zee Bridge Sediment Resuspension Rate Findings.
- Attachment 5—Projected Total Suspended Sediment Concentrations During Construction of the Replacement Bridge Alternative.
- Attachment 6—Pollutant Loading Calculations Table 1 and Table 2 estimating the pollutant loading from stormwater discharges to the Hudson River.
- Attachment 7—Memorandum from Donald F. Hayes, Ph.D., P.E., BCEE, Tappan Zee Hudson River Crossing Project, Dredging Water Quality Assessment, dated April 24, 2012, presenting an assessment of potential water column concentrations of sediment constituents due to the resuspension of river sediments during dredging of the construction access channels..

For the Hudson River, the principal water quality resources issue for the construction of the Replacement Bridge Alternative is the resuspension of river sediments during construction and removal of the existing bridge foundations, and the transport and eventual deposition of this resuspended sediment elsewhere in the Hudson River. While the sand fraction of river sediment settles out relatively quickly after being resuspended, the finer sediment fractions will remain suspended and will be transported away from the construction area.

## **E-2 HYDRODYNAMIC MODELING**

Hydrodynamic modeling was used to project the plume of resuspended sediment that would result from sediment-disturbing construction activities and the fate and transport of this plume within the Hudson River estuary. Two public domain models were employed in the modeling:

- The EFDC model simulates three dimensional flow, sediment transport and water quality. Originally developed at the Virginia Institute of Marine Science it is currently supported by the US Environmental Protection Agency (USEPA) and has been extensively tested and documented in numerous modeling studies.
- The RMA-2 model is a widely tested model that is used extensively for bridge scour evaluations in estuaries. It was used to evaluate the results of the EFDC modeling during the periods when the Hudson River Estuary is well-mixed throughout its depth (e.g., during the spring freshet—a time of high freshwater inflows). The model was originally developed for the US Army Corps of Engineers (USACE).

EFDC is a numerically sophisticated model capable of simulating a large number of complex physical processes, including density induced circulation and sediment transport. These physical processes may also evolve over long time scales, on the order of months or years. When considering the numerical requirements of the processes and the time scales over which they occur, the EFDC model is inherently computationally intensive. These computational requirements create practical constraints on the model grid size and the resolution of near-field processes.

- The RMA-2 model simulates fewer physical processes (which typically evolve over shorter time scales) than the EFDC model and also utilizes a more flexible numerical grid. These characteristics allow for significantly more detailed numerical grids in areas of interest. Subsequently, the RMA-2 model can typically produce more detailed near-field data but may also produce progressively worse approximations of transport processes over large periods of time due to the physical processes it does not describe. Subsequently, the EFDC model was used as a far-field model, considering processes such as sediment transport, while the RMA-2 model was used as a near-field model, modeling processes which evolve over periods less than those of tidal cycles.

Inputs to the hydrodynamic models included the following:

- Results of site-specific monitoring and studies conducted for the Replacement Bridge Alternative within the study area, including a bathymetric study, grain size analysis, total suspended solids and turbidity measurements, monitoring of tide gauges installed for the project, dye study, water quality monitoring (i.e., conductivity, temperature, and turbidity), channel salinity profile mapping, and river velocity monitoring to create a cross-sectional profile of the river velocities.
- Results of SedFlume analysis of sediments within the vicinity of the area to be dredged, which indicated sediments within the study area are highly susceptible to resuspension (see Attachment 2).
- Existing information to characterize the Hudson River Estuary within the study area. Examples include bathymetry from the National Oceanic and Atmospheric

Administration (NOAA) navigational charts, tidal data from US Geological Survey (USGS) and NOAA tide stations, USGS freshwater discharge, and USGS salinity and suspended sediment concentration data.

- Results of numeric models developed to estimate suspended sediment loadings that would result from dredging; pile driving, coffer dam installation, dewatering, and removal; and vessel movement as described below and in Attachments 3 and 4. Inputs to these models are presented below.
  - Suspended sediment generated by dredging—Assessment assumed the use of environmental/closed bucket with no barge overflow and a sediment loss rate of about 1 percent. This conservative loss rate of 1 percent, combined with the projected dredging rate and the sediment characteristics results in an average sediment resuspension rate for each dredge of 39 kilograms per minute (kg/min), and a maximum rate of 94 kg/min (See Attachment 4).
  - Suspended sediment generated by cofferdam construction and dewatering—In the absence of existing information on sediment resuspension rates associated with cofferdam construction, resuspension of sediment during installation of sheet pile for cofferdams was developed on the basis of results of suspended sediment monitoring conducted for the San Francisco-Oakland Bay Bridge East Span Seismic Safety Project during dredging and in-water construction activities ([http://biomitigation.org/bio\\_overview/subjects\\_overview.asp#water](http://biomitigation.org/bio_overview/subjects_overview.asp#water)). Results of monitoring for that project indicated that installation of sheet pile for coffer dam construction resulted in average resuspension of bottom material that was about 30 percent of the average resuspension during dredging. (See Attachment 4).
  - Suspended sediment generated by pile driving and dewatering—Existing information on sediment resuspension from pile driving and dewatering was similarly absent and was estimated to be approximately 40 percent of that observed during dredging on the basis of the suspended sediment monitoring for the San Francisco-Oakland Bay Bridge East Span Seismic Safety Project (See Attachment 4).
  - Suspended sediment generated by vessel movement and prop scour— Since the results of the SedFlume analysis and scour modeling (see Attachment 3) indicated that the bottom sediment following dredging would be highly susceptible to resuspension due to scouring by the props on the tugs needed to move the construction barges along the dredged access channel, the project included the placement of sand/gravel armoring material within the dredged channel following dredging. Therefore, the resuspension resulting from vessel movement would be limited to sediment that has been naturally deposited in the dredged access channel which will act as a sediment trap. Using an estimated depositional rate of sediment within the dredged channel of 104 kilograms per meter per day developed on the basis of van Rijn (1986), described in Attachment 4 and below, and total suspended sediment concentrations measured during studies conducted for the Replacement Bridge Alternative, the hourly scour rate of sediment as the vessels move along the armored channel was estimated as 8.7 kg per meter per hour (kg/m/hr) (See Attachment 4).



### **E-3 20TH CENTURY SEDIMENT DEPOSITION**

As described in Attachment 1, the main objectives of this study by LDEO were to identify the extent and thickness of sediments potentially containing elevated levels of contaminants, as well as areas where sediments were eroding or non-depositing. Locations of these sediments can be used to determine areas of recent and historical deposition. Results are based on 14 sediment cores collected in September 2001 and 15 sediment cores collected in May 2006 in the vicinity of the proposed Tappan Zee construction zone.

LDEO used the presence of lead concentrations in sediments above natural background levels (15 to 30 parts per million (ppm)) as a proxy for identifying those sediments impacted by twentieth century activities. Sediments containing elevated lead concentrations also potentially contain other contaminants of concern, while sediments containing background levels of lead represent sediments deposited prior to the onset of industrial activities and do not pose a significant contamination issue.

The majority of sediments collected were terrigenous, bioclastic, clays and sandy clays. Lead concentrations ranged from a few ppm to about 225 ppm. The majority of samples measured had concentrations lower than 25 ppm and in the range of natural background levels. The depth to which elevated lead levels penetrated the sediments varied considerably throughout the study site. The majority of penetration depths were between 0 and 20 inches, with depths exceeding 60 inches at a few sites.

Sediments collected north of the existing Tappan Zee Bridge exhibited elevated lead concentrations penetrating between 0 and 20 inches, with the majority between 0 and 8 inches, suggesting that deposition of recent sediments in this portion of the study site was limited. Depositional patterns observed south of the existing bridge were more complex. Many of the cores along the western side of the river indicated limited penetration of elevated levels of lead, which may indicate limited deposition of recent sediments. On the eastern side of the river, lead was consistently found at greater depths, suggesting that deposition of recent sediments can be localized.

### **E-4 SEDFLUME AND PROP SCOUR ANALYSES**

The SedFlume is a straight rectangular flume designed to evaluate erosion rates using adjustable sediment heights and constant flow rate. The primary purpose of this analysis is to understand the relationship between flow velocity and sediment erosion. Water flows through the flume, and an adjustable layer of sediment rests on the bottom. Once the proper flow is established, the sediment core is raised manually until the sediment surface is even with the bottom flow surface of the SedFlume. This continues until the water becomes too turbid to see the sediment level in the flume. Sediment erosion rate is recorded in centimeters per minute as the average erosion over the testing period (Attachment 2).

To assess the potential for sediment scour, the SedFlume results were used in combination with the following two propeller-induced shear stress models (Attachment 3):

- Bottom Shear Stress: This model incorporates both propeller velocity and vessel wake velocity, and adjusts for the fact that tugs and barges associated with the

construction project should be maneuvering at low speeds resulting in minimal wake effects.

- **Propeller-induced Velocities at Sediment Surface:** This model designates two velocity fields, or zones, located immediately behind the vessels' propellers. The zones act independently, but eventually join to create a single flow field.

For this analysis, four 5-gallon composite samples of fine-grained depositional sediment were collected at multiple locations in two general areas along the study area for the project. SedFlume testing of bottom sediments in shallow areas of the Hudson River showed that these sediments begin to erode at shear stress of 1.14 Pa, which occurred at a velocity of 2 feet per second.

## **E-5 SEDIMENT RESUSPENSION RATE FROM IN-WATER CONSTRUCTION ACTIVITIES**

In-water bridge construction activities have the potential to resuspend sediments. The primary construction activities of concern are sheet pile installation, dewatering of cofferdams during pier construction, and pile driving activities. The most comprehensive and applicable data set regarding resuspension rates came from the San Francisco – Oakland Bay Bridge East Span Seismic Safety Project. Thousands of water quality measurements, mostly turbidity, were taken during various aspects of the project, including dredging, sheet pile installation, cofferdam dewatering, and pile driving. As presented in Attachment 4, the results of the water quality monitoring for the San Francisco – Oakland Bay Bridge East Span Seismic Safety Project were used to project sediment resuspension rates resulting from in-water construction activities for the Replacement Bridge Alternative.

## **E-6 DEPOSITIONAL RATES IN ARMORED DREDGED CHANNEL**

### **E-6-1 INTRODUCTION AND BACKGROUND**

A procedure for estimating sedimentation rates in dredged channels is outlined in *Sedimentation of Dredged Channels by Currents and Waves* (van Rijn 1986). This procedure describes a means of determining a “trapping efficiency” (the percent of the sediment load passing over the channel that remains in the channel) based on the orientation of the channel relative to the flow, the angle of the channel side slopes, the ratio of settling velocity to shear velocity, and the ratios of the depth and width of the dredged channel relative to the upstream depth. The trapping efficiency in turn defines the rate at which a dredged channel will fill in over time.

The simplified procedure described in van Rijn (1986) uses nomographs to relate the various parameters described above for several combinations of factors, and was used to determine the sedimentation rate in the dredged channel. Because only a limited number of nomographs have been developed, it was necessary to approximate certain parameters in order to develop a “typical” condition for analysis. For example, the channel was assumed to have side slopes of 1:20 (a conservative assumption; a nomograph of the proposed 1:10 slope is not available).

Based on the available data and necessary approximations, the trapping efficiency of the proposed dredged channel was estimated at 0.05. For a typical suspended sediment concentration of 35 mg/L and an average current velocity of 1.3 ft/s, the resulting rate of sediment accumulation is estimated at approximately 1 foot per year. However, the actual rate of sedimentation at any given location within the dredged channel will vary with the changing physical conditions across the length of the channel. Overall, it is expected that actual sedimentation rates at any given location might vary by as much as 50 percent from the “average” prediction and are likely to be greater (i.e., fill in more quickly) in areas of deeper dredging, and lesser (slower) in areas of shallower dredging.

#### **E-6-2 DEPOSITIONAL RATES IN DREDGED CHANNEL**

Quantitative estimates of sedimentation rates in dredged channels were calculated using procedures outlined in *Sedimentation of Dredged Channels by Currents and Waves* by Leo C. van Rijn (van Rijn, 1986). The calculation method used in this subchapter is based on the nomographs developed in that paper for simplified estimates of sedimentation rates.

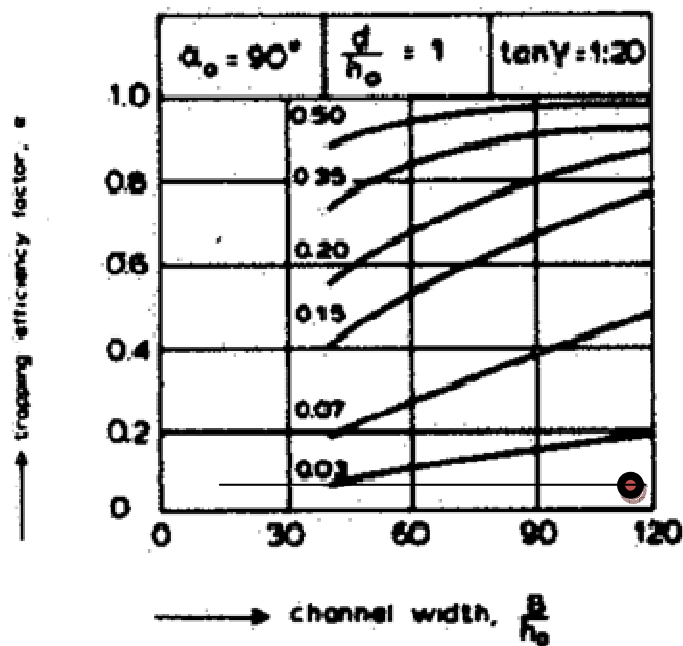
The nomographs of trapping efficiency (the percent of the sediment load passing over the channel that remains in the channel) are based on the orientation of the channel to the flow, the angle of the side slopes, and several dimensionless parameters: the ratio of settling velocity to shear velocity; the depth of the dredged channel to the upstream depth; and the width of the channel to the upstream depth.

The proposed dredged channel is perpendicular to the typical ebb and flood flow directions ( $\alpha=90^\circ$ ). The side slopes are assumed to be 1:20 due to the low shear strength of the soil (a nomograph of the proposed 1:10 slope is not available). The settling velocity was calculated assuming 95% of the suspended material is in the silt to clay fraction based on sampling by the USGS (USGS 2006). Assuming the ambient silt to clay material is represented by a typical silt particle with a diameter of 16 microns, the settling velocity, based on relationships developed by van Rijn, is 0.00023 m/s. Shear velocity is defined as:

$$u_* = \frac{K}{-1 + \ln\left(\frac{h}{z_0}\right)} \frac{Q}{bh}$$

where  $K$  = the Von Karman constant ( $\sim 0.4$ ),  $h$  is the water depth,  $z_0$  is  $0.33k_s$ , where  $k_s$  is the effective roughness height, and  $Q/bh$  is the depth averaged velocity. The maximum value of either  $3 \cdot D_{90}$  or 0.01 meters was used to define  $k_s$ . Using a  $k_s=0.01$  meters, a water depth of 2 meters, and a typical velocity of 0.4 m/s, the upstream shear velocity  $u_{*,0}$ , was calculated as 0.03 m/s. The ratio of settling velocity to shear velocity,  $w_s/u_{*,0}$  is approximately 0.008.

A representative depth of the dredged channel is 2 meters, a representative depth of the upstream depth is also 2 meters, leading to a ratio of  $d/h_o=1$ . The width of the channel is approximately 200 meters, leading to a ratio of  $B/h_o$  of 100. An estimate of trapping efficiency can be estimated based on the following nomograph presented by van Rijn:



Deposition Nomograph

The trapping efficiency was estimated as 0.05. Based on a typical suspended sediment concentration of 35 mg/L and velocity of 0.4 m/s, the mass of sediment passing through the channel, per meter width, over a 5 year period is  $(0.05)(2\text{m})(1\text{m})(0.4\text{m/s})(0.035\text{kg/m}^3)(31,536,000\text{s/yr})(5\text{yr}) = 221,000 \text{ kg}$ . Using a dry sediment density of  $900 \text{ kg/m}^3$ , the volume is  $250 \text{ m}^3/\text{m}$ . The depth of sediment is  $250 \text{ m}^3/\text{m}/200\text{m} = 1.3 \text{ m}$ , or approximately 1 foot per year.

## E-7 PROJECTED TOTAL SUSPENDED SEDIMENT CONCENTRATIONS DURING CONSTRUCTION OF THE REPLACEMENT BRIDGE ALTERNATIVE

Figures 1 through 18 (Attachment 5) indicate the increase in total suspended sediment over ambient concentrations projected by the hydrodynamic modeling resulting from the anticipated schedule for in-water construction activities. These figures depict the projected suspended sediment concentrations due to dredging with other concurrent in-water construction activities for the Replacement Bridge Alternative Long Span and Short Span Options at a given point of time during these construction activities under three tidal conditions, flood, ebb and slack.

The results of the modeling of the scenarios expected to result in the greatest resuspension of sediment indicated in Attachment 5 suggest that total suspended sediment concentrations in the range of 50 to 100 mg/L above ambient conditions will only occur in the immediate vicinity of the dredges, and that a much smaller contribution would result from the other sediment disturbing construction activities (i.e., driving of piles for the cofferdams, pile driving, vessel movement, and cofferdam dewatering). On flood and ebb tides, concentrations of 10 mg/L above ambient conditions may extend in

a relatively thin band approximately 1,000 to 2,000 feet from the two dredges, while concentrations of 5 mg/L may extend a greater distance.

## **E-8 POLLUTANT LOADING CALCULATIONS**

Potential effects to Hudson River water quality due to the discharge of stormwater runoff from the project were assessed by considering the change in impervious surfaces and changes in pollutant loadings discharged to the Hudson River. Attachment 6 presents the pollutant loading calculations for total phosphorus (TP) and total suspended solids (TSS) for the landings and bridge with treatment of only the landings (Table 1 of Attachment 6) and for the landings only (Table 2 of Attachment 6).

This pollutant loading analysis was performed to evaluate the quality of the stormwater runoff in existing and proposed conditions using the pollutant coefficient method, as outlined in *Reducing the Impacts of Stormwater Runoff from New Development* published by the New York State Department of Environmental Conservation (NYSDEC) in April 1992. Pollutant coefficient values were used to best evaluate the pre- and post-development conditions based on the land use type, which was predominantly impervious surfaces. Following the pollutant coefficient method, the upland portion of the study area was broken up into three major drainage areas on the basis of topography: Rockland landing, bridge, and Westchester landing. The predominant land use within these three drainages is roadways or impervious surface. Therefore, a pollutant loading coefficient of 0.6 pounds per year (lbs/acre/year) was used for phosphorus and 833 lbs/acre/year was used for total suspended solids (TSS). The contributing drainage areas are multiplied by the pollutant loading coefficient for the associated land use resulting in the total annual pollutant load to the Hudson River. Appendix E provides the detailed pollutant loading calculations: On the basis of the New York State Stormwater Management Design Manual (SWMDM), the stormwater management practices that would be implemented to treat the stormwater runoff are capable of reducing Total Suspended Solids (TSS) by 80 percent and total phosphorus (TP) by 40 percent. These pollutant removal rates are then applied to the calculated total pollutant load to determine the final pollutant load to the Hudson River.

## **E-9 ASSESSMENT OF POTENTIAL WATER COLUMN CONCENTRATIONS OF SEDIMENT CONSTITUENTS DURING DREDGING**

Potential increases in water-column constituent concentrations resulting from sediment resuspension during dredging was assessed by Hayes (2012) and is presented in Attachment 7. This analysis used: information on sediment and hydrodynamic characteristics at the Replacement Bridge Alternative site, settling properties of the sediments that would be dredged, actual sediment constituent concentrations and anticipated dredging operating procedures to model the spatial extent of the sediment plume. The dissolved water column concentration of chemical constituents at the edge of the plume was also determined through this modeling effort.

Two dredge operation scenarios were modeled to provide estimates of constituent concentrations resulting from sediment resuspension during dredging: 1) average conditions (39 kg/min) and 2) maximum conditions (94 kg/min). On the basis of criteria

presented in the New York State Division of Water Technical and Operational Guidance Series 5.1.9 (TOGS 5.1.9), the mixing zone was assumed to extend 500 ft from the dredging location. Sediment resuspension and particulate and dissolved constituent concentrations within the water column within the active dredging area was projected using a near-field model. Once the sediment resuspended during dredging leaves the well-mixed active dredging area, its transport can be modeled using a two dimensional depth averaged analytical model (far-field model) that is the basis of transport computations in the U.S. Army Corps of Engineer's (USACE's) DREDGE model. Modeling did not assume any loss of the particle-bound constituents to the dissolved phase between the point where the suspended sediment exits the near-field region to the edge of the 500-foot mixing zone, resulting in a conservative estimate (higher than actual) of contaminant concentrations within the water column.

As summarized in Table 7 of Attachment 7, dissolved water-column concentrations of the sediment constituents predicted by the DREDGE model are substantially less than the water-quality criteria for aquatic exposure selected for comparison at the edge of the mixing zone.

## **E-10 SUPPLEMENT TO ATTACHMENT 7, MEMORANDUM FROM DONALD F. HAYES, IN RESPONSE TO MAY 31, 2012 COMMENTS RECEIVED FROM NYSDEC**

### **E-10-1 COMPARISON OF DISSOLVED CONSTITUENT CONCENTRATIONS TO NYSDEC USE CLASS SB AQUATIC CHRONIC WATER QUALITY STANDARDS**

NYSDEC submitted comments to the NYS Department of Transportation dated May 31, 2012 noting an incorrect application of the water quality criteria for aquatic exposure used to compare the results of the modeled dissolved constituent concentrations in the April 24, 2012 memorandum from Dr. Hayes (Attachment 7). NYSDEC indicated that rather than applying an Aquatic Acute water-quality standard from Class B when a standard for Class SB waters was not specified, the most stringent Class SB standards (i.e., other than the acute criterion) should be used in the analysis. NYSDEC also stated that the water-quality criteria that should be used to compare the dissolved water-column concentrations predicted by the DREDGE model for arsenic, cadmium, copper, lead, PCBs, PAHs, and mercury should be as follows:

- Class SB aquatic chronic (A(C)) for arsenic, cadmium, copper, and lead;
- Class SB health fish consumption (H(FC)) for PCBs;
- Class SB criteria for individual PAHs rather than total PAHs; and
- 0.05 µg/L for mercury.

Table 1 presents a comparison of the predicted dissolved constituent concentrations from Hayes (2012) to the Class SB standard specified in your May 31, 2012 correspondence. Predicted dissolved heavy metal concentrations are below the aquatic water-quality criteria at the edge of the modeled 500-foot mixing zone for dredging. Predicted dissolved total PCB concentration exceed the Class SB fish consumption criterion. However, PCB sediment contamination occurs throughout the Hudson River estuary and the concentrations observed within the study area for the project are similar

## **Tappan Zee Hudson River Crossing Project Environmental Impact Statement**

---

to average levels found elsewhere in the Hudson River as indicated by the Hudson River Benthic Mapping Project. For example, the average total PCB concentrations reported for sediments to be dredged at the U.S. Gypsum facility about 12 miles upriver in Haverstraw Bay<sup>1</sup> are over three times higher than the average total PCB concentrations observed in sediments within the project site, and the NYSDEC and the USACE authorized dredging at the U.S. Gypsum facility (USACE Number 2005-00053, and NYSDEC3-3928-00030/00045). Furthermore, on June 22, 2012, we received a letter from the USCOE indicating that that all of the proposed dredged sediments are of sufficient quality to be suitable for placement at the HARS. Therefore, the proposed project would be expected to comply with the conditions anticipated to be issued by the NYSDEC under Section 401 water quality certification for the project and would not result in adverse impacts to water quality of the Hudson River.

Table 2 presents a comparison of the predicted dissolved constituent concentrations of individual PAHs estimated at the edge of a 500-foot mixing zone to their most restrictive Class SB criterion. The estimated dissolved PAH concentrations were developed by multiplying the dissolved total PAH concentration estimated by Hayes (2012) by the relative percentage of the average total PAH concentration (see Table 15-4 in Chapter 15 of the DEIS) that each PAH comprised in the sediment samples collected within the project site. Estimated dissolved PAH concentrations for four of fifteen PAHs tested would be above the Class SB standard using the maximum predicted total dissolved PAH concentration, but only two would be above the standard using the average predicted total dissolved PAH concentration. As indicated by Hayes (2012), the dissolved constituents predicted by the DREDGE model should be considered conservative because the analysis did not take into account “washing” of particle-bound constituents<sup>2</sup>. Therefore, the dissolved concentrations would be expected to be lower than those predicted by the model. Sediment PAH concentrations observed within the study area are within the range of concentrations observed elsewhere within the river, and the average total PAH concentration is about half as much as reported for Haverstraw Bay north of the project site<sup>3</sup> where dredging has been authorized by NYSDEC (Permit Number3-3928-00030/00045) and the USACE (Permit Number 2005-00053). Additionally, the estimated dissolved concentration of the PAH phenanthrene, which was used as an indicator for the total concentration of PAHs in the Section 401 water quality certification issued to Champlain Hudson Power Express, Inc., would be below the Class SB aquatic chronic standard and the acute standard of 14 µg/L specified in the Champlain Hudson water quality certification. Therefore, the proposed project would be expected to comply with the conditions anticipated to be issued by the

---

<sup>1</sup> United States Gypsum Company, 2005. Joint Application for maintenance dredging, US Gypsum Company, Stony Point, Rockland County.

<sup>2</sup> As a particle resuspended by dredging moves downriver, a portion of the particle-bound contaminants dissolves into the water column before that that particle reaches the edge of the mixing zone. The dissolved concentration predicted by the dredge model assumes no loss of sediment bound constituents and therefore overestimates the amount that can move into the dissolved phase at the edge of the mixing zone. The amount of this overestimate varies with the constituent.

<sup>3</sup> United States Gypsum Company, 2005. Joint Application for Maintenance Dredging, US Gypsum Company, Stony Point, Rockland County.

NYSDEC under Section 401 water quality certification for the project and would not result in adverse impacts to water quality of the Hudson River.

**Table 1**  
**Comparison of Dissolved Water-Column Constituent Concentrations**  
**Predicted by the DREDGE Model to Class SB Water-Quality Criteria**

Constituent	Water Quality Criteria Used in DREDGE Model <sup>(1)</sup> (µg/L)	Class SB A(C) Chronic Criterion (µg/L)	Modeled Dissolved Concentrations at 500 ft from Dredge		Standard Exceeded?
			MR(avg) (µg/L)	MR(max) (µg/L)	
Arsenic	340	63	0.133	0.26	No
Cadmium	3.2	7.7	0.0189	0.0267	No
Copper	4.8	3.4	0.318	0.45	No
Lead	204	8	0.0802	0.0859	No
Mercury	1.4	0.05 <sup>(2)</sup>	0.00356	0.00404	No
Total PCBs	-	1.00E-06 <sup>(3)</sup>	4.99E-04	5.46E-04	Yes
Total PAHs	-	See Table 2 <sup>(4)</sup>	0.0309	0.068	See Table 2 <sup>(4)</sup>
<b>Notes:</b> (1) April 24, 2012 Memorandum from Dr. Donald F. Hayes, Tappan Zee Hudson River Crossing Project, Dredging Water Quality Assessment. (2) Statewide variance for mercury (3) Total PCB is H(FC) (4) PAHs are regulated individually. Estimated dissolved concentrations of individual PAHs are presented in Table 2.					



**Table 2**

**Comparison of Dissolved Water Column PAH concentrations to Class SB  
Water Quality Criteria**

Constituent	Average Concentration in Sediment Samples <sup>(1)</sup> (µg/kg)	Percentage of Average Total PAHs <sup>(1)</sup>	Estimated Dissolved Concentration at 500 Feet Based on Predicted Total Dissolved PAHs (0.0309 µg/L average and 0.0680 µg/L max)		Class SB A(C) Standard (µg/L)	Standard Exceeded?
			Adjusted M <sub>R</sub> (average)	Adjusted M <sub>R</sub> (maximum)		
2-Methylnaphthalene	0.96	0.06%	0.000019	0.000041	4.2	No
Naphthalene	11	0.67%	0.00021	0.00046	16	No
Acenaphthylene	13	0.79%	0.00024	0.00054	6.6	No
Dibenzo(a,h)anthracene	14	0.85%	0.00026	0.00058	-	-
Fluorene	28	1.7%	0.00053	0.0012	2.5	No
Acenaphthene	36	2.18%	0.00067	0.0015	6.6	No
Anthracene	47	2.85%	0.00088	0.0019	3.8 <sup>(2)</sup>	No
Indeno(1,2,3-c,d)pyrene	53	3.21%	0.001	0.0022	0.002 <sup>(2)</sup>	No
Benzo(g,h,i)perylene	64	3.88%	0.0012	0.0026	-	-
Benzo(k)fluoranthene	91	5.52%	0.0017	0.0038	0.002 <sup>(2)</sup>	Yes only for adjusted M <sub>R</sub> (maximum)
Benzo(b)fluoranthene	110	6.67%	0.0021	0.0045	0.002 <sup>(2)</sup>	Yes only for adjusted M <sub>R</sub> (maximum)
Benzo(a)anthracene	130	7.88%	0.0024	0.0054	0.03	No
Benzo(a)pyrene	133	8.07%	0.0025	0.0055	0.0006	Yes
Chrysene	134	8.13%	0.0025	0.0055	0.002 <sup>(2)</sup>	Yes
Phenanthrene	163	9.89%	0.0031	0.0067	1.5	No
Pyrene	288	17.47%	0.0054	0.012	4.6 <sup>(2)</sup>	No
Fluoranthene	333	20.19%	0.0062	0.014	50	No
2-Chloronaphthalene <sup>(3)</sup>	-	-		-	10 <sup>(2)</sup>	
<b>Notes:</b> (1) Individual PAH concentrations from Tappan Zee sediments can be found in Table 15-4 in Chapter 15, "Water Resources" of the Draft Environmental Impact Statement. (2) No standard listed for Class SB. Used most stringent standard available for the PAH. (3) Not measured in sediment samples.						

**E-10-2 ASSESSMENT OF WATER-QUALITY IMPACTS RESULTING FROM EROSION OF SEDIMENT THAT HAS MOUNDED DUE TO PRESENCE OF EXISTING BRIDGE PIERS**

Section 18-4-12-4, "Existing Bridge Demolition," of the DEIS evaluated the potential for sediment that has been deposited within mounds in the vicinity of the existing bridge piers to adversely affect water quality of the Hudson River. The DEIS concluded that the sediment that has been deposited within these mounds would be expected to erode over time until reaching a new equilibrium elevation. Because the Tappan Zee portion of the Hudson River is considered to be neither a depositional nor an erosional environment (i.e., in equilibrium), as indicated by the results of the 20th century sediment mapping presented in this appendix, minimal erosion of sediments in the vicinity of the existing bridge would be expected to occur under normal river conditions, and would most likely occur only during high flow events. While some of these sediment deposits have elevated concentrations of certain contaminants (Class B or Class C categories), these elevated concentrations do not extend more than a few feet below the mudline. Therefore, the gradual erosion of some areas of contaminated sediment following the removal of the bridge in accordance with conditions issued by the NYSDEC would not be expected to result in adverse impacts to water quality or result in water quality conditions that fail to meet the Class SB standards.

Subsequent to the publication of the DEIS and in response to a May 31, 2012 letter from the NYSDEC, the NYSDOT provided additional information on the quality of the sediment within the mound areas, and a further assessment of the potential for the erosion of these mounds to result in water-quality conditions that fail to meet Class SB water-quality standards.

In order to estimate dissolved constituent concentrations resulting from mound erosion, the dissolved concentrations modeled at the edge of the mixing zone by Hayes (2012) for dredge-induced resuspension were scaled up to account for higher sediment concentrations in the mounds compared to the dredged sediments (see Tables 3 and 4). This approach required the assumption that sediment resuspension from the mounds would occur at the same rates as for dredging (i.e., 39 kg/min on average, or 94 kg/min as a maximum). Based on literature review of erosion and deposition rates in the estuary, calculations for dredged induced resuspension rates, estimated mound size, and sediment density, erosion from the mounds would need to be more than 1,000 times greater than natural erosion rates to achieve the same level of sediment removal as the dredges. Therefore, natural erosion of the mounds would be expected to result in a resuspension rate that would be much less than that generated by dredging.

Even under the conservative assumption that mound sediment is resuspended at the same rate as would occur during dredging, dissolved concentrations of arsenic, cadmium, copper, lead and mercury would not exceed the Class SB standard (Table 4). As was the case for the predicted total dissolved PCBs due to dredging, dissolved total PCBs estimated to result from mound erosion also exceeded the standard. Since this is an unrealistic assumption, the dissolved total PCB concentration due to mound erosion would be considerably lower than that predicted for dredging and would not be expected to result in an exceedance of the standard.

**Tappan Zee Hudson River Crossing Project  
Environmental Impact Statement**

Table 5 presents the estimated PAH concentrations at the edge of a 500-foot mixing zone from eroding mounds. Because there was such a disparity between the maximum total PAH concentration measured in sediments from depositional mounds (48,211 µg/kg and 14,303.5 µg/kg from two samples) and the maximum concentrations for the remaining 46 of 48 mound locations which were less than or equal to 3,116 µg/kg, both 48,211 µg/kg and 3,116 µg/kg concentrations were used to estimate the dissolved concentrations resulting from mound erosion. The dissolved PAH concentrations presented in Table 5 were derived by adjusting the total dissolved PAH concentration predicted from the DREDGE model by the maximum relative percentage each PAH comprised in the mound sediments.

**Table 3**

**Range of Constituent Concentrations in Mound Sediment**

Parameter	Location	Sample Depth (ft)	Minimum Sediment Conc.	Maximum Sediment Conc.	Average Concentration Used in DREDGE Model	Difference Between Maximum Sediment Concentration in Mounds and Sediment Concentration Used in DREDGE Model
Mercury (mg/kg)	East Mound 2, North, VC-34	3.0 - 4.0	0.045	2.3	0.89	2.6
Total PCBs (µg/kg)	East Mound 2, North, VC-34	4.0 - 5.0	52	1,144	169	6.8
Total PAHs (µg/kg)	East Mound 3, South, VC-31	2.0 - 2.5	53.88	48,211	1,673	28.8
Arsenic (mg/kg)	East Mound 3, North, VC-35	5.0 - 6.0	5.2	16.1	8.06	2.0
Cadmium (mg/kg)	East Mound 3, North, VC-35	2.0 - 3.0	0.33	3.1	1.9	1.6
Copper (mg/kg)	West Mound 1, South, VC-29	4.0 - 5.0	9.4	95.9	32	3.0
Lead (mg/kg)	East Mound 3, North, VC-35	0.0 - 1.0	6.9	604	36	16.8
Total DDT, DDD, and DDE (µg/kg)	West Mound 1, North, VC-13	2.0 - 3.0	3.7	371.1	Not modeled	-

**Table 4**

**Estimated Dissolved Constituent Concentrations Released During Mound Erosion**

Constituent	Dissolved Concentrations (µg/L) Predicted by DREDGE Model		Difference Between Maximum Sediment Concentration in Mounds and Sediment Concentration Used in DREDGE Model	Estimated Dissolved Concentrations (µg/L) <sup>(1)</sup>		Class SB A(C) Standard (µg/L)	Standard Exceeded?
	MR (avg)	MR (max)		MR (avg)	MR (max)		
Arsenic	0.133	0.26	2.0	0.266	0.520	63	No
Cadmium	0.0189	0.0267	1.6	0.0308	0.0436	7.7	No
Copper	0.318	0.450	3.0	0.953	1.349	3.4	No
Lead	0.0802	0.0859	16.8	1.346	1.441	8	No
Mercury	0.00356	0.00404	2.6	0.0092	0.0104	0.05	No
Total PCBs	4.99E-04	5.46E-04	6.8	3.38E-03	3.70E-03	1.00E-06	Yes
Total PAHs	0.0309	0.0680	28.8	-	-	-	See Table 5 <sup>(2)</sup>
<b>Notes:</b> (1) Estimated dissolved concentration represents the dissolved concentration predicted by the DREDGE model adjusted by the difference between the average concentration used as input to the DREDGE model and the maximum concentration of a constituent in the sediment mounds. (2) PAHs are regulated individually. Estimated dissolved concentrations of individual PAHs are presented in Table 5.							

**Table 5**

**Estimated Dissolved PAH Concentrations at the Edge of the Mixing Zone During Mound Erosion**

Constituent	Maximum Percentage Of Total PAH in Mound Sediment Samples <sup>(1)</sup>	Estimated Dissolved Concentration Based on Maximum Total PAH Concentration in Mound Sediment of 3,115 µg/kg <sup>(2)</sup>		Estimated Dissolved Concentration Based on Maximum Total PAH Concentration in Mound Sediment of 48,211 µg/kg <sup>(2)</sup>		Class SB A(C) Standard (µg/L)
		Adj M <sub>R</sub> (avg) <sup>(3)</sup>	Adj M <sub>R</sub> (max) <sup>(3)</sup>	Adj M <sub>R</sub> (avg) <sup>(3)</sup>	Adj M <sub>R</sub> (max) <sup>(3)</sup>	
2-Chloronaphthalene	9.90%	0.0057	0.0125	0.0881	0.1939	10 <sup>(4)</sup>
2-Methylnaphthalene	9.90%	0.0057	0.0125	0.0881	0.1939	4.2
Acenaphthene	5.10%	0.0029	0.0065	0.0454	0.0999	6.6
Acenaphthylene	5.10%	0.0029	0.0065	0.0454	0.0999	-
Anthracene	5.10%	0.0029	0.0065	0.0454	0.0999	3.8 <sup>(4)</sup>
Benzo(a)anthracene	7.50%	0.0043	0.0095	<b>0.0667</b>	<b>0.1469</b>	0.03
Benzo(a)pyrene	7.20%	<b>0.0041</b>	<b>0.0091</b>	<b>0.0641</b>	<b>0.1410</b>	0.0006
Benzo(b)fluoranthene	6.40%	<b>0.0037</b>	<b>0.0081</b>	<b>0.0570</b>	<b>0.1253</b>	0.002 <sup>(4)</sup>
Benzo(g,h,i)perylene	5.10%	0.0029	0.0065	0.0454	0.0999	-
Benzo(k)fluoranthene	8.00%	<b>0.0046</b>	<b>0.0101</b>	<b>0.0712</b>	<b>0.1567</b>	0.002 <sup>(4)</sup>
Chrysene	7.40%	<b>0.0043</b>	<b>0.0094</b>	<b>0.0659</b>	<b>0.1449</b>	0.002 <sup>(4)</sup>
Dibenz(a,h)anthracene	5.10%	0.0029	0.0065	0.0454	0.0999	-
Fluoranthene	26.00%	0.0150	0.0329	0.2314	0.5092	50
Fluorene	5.10%	0.0029	0.0065	0.0454	0.0999	2.5
Indeno(1,2,3-cd)pyrene	5.10%	<b>0.0029</b>	<b>0.0065</b>	<b>0.0454</b>	<b>0.0999</b>	0.002 <sup>(4)</sup>
Naphthalene	6.20%	0.0036	0.0079	0.0552	0.1214	16
Phenanthrene	13.50%	0.0078	0.0171	0.1201	0.2644	1.5
Pyrene	19.60%	0.0113	0.0248	0.1744	0.3838	4.6 <sup>(4)</sup>
<p><b>Notes:</b> (1) Maximum percentage of Total PAH concentration developed from results of laboratory analysis of individual PAHs and Total PAHs for each of the 10 mound sediment sampling locations.</p> <p>(2) Total PAH used by Hayes (2012) to model sediment concentration equals 1,673 µg/kg. Maximum and near-maximum total PAH concentrations measured in mound sediment equal to 48,211 µg/kg and 3,115 µg/kg, resulting in a difference of 28.8x and 1.9x greater for mound sediments.</p> <p>(3) PAH concentrations for average M<sub>R</sub> (avg) and maximum M<sub>R</sub> (max) resuspension scenarios were estimated as the percentage of the total dissolved PAH concentration (0.0309 µg/L and 0.068 µg/L) for each PAH weighted by the difference in sediment concentration.</p> <p>(4) No standard listed for Class SB. Used most stringent standard available for the PAH.</p> <p>Concentrations in <b>bold</b> exceed the standard.</p>						

As presented in Table 5, the estimated dissolved concentration for only five of eighteen and six of eighteen PAHs exceeded the standard concentration when estimated using the near-maximum and maximum total PAH concentrations for the mounds of 3,116

and 48,211 µg/kg, respectively. Six of the eighteen PAHs are predicted to exceed the standard using the maximum total PAH concentration of 48,211 µg/kg: benzo(a)anthracene, benzo(a)pyrene, benzo(b)fluoranthene, benzo(k)fluoranthene, chrysene, and indeno(1,2,3-cd)pyrene. Benzo(a)anthracene would not exceed the standard using the lower total PAH concentration of 3,115 µg/kg. However, these estimated exceedences assume a rate of resuspension for mound erosion identical to dredging. Since this is an unrealistic assumption, dissolved PAH concentrations resulting from mound erosion would be far less and would not be expected to exceed the water quality standard. Even assuming that the rate of sediment resuspension from the mounds was half that of the estimated average rate of resuspension, dissolved concentrations of PAHs would all be below the individual PAH standards with the exception of possibly benzo(a)anthracene. Even under the extremely conservative assumption that mound erosion resuspends sediment at the same rate as dredging, phenanthrene, which was the PAH used as an indicator for the total concentration of PAHs in the Section 401 water quality certification issued to Champlain Hudson Power Express, Inc., would be below the Class SB aquatic chronic and acute standards.

Therefore, the gradual erosion of some areas of contaminated sediment following the removal of the bridge would be expected to comply with the conditions anticipated to be issued by the NYSDEC under Section 401 water quality certification for the project and would not be expected to result in adverse impacts to water quality of the Hudson River. Furthermore, if in the event the erosion rate resulted in a sediment loading approaching that of the dredging operation, they would be eroded quickly and result in elevated dissolved constituent concentrations for a very short time in the vicinity of the mounds, and would not result in adverse impacts to water quality.

## **E-11 LITERATURE CITED**

- United States Geological Survey (USGS). 2006. Use of an ADCP to Compute Suspended – Sediment Discharge in the Tidal Hudson River, New York. Scientific Investigations Report 2006-5055. 16 pp.
- Van Rijn, L.C. 1986. Sedimentation of Dredged Channels by Currents and Waves. *Journal of Waterway, Port, Coastal, and Ocean Engineering*, Vol. 112, No. 5, September, 1986.

Assessment of the deposition of sediments impacted by  
Twentieth Century activities in the vicinity of the Tappan Zee Bridge

Principal Investigator: Dr. Timothy Kenna  
Co Investigators: Dr. Frank Nitsche,  
Dr. Robin Bell, Dr. William B.F. Ryan

Preliminary Report to:

EarthTech  
655 Third Avenue  
New York, NY 10017

From

Lamont-Doherty Earth Observatory  
of Columbia University in the City of New York

DUNS #049179401

## Introduction

Alternatives being considered as part of the Tappan Zee Bridge/I-287 Environmental Review include significant modification of the current bridge or construction of a new one, requiring that the existing structure be removed. With the exception of the no-build alternative, the remaining and more likely options will result in significant disturbance and/or removal of river bottom sediments. Work required for the DEIS and FEIS will include the assessment of the levels and penetration depths of a variety of contaminants in sediments residing within the proposed construction zone.

Sediment work typically entails collection of sediment cores, followed by costly and time consuming analysis for specific contaminants such as heavy metals, organic contaminants, etc. Because there is little depositional information available for the sediment cores prior to sectioning, some pre-determined increment is used regardless of the specific depositional setting of each core. Depending on the individual sedimentation regime, this results in the over-sampling of sediment cores where anthropogenic contamination is low or absent and under-sampling of sediment cores where anthropogenic contamination is present and higher-resolution sampling would provide additional and valuable information— in short, there is currently no way to optimize core sampling to obtain the highest quality information from the fewest number of samples.

As part of several sediment coring projects at LDEO, we have developed techniques to rapidly assess sediment deposition on split, wet sediment cores shortly after collection and prior to the commencement of further analyses. To identify sediments impacted by twentieth century activities, we use down-core sediment distributions of lead as a proxy to identify sediments deposited within the last ~100 years. Increases in the concentration of lead and other industrial metals have been used in numerous studies to provide constraints on deposition timing. The timing of the majority of industrial activities generally overlaps with the period of the 20<sup>th</sup> century. As a result, elevated lead concentrations in sediments also allow the identification of sediments that likely contain other anthropogenic particle-reactive contaminants of concern.

Our approach entails the measurement of lead and several other elements using a hand-held x-ray fluorescence spectrometer (XRF). Measurements are made at 5-10cm increments on split, wet sediment cores. Using *in-situ* wet-bulk density estimates obtained from our core logging system, we are able to calculate water content and correct XRF measurements to a dry weight basis. We use the presence of lead concentrations in sediments above natural background levels (15-30ppm) as a proxy for identifying those sediments impacted by twentieth century activities. As mentioned above, sediments containing elevated lead concentrations will also potentially contain other contaminants of concern, while sediments containing background levels of lead represent sediments deposited prior to the onset of industrial activities and do not pose a contamination issue. Using this information, one can gain baseline information regarding sediment deposition regimes and design a more cost-effective core sectioning strategy limiting the number of analyses performed on uncontaminated sediments. For future field sampling, the results of the proposed work will aid in targeting areas where additional cores are needed as well as specific regions where longer sediment cores (vibra-cores) will be necessary to assess contaminant levels.



## Main Objectives

The main objectives of this project are to identify the extent and thickness of sediments potentially containing elevated levels of contaminants as well as areas where sediments are eroding or non-depositing and contamination issues are limited. This information is based on 14 sediment cores collected in September 2001 as well as 15 sediment cores collected in May 2006 in the vicinity of the proposed Tappan Zee construction zone. This report contains the following information:

- (1) Map with coring locations
- (2) Lead distribution profiles for both archived and new sediment cores collected in the vicinity of the proposed study site, including data interpretation.
- (3) Basic information for sediment cores, including megascopic sediment core descriptions, digital color photographs of split sediment cores, and sediment physical properties.

Note: Surface sediment grain size distributions, potentially contaminated sediment volume estimates resulting from the integration of geochemical data with geophysical results from the high-resolution acoustic mapping work are contained in the final project report.

## Methods

### *Study site*

The Tappan Zee Bridge study site is shown in Figure 1. The shaded region is a corridor running the length of the existing bridge, extending approximately 500 meters north and south. The symbols represent the core sample locations.

### *Sediment core collection*

The sediment cores analyzed as part of this study were collected of two separate sampling expeditions (Figure 1). The LWB2 coring series (yellow squares) was collected on September 5, 2001 aboard the R/V Lionel A. Walford operated by the New Jersey Marine Science Consortium. The DPB2-06 coring series was collected on May 10 and 11, 2006 aboard the R/V Donald W. Pritchard operated by SUNY- Stony Brook. On both expeditions, sediment cores were collected using a gravity coring device fitted with 4" diameter PVC pipe. The gravity corer is equipped with a check valve, which maintains a vacuum above the collected sediments and permits the collection of samples without the use of a core catcher, which can cause disturbances. In many cases, clear PVC was used in order to assess core length and quality in the field. Table 1 contains information regarding sediment core collection.

### *Sediment core processing*

After cores were collected, they were stored and transported upright in order to preserve the integrity of the core tops. At the end of each day, cores were transported to LDEO's core

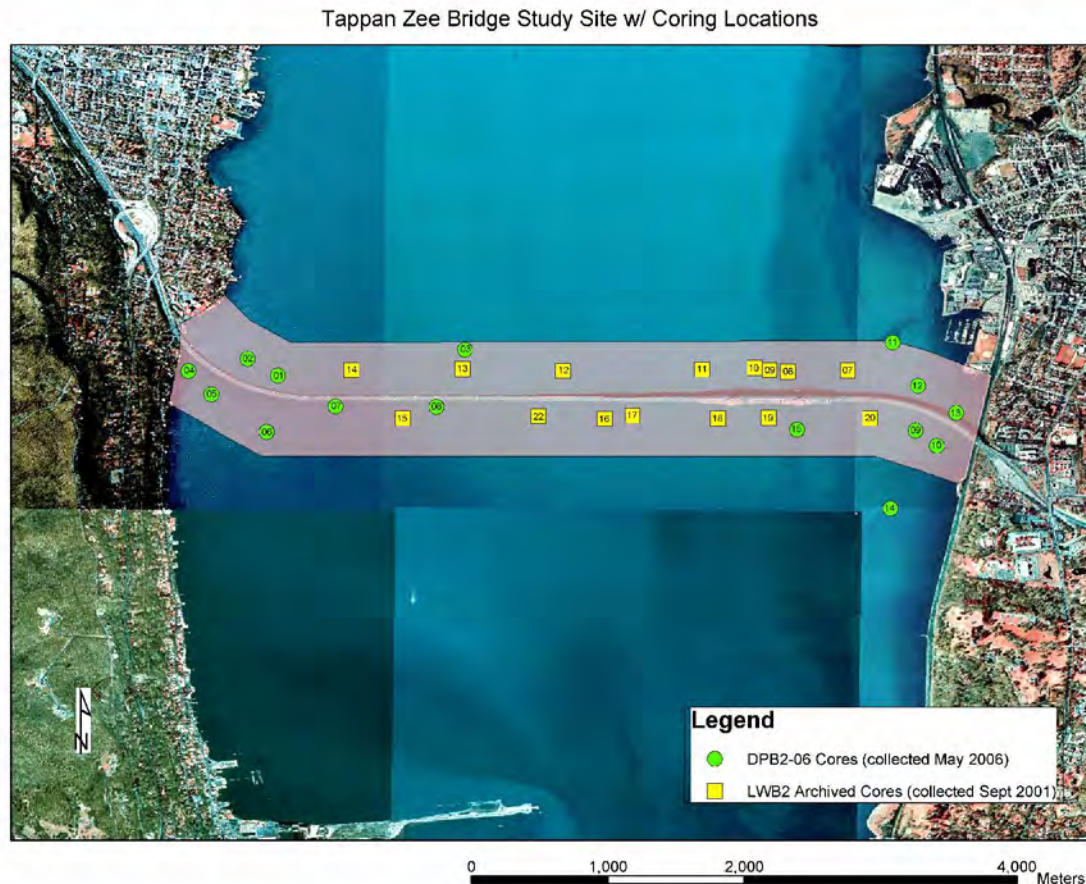


**Figure 1.** Tappan Zee Bridge study site with sediment core locations. Yellow squares represent archived cores collected September 2001; green circles represent new cores collected May 2006. Numbers within symbols indicate sample number for the respective coring series. See Table 1 for additional information.

facility and stored in a walk-in refrigerator at 4°C to before processing. Sediment cores were then carefully de-watered, excess PVC above the core top was removed and a foam plug was securely fitted to stabilized sediments. Sediment cores were then logged for physical properties, after which they were split longitudinally, archived, which includes inserting depth markers, digitally photographing both core halves, and conducting megascopic descriptions. In between various processing steps and upon completion of analysis, sediment core samples were placed in D-tubes and stored at 4°C.

#### *Physical properties*

Once dewatered and prior to splitting, sediment cores were logged for physical properties at 1cm intervals using a GEOTEK Multi-Sensor Core Logger. Properties measured

included gamma ray attenuation, magnetic susceptibility, as well as P-wave velocity and amplitude.

**Table 1. Sediment core locations and information**

Core ID	Latitude	Longitude	Collection Date	Core length (cm)	Water Depth (m)
LWB2-07	41° 4.313' N	73° 52.532' W	09/05/01	177	5.5
LWB2-08	41° 4.308' N	73° 52.769' W	09/05/01	140.6	12.9
LWB2-09	41° 4.314' N	73° 52.841' W	09/05/01	65	14.3
LWB2-10	41° 4.323' N	73° 52.900' W	09/05/01	88	14
LWB2-11	41° 4.316' N	73° 53.108' W	09/05/01	161	9.6
LWB2-12	41° 4.311' N	73° 53.657' W	09/05/01	41.5	3.5
LWB2-13	41° 4.318' N	73° 54.055' W	09/05/01	39.5	3.1
LWB2-14	41° 4.314' N	73° 54.494' W	09/05/01	151	2.7
LWB2-16	41° 4.121' N	73° 53.493' W	09/05/01	121.6	3.4
LWB2-17	41° 4.134' N	73° 53.383' W	09/05/01	42	3.1
LWB2-18	41° 4.122' N	73° 53.045' W	09/05/01	156.3	10.8
LWB2-19	41° 4.126' N	73° 52.844' W	09/05/01	78.5	13.5
LWB2-20	41° 4.124' N	73° 52.444' W	09/05/01	165.6	2.4
LWB2-22	41° 4.131' N	73° 53.755' W	9/8/2001	39	3
DPB2-06-01	41° 4.292' N	73° 54.785' W	05/11/06	116	3.3
DPB2-06-02	41° 4.359' N	73° 54.905' W	05/11/06	151.5	3
DPB2-06-03	41° 4.395' N	73° 54.045' W	05/11/06	87	2.4
DPB2-06-04	41° 4.310' N	73° 55.139' W	05/11/06	115.5	2.3
DPB2-06-05	41° 4.218' N	73° 55.048' W	05/10/06	162.5	1.8
DPB2-06-06	41° 4.069' N	73° 54.829' W	05/10/06	164.5	2.1
DPB2-06-07	41° 4.171' N	73° 54.557' W	05/10/06	195	2.8
DPB2-06-08	41° 4.169' N	73° 54.158' W	05/10/06	135	3.7
DPB2-06-09	41° 4.075' N	73° 52.263' W	05/10/06	53	2.9
DPB2-06-10	41° 4.014' N	73° 52.179' W	05/10/06	71	2.5
DPB2-06-11	41° 4.423' N	73° 52.354' W	05/11/06	105.5	3.5
DPB2-06-12	41° 4.252' N	73° 52.253' W	05/10/06	49	3
DPB2-06-13	41° 4.145' N	73° 52.103' W	05/11/06	65.5	2.7
DPB2-06-14	41° 3.769' N	73° 52.363' W	05/10/06	103	3
DPB2-06-15	41° 4.078' N	73° 52.732' W	05/10/06	156	12.5

### *X-ray Fluorescence Spectrometry*

Split sediment cores were analyzed for lead concentrations every 10cm using an Innov-X Alpha series 4000 handheld X-ray fluorescence (XRF) spectrometer. To prevent contamination of the instrument between measurements, the sediment surface was covered with plastic wrap during analysis. Each measurement was conducted for 120 seconds, which reduced analytical uncertainties to less than a few percent. Lead concentrations made on wet sediments were corrected for water content and are reported on a dry weight basis. Although confirmatory analyses were not conducted as part of this study, previous work on other Hudson River cores has indicated good agreement between lead concentration measurements obtained via the wet corrected XRF technique and sub-samples analyzed by total digestion ICP-MS

analysis using established procedures ( $r^2 = 0.92$ ;  $n = 24$ ). Wet bulk density, derived from gamma ray attenuation was used to calculate water content using the following equation:

$$\text{Water content} = \frac{\left( \frac{(\rho_{H_2O} \cdot \rho_{Sed})}{WBD} - \rho_{H_2O} \right)}{(\rho_{Sed} - \rho_{H_2O})} \quad (\text{eq. 1})$$

where :

$\rho_{H_2O}$  = water density

$\rho_{Sed}$  = dry grain density

In this study, we assumed  $1 \text{ g cm}^{-3}$  and  $2.6 \text{ g cm}^{-3}$ , for water and dry grain density, respectively.

### *Sediment grain size analysis*

Sub-samples from selected core tops were disaggregated in distilled water and washed through a 63-  $\mu\text{m}$  sieve to determine the coarse fraction. The  $<63 \mu\text{m}$  fraction was then analyzed using a Micromeritics SediGraph 5100 particle-size analyzer to obtain a continuous grain size distribution down to  $0.8 \mu\text{m}$ . Sediment size fractions greater than  $63 \mu\text{m}$  were dried, and sieved using an ATM sonic sifter, individual sieved fractions were weighed using a Mettler micro-balance.

## **Results**

### *Lead concentrations*

Lead concentrations are reported in ppm on a corrected dry weight basis. Figures 2 and 3 show down core lead distribution profiles measured for all cores in the study site. For comparison, the depth and concentrations scales are set at 0-200 cm and 0-250ppm for all profiles. Lead concentrations ranged from a few ppm to  $\sim 225 \text{ ppm}$ . The majority of samples measured were less than 25ppm and in the range of natural background levels. In several instances, lead levels elevated above natural background are observed in the upper portions of the sediment cores. The depth to which elevated lead levels penetrate the sediments varied considerably throughout the study site; the majority of penetration depths are between 0 and 50 cm, with penetration depths exceeding 150cm at a few sites. The deepest sediments recovered in all but two cores (LWB2-16 and DPB2-06-14) contain lead levels consistent with expected natural background.

### *Lithologies, Physical properties, and Core images*

Physical properties, core images, along with megascopic descriptions are contained in Appendix A. The majority of sediments collected are terrigenous, bioclastic, clays and sandy clays. Carbonate content is generally low, and quartz is the most abundant mineral observed in the coarse fraction. Lesser amounts of observed minerals in the coarse fraction include mica,

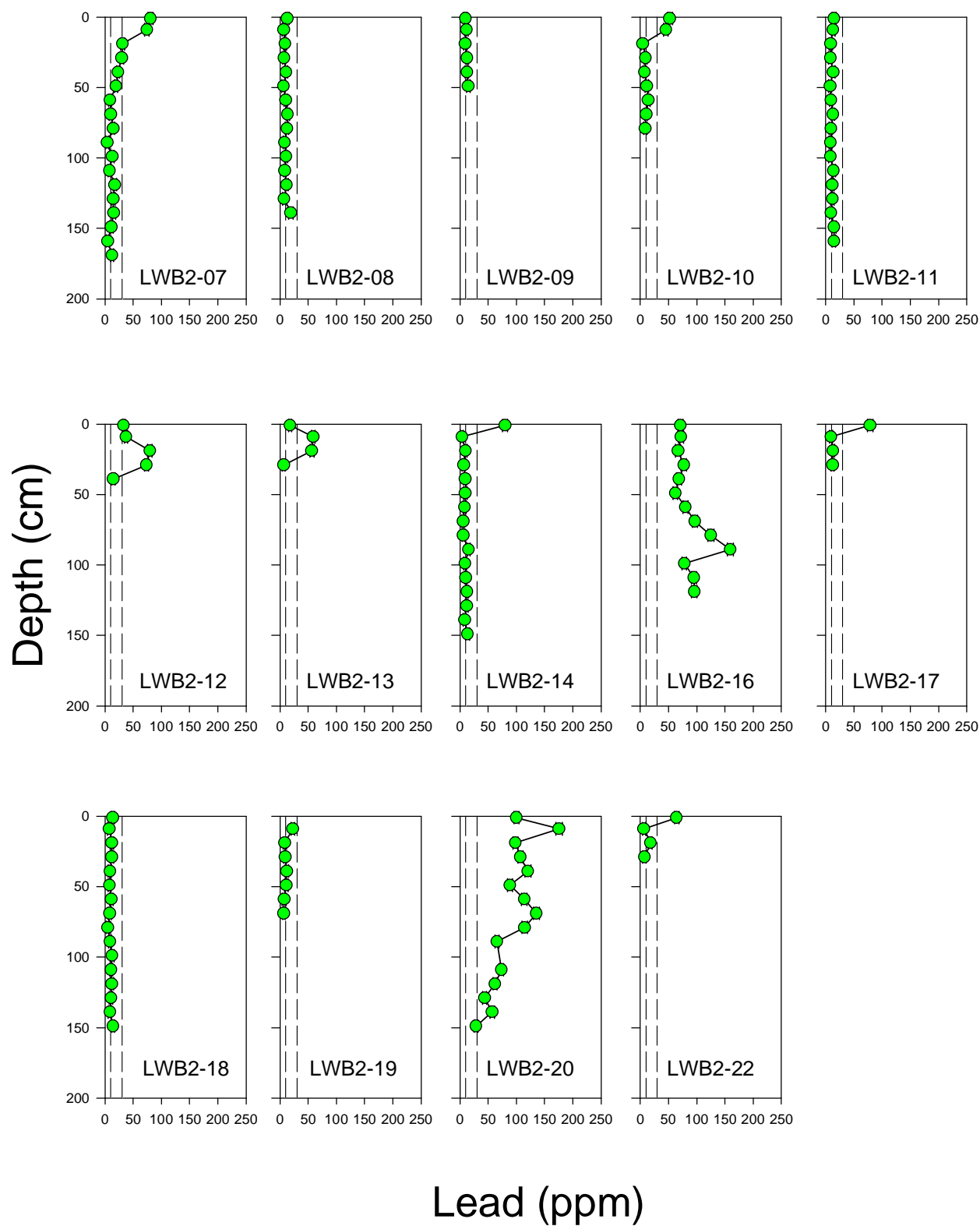


Figure 2. Down core lead distribution profiles for LWB2 series cores collected September 2001. The concentration range between the dashed lines is 10-30ppm and represents natural background lead levels.

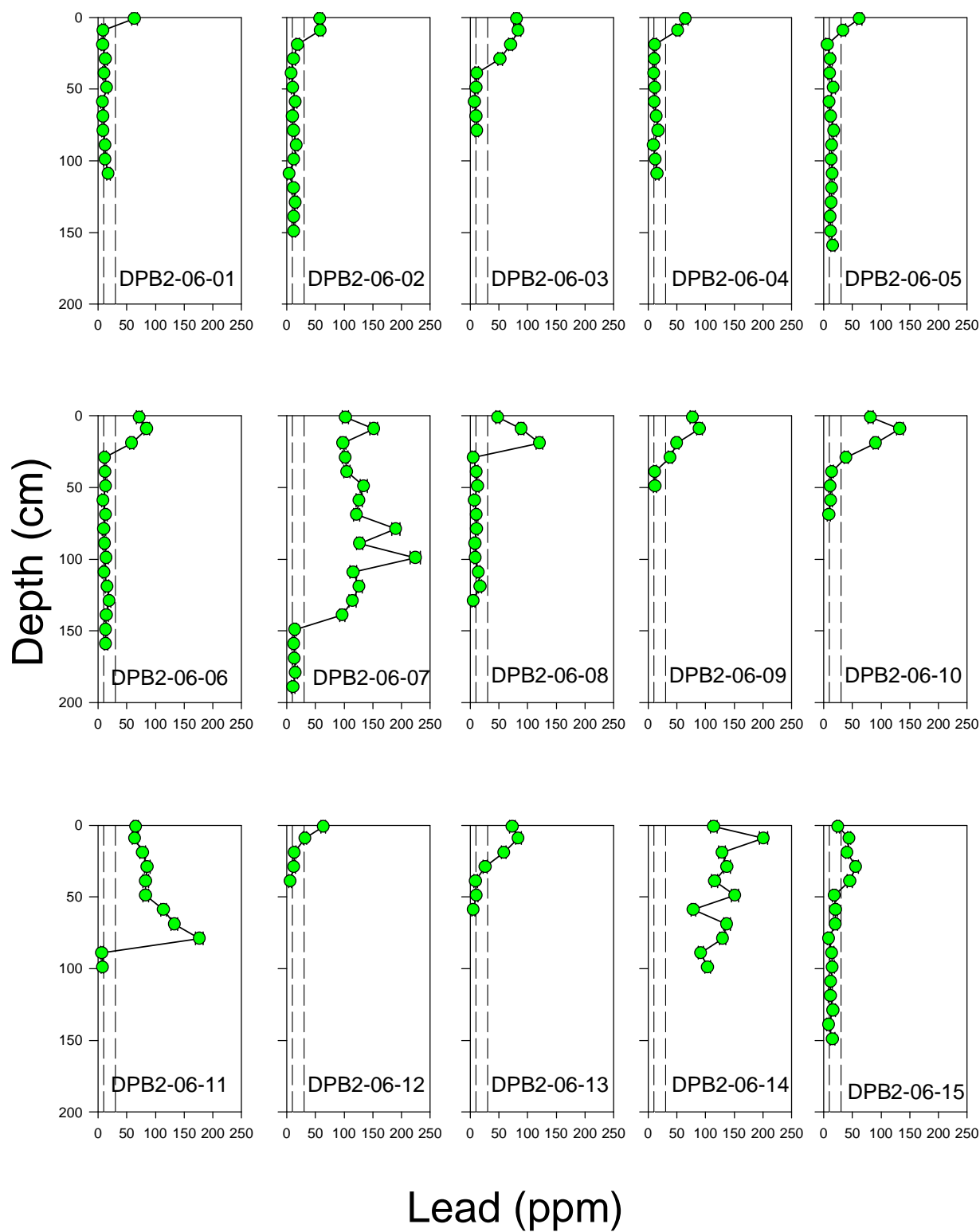


Figure 3. Down core lead distribution profiles for DPB2-06 series cores collected May 2006. The concentration range between the dashed lines is 10-30ppm and represents natural background lead levels.

iron oxide stained grains, feldspar, hornblende, framboidal pyrite, and pyroxene (see individual log sheets in Appendix A, for specific details). In general bulk densities ranged between ~1.2 and ~1.6 g/cc. In several cases, the depth at which lead concentrations decreased to expected natural background coincided with a clear increase in wet-bulk density values. In a few cases, we also observe a coincident decrease in magnetic susceptibility readings. Color images of each core also appear in Appendix A as bitmapped images. It should be noted that in several cases, the bitmapped images are stretched to match the depths of the physical property and lead data. In cases where very short cores were collected, this distortion is noticeable. In addition to these images included in Appendix A, we can provide the original high-resolution composite images with the final report. As noted above, sediment grain size analyses are not yet complete; these results will be included in the final report.

## Data interpretation

We use the presence of lead concentrations in sediments above natural background levels (15-30ppm) as a proxy for identifying those sediments impacted by twentieth century activities. As mentioned above, sediments containing elevated lead concentrations will also potentially contain other contaminants of concern, while sediments containing background levels of lead represent sediments deposited prior to the onset of industrial activities and do not pose a significant contamination issue.

Figure 4 shows the study site, core locations, as well as the lead profiles obtained for each core. With the exception of DPB2-06-11, all the sediment cores collected north of the existing Tappan Zee Bridge exhibit elevated lead concentrations penetrating between 0 and 50 cm, with the majority penetrating between 0 and 20cm. These data suggest that deposition of recent sediments in this portion of the study site is limited. The deeper penetration observed in DPB2-06-11, and relatively sharp decline to background levels at ~90cm suggest a dredge boundary. This interpretation is consistent with acoustic and bathymetric data identifying the coring site as being located in the channel leading the marina in Tarrytown and subject to frequent dredging.

In contrast, the depositional patterns observed in sediment cores collected within the study site and south of the existing bridge are more complex. While many of the cores indicate limited penetration of elevated levels of lead, which can be interpreted as limited deposition of recent sediments (e.g. the western margin), there are several instances of deeper penetration, suggesting that deposition of recent sediments can be significant in specific areas. Sediment cores collected from the area south of the existing bridge along the eastern side of the river, exhibit consistently deeper lead penetration than other areas. Individual cores such as LWB2-16 and DPB2-06-07 also exhibit relatively deep lead penetration and are likely indicative of drift bodies related to bridge pilings.



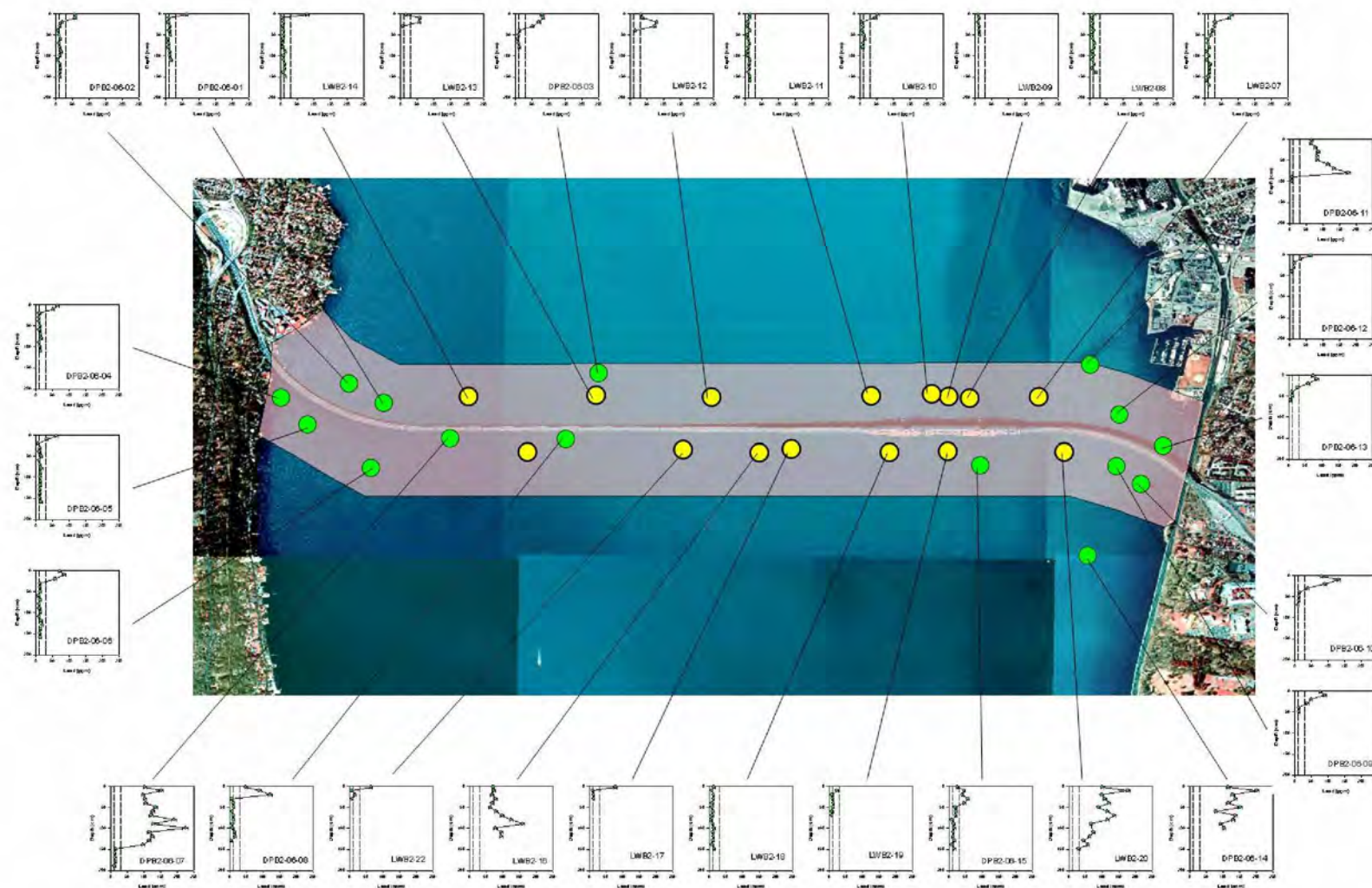


Figure 4. Tappan Zee Bridge study site with sediment core locations and lead distribution profiles. See Table 1 for additional information.



## Recommendations

Interpretation of sediment core data collected at 29 locations in the vicinity of the existing Tappan Zee Bridge and within the proposed study site suggests that deposition of sediments impacted by Twentieth Century activities is limited in the portion of the study site north of the existing bridge. The collection of significantly longer cores (i.e., vibra-cores) does not appear to be necessary. For the purposes of assessing levels of other anthropogenic particle-reactive contaminants of concern in the northern portion, we also suggest higher resolution sub-sampling of cores in the upper 50cm, and lower resolution below this depth.

Although the lead penetration in cores collected from the western margin south of the bridge suggests limited deposition in this area, the variability of lead penetration observed in the remainder of the southern portion of the study site may indicate the need of additional core samples to adequately characterize the depositional patterns. The area that appears to have consistently experienced the highest deposition of recent sediments is the southeastern portion of the study site. In two cores (LWB2-16 and DPB2-06-14), the deepest sediments recovered (~120cm and ~100cm, respectively), contained lead levels elevated above natural background. Assessing the actual thickness of the impacted layer at these two sites is not possible without the acquisition of longer sediment cores.

## **Appendix A**

**Core Log Data:  
Physical Properties  
Core images  
Lithology**

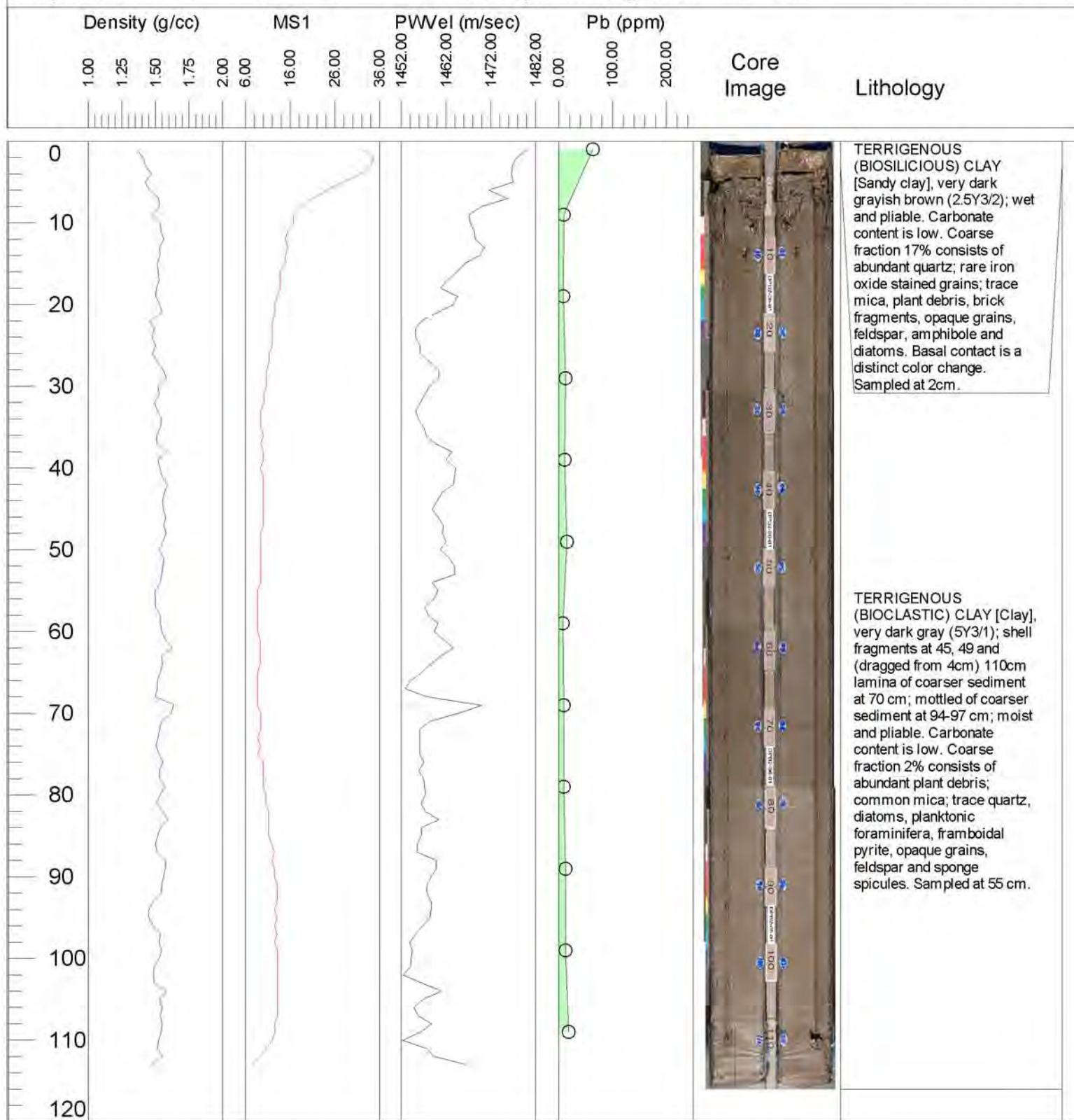
## Lamont-Doherty Earth Observatory

DPB2-06-01

Project Title: Assessment of the deposition of sediments impacted by Twentieth Century activities in the vicinity of the Tappan Zee Bridge

Project No.: EARTHT D213123

Principle Investigators: Timothy C. Kenna and Frank Nitsche



Core ID: DPB2-06-01

Latitude: 41° 4.292' N

Date Opened: 05/19/06

Core Length: 116 cm

Longitude: 73° 54.785' W

Date Photographed: 05/19/06

Collection Date: 05/11/06

PDR Depth: 3.3 m

Date Described: 06/01/06

Described by: N. Anest

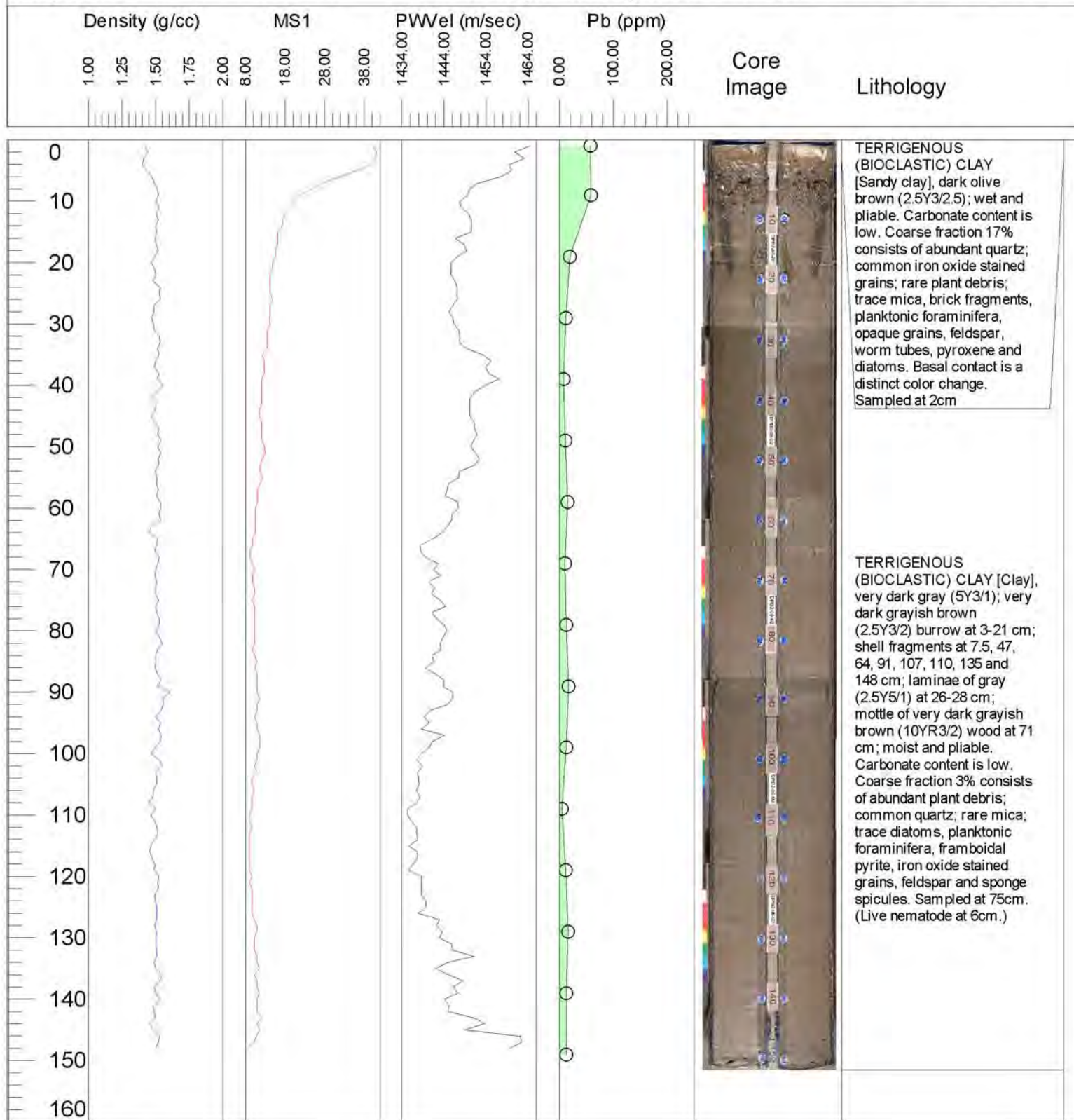
## Lamont-Doherty Earth Observatory

DPB2-06-02

Project Title: Assessment of the deposition of sediments impacted by Twentieth Century activities in the vicinity of the Tappan Zee Bridge

Project No.: EARTH D213123

Principle Investigators: Timothy C. Kenna and Frank Nitsche



Core ID: DPB2-06-02

Latitude: 41° 4.359' N

Date Opened: 05/17/06

Core Length: 151.5 cm

Longitude: 73° 54.905' W

Date Photographed: 05/17/06

Collection Date: 05/11/06

PDR Depth: 3.0 m

Date Described: 06/01/06

Described by: N. Anest



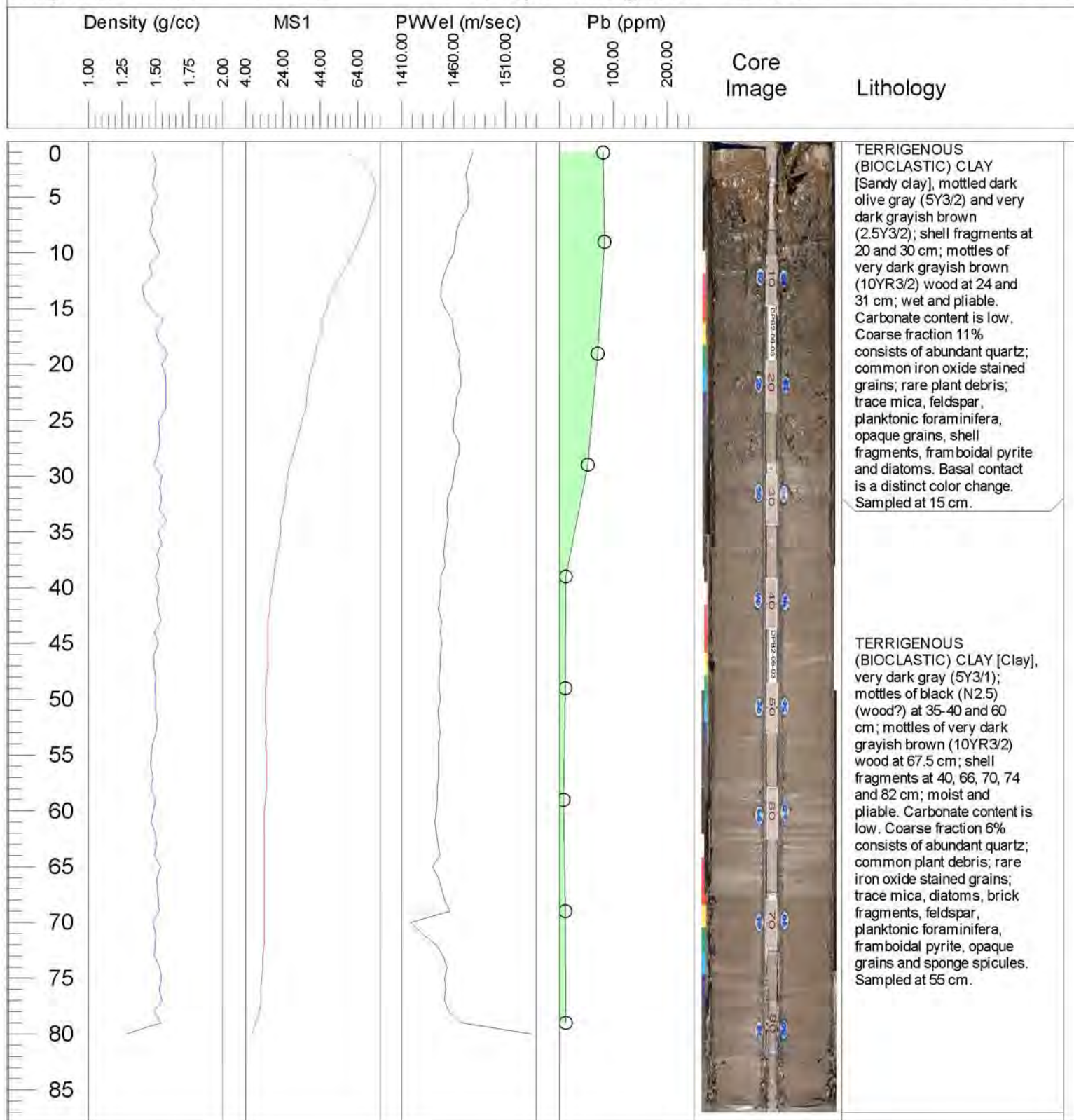
## Lamont-Doherty Earth Observatory

DPB2-06-03

Project Title: Assessment of the deposition of sediments impacted by Twentieth Century activities in the vicinity of the Tappan Zee Bridge

Project No.: EARTH D213123

Principle Investigators: Timothy C. Kenna and Frank Nitsche



**TERRIGENOUS (BIOCLASTIC) CLAY** [Clay], very dark gray (5Y3/1); mottles of black (N2.5) (wood?) at 35-40 and 60 cm; mottles of very dark grayish brown (10YR3/2) wood at 67.5 cm; shell fragments at 40, 66, 70, 74 and 82 cm; moist and pliable. Carbonate content is low. Coarse fraction 6% consists of abundant quartz; common plant debris; rare iron oxide stained grains; trace mica, diatoms, brick fragments, feldspar, planktonic foraminifera, framboidal pyrite, opaque grains and sponge spicules. Sampled at 55 cm.

Core ID: DPB2-06-03

Latitude: 41° 4.395' N

Date Opened: 05/19/06

Core Length: 87 cm

Longitude: 73° 54.045' W

Date Photographed: 05/19/06

Collection Date: 05/11/06

PDR Depth: 2.4 m

Date Described: 06/01/06

Described by: N. Anest

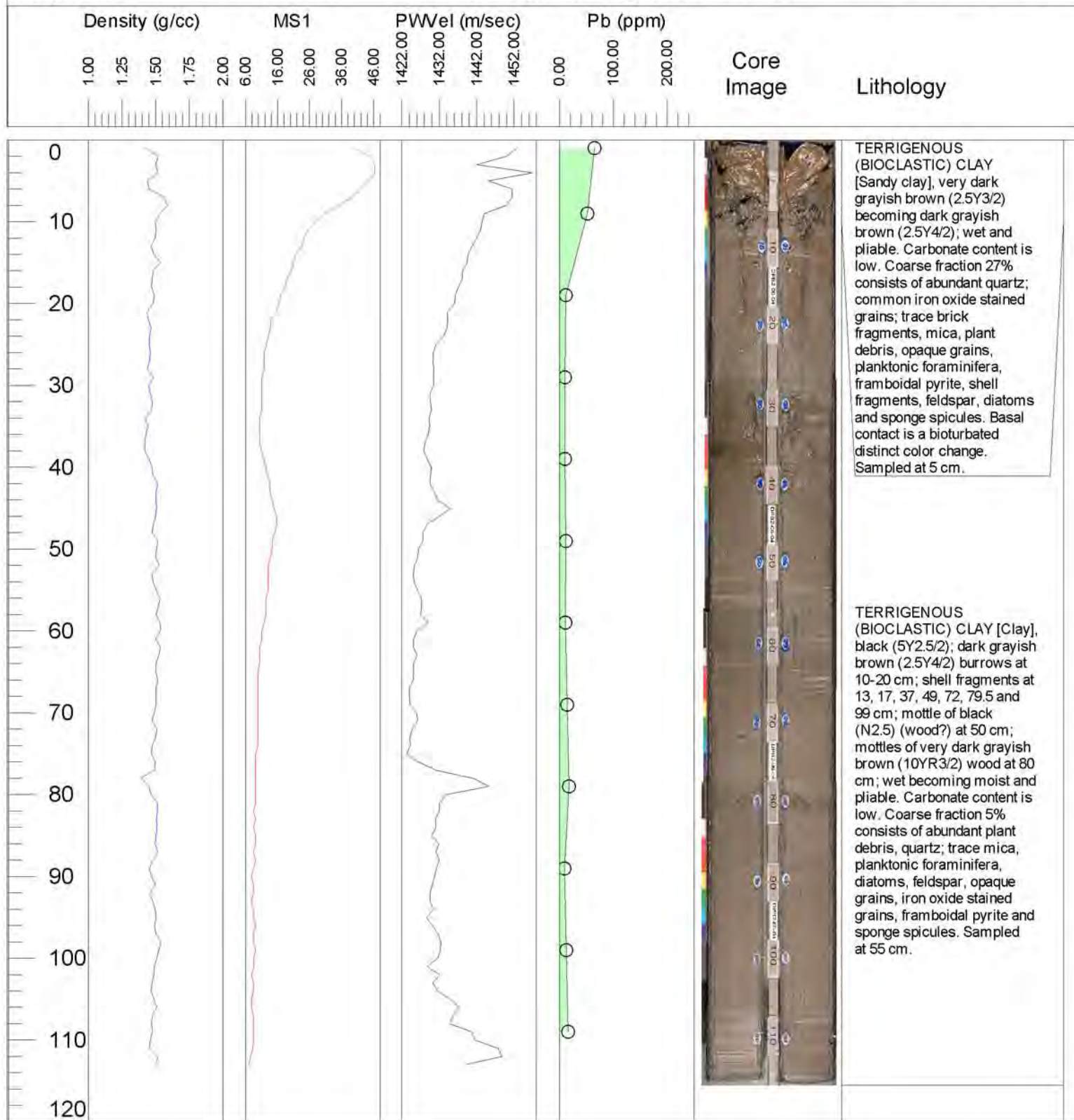
## Lamont-Doherty Earth Observatory

DPB2-06-04

Project Title: Assessment of the deposition of sediments impacted by Twentieth Century activities in the vicinity of the Tappan Zee Bridge

Project No.: EARTH D213123

Principle Investigators: Timothy C. Kenna and Frank Nitsche



Core ID: DPB2-06-04

Latitude: 41° 4.310' N

Date Opened: 05/19/06

Core Length: 115.5 cm

Longitude: 73° 55.139' W

Date Photographed: 05/19/06

Collection Date: 05/11/06

PDR Depth: 2.3 m

Date Described: 06/01/06

Described by: N. Anest



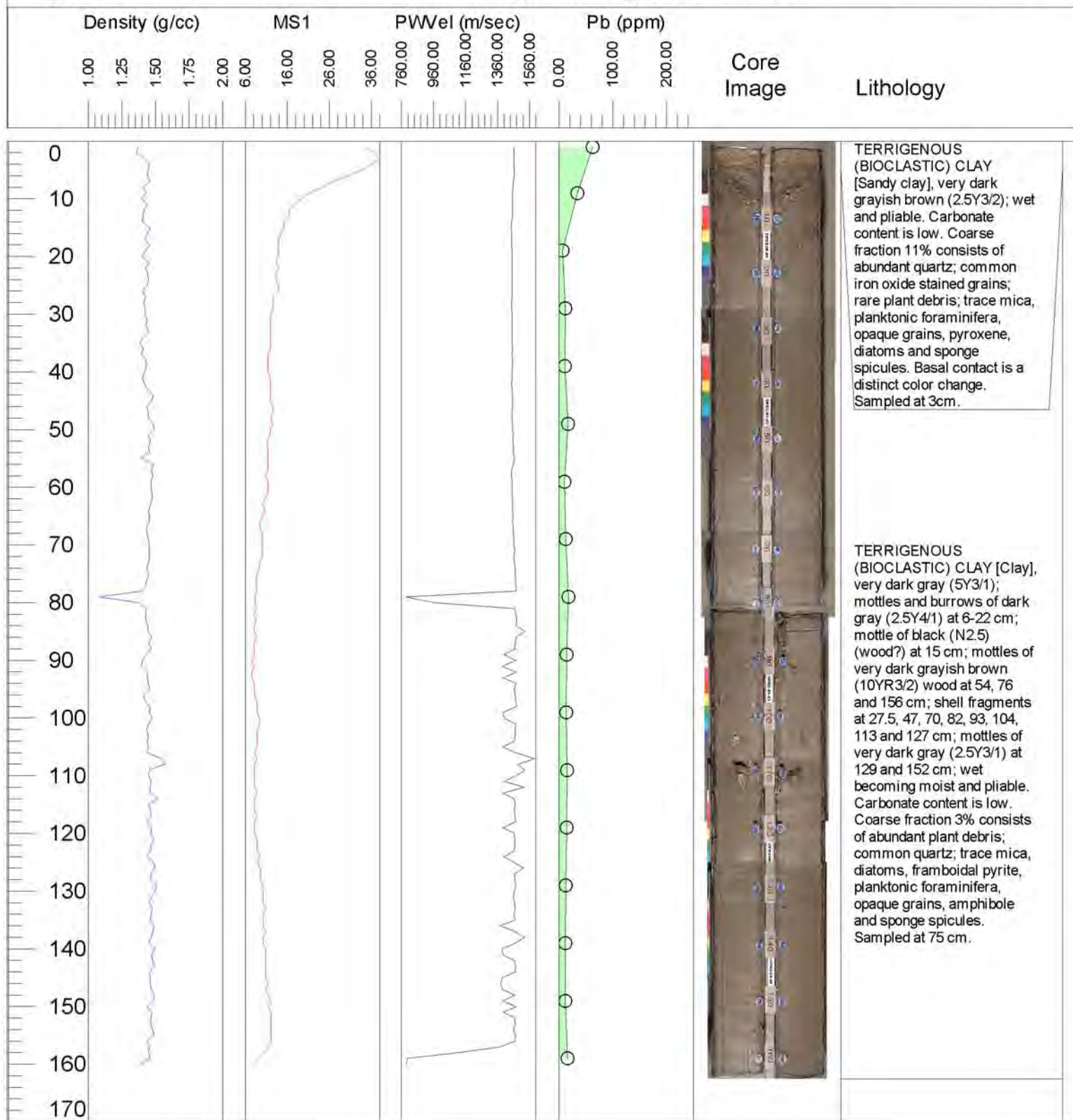
## Lamont-Doherty Earth Observatory

DPB2-06-05

Project Title: Assessment of the deposition of sediments impacted by Twentieth Century activities in the vicinity of the Tappan Zee Bridge

Project No.: EARTH D213123

Principle Investigators: Timothy C. Kenna and Frank Nitsche



Core ID: DPB2-06-05

Latitude: 41° 4.218' N

Date Opened: 05/23/06

Core Length: 162.5 cm

Longitude: 73° 55.048' W

Date Photographed: 05/23/06

Collection Date: 05/10/06

PDR Depth: 1.8 m

Date Described: 06/02/06

Described by: N. Anest

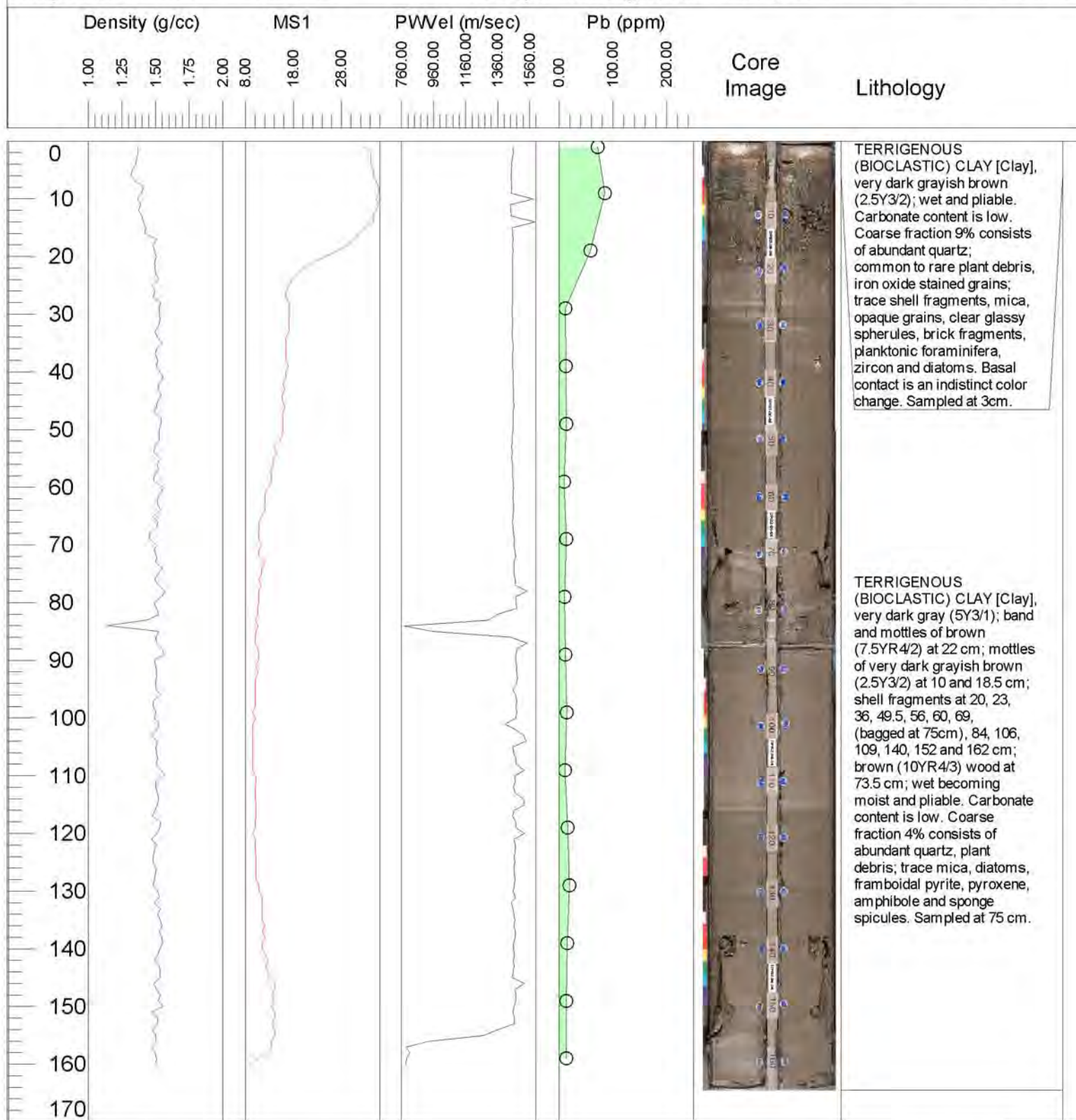
## Lamont-Doherty Earth Observatory

DPB2-06-06

Project Title: Assessment of the deposition of sediments impacted by Twentieth Century activities in the vicinity of the Tappan Zee Bridge

Project No.: EARTH D213123

Principle Investigators: Timothy C. Kenna and Frank Nitsche



Core ID: DPB2-06-06

Latitude: 41° 4.069' N

Date Opened: 05/23/06

Core Length: 164.5 cm

Longitude: 73° 54.829' W

Date Photographed: 05/23/06

Collection Date: 05/10/06

PDR Depth: 2.1 m

Date Described: 06/02/06

Described by: N. Anest



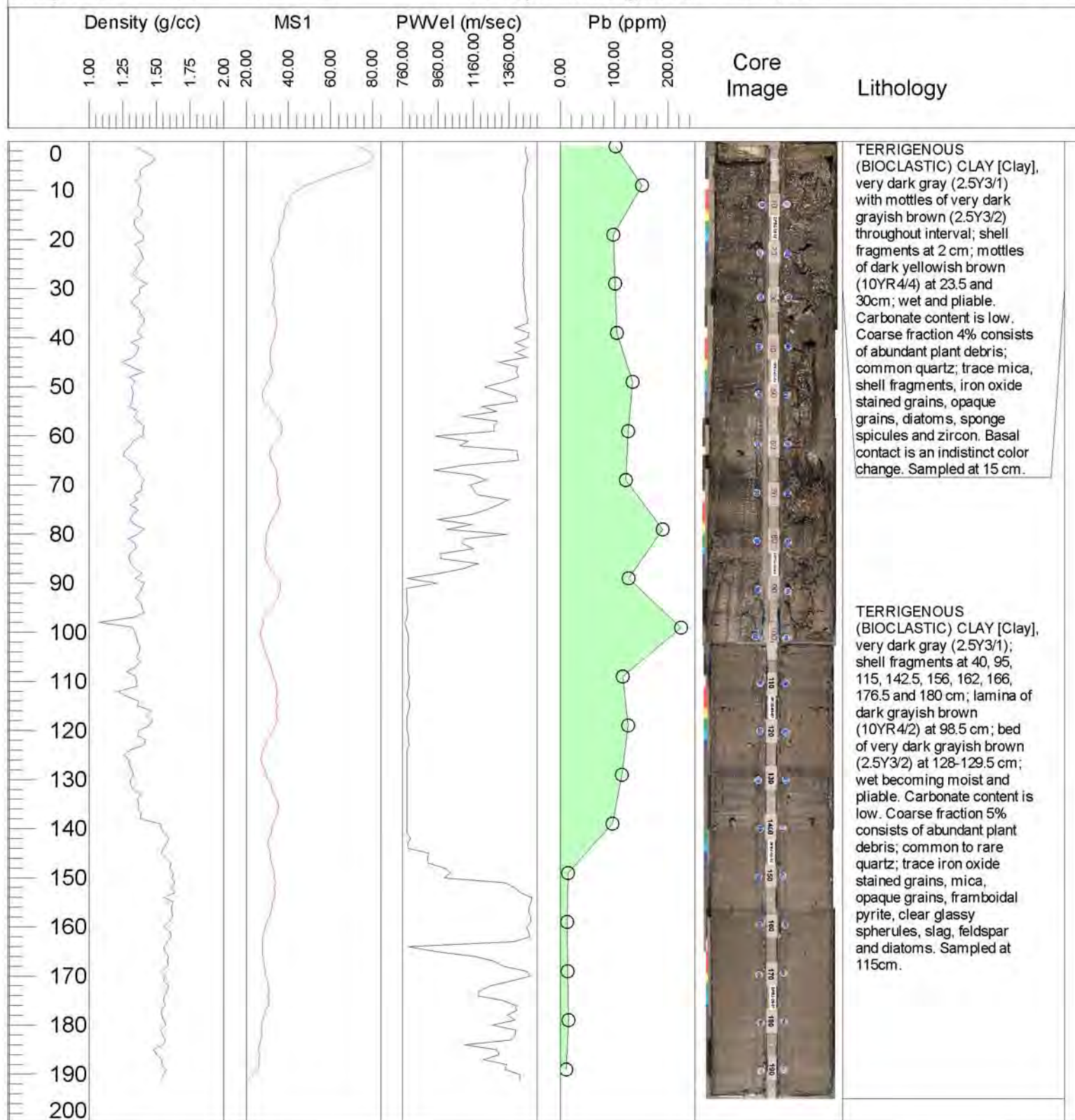
## Lamont-Doherty Earth Observatory

DPB2-06-07

Project Title: Assessment of the deposition of sediments impacted by Twentieth Century activities in the vicinity of the Tappan Zee Bridge

Project No.: EARTH D213123

Principle Investigators: Timothy C. Kenna and Frank Nitsche



Core ID: DPB2-06-07

Latitude: 41° 4.171' N

Date Opened: 05/23/06

Core Length: 195 cm

Longitude: 73° 54.557' W

Date Photographed: 05/23/06

Collection Date: 05/10/06

PDR Depth: 2.8 m

Date Described: 06/02/06

Described by: N. Anest

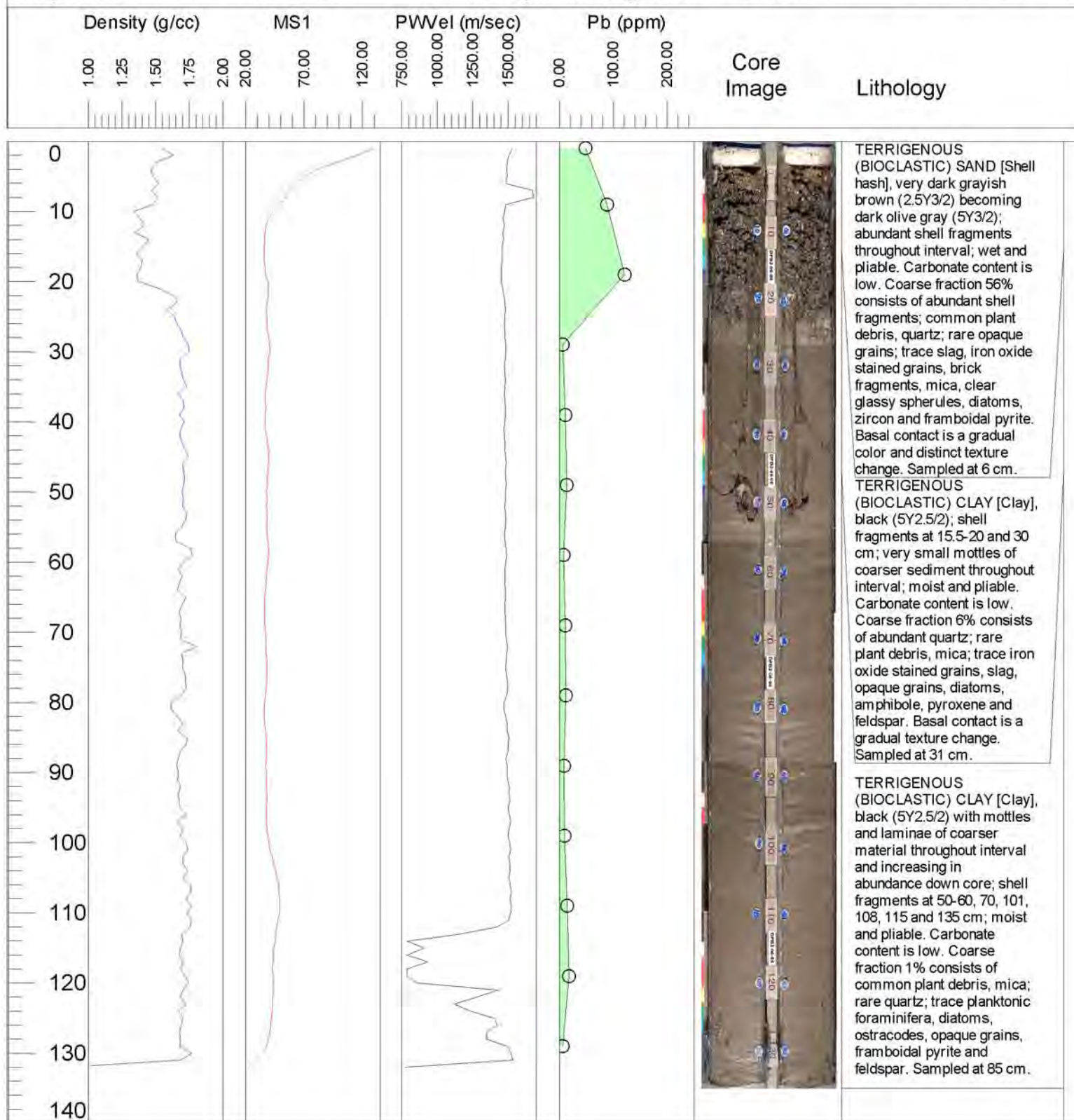
## Lamont-Doherty Earth Observatory

DPB2-06-08

Project Title: Assessment of the deposition of sediments impacted by Twentieth Century activities in the vicinity of the Tappan Zee Bridge

Project No.: EARTHT D213123

Principle Investigators: Timothy C. Kenna and Frank Nitsche



Core ID: DPB2-06-08

Latitude: 41° 4.169' N

Date Opened: 05/17/06

Core Length: 135 cm

Longitude: 73° 54.158' W

Date Photographed: 05/17/06

Collection Date: 05/10/06

PDR Depth: 3.7 m

Date Described: 06/08/06

Described by: N. Anest



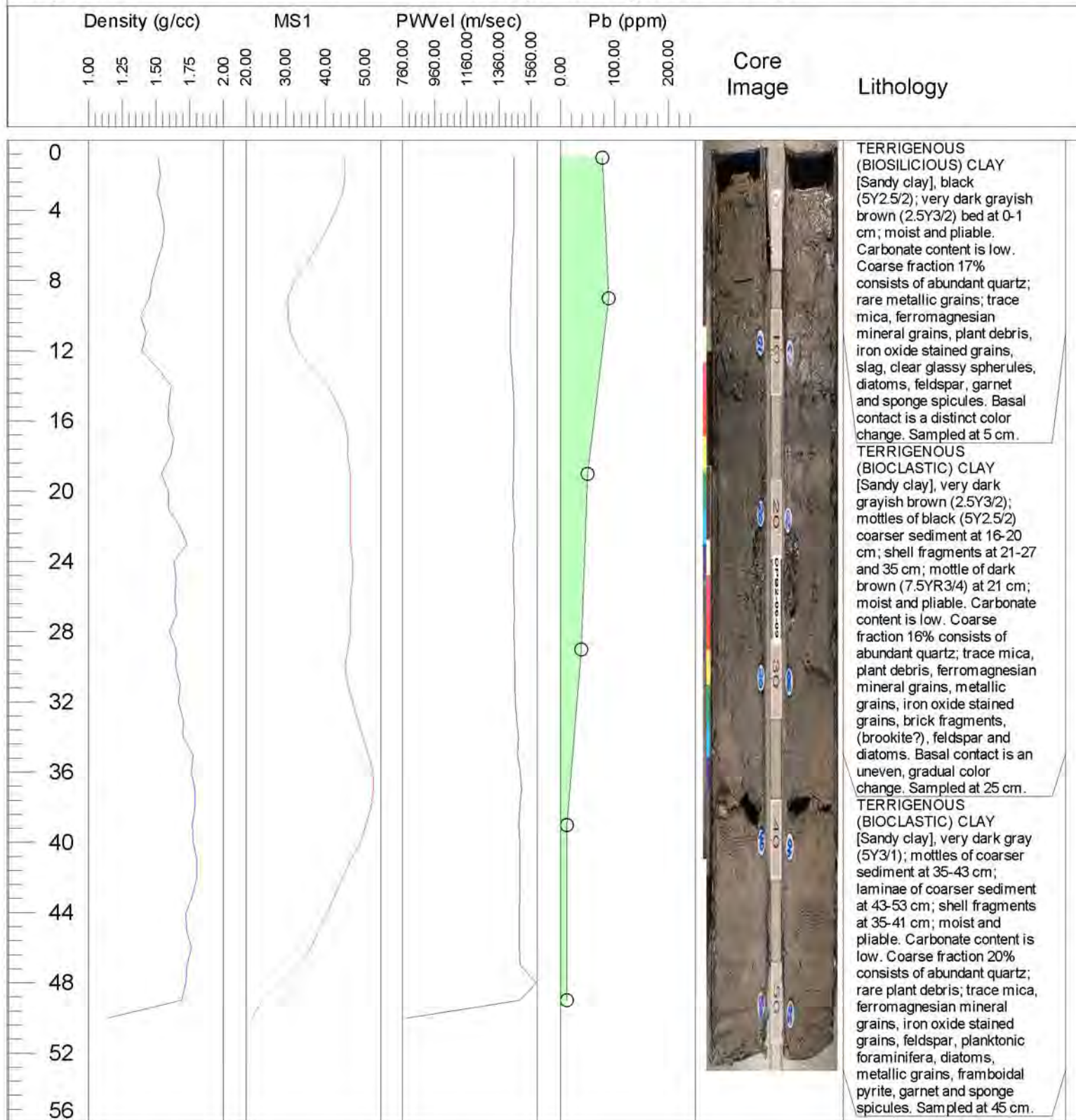
## Lamont-Doherty Earth Observatory

DPB2-06-09

Project Title: Assessment of the deposition of sediments impacted by Twentieth Century activities in the vicinity of the Tappan Zee Bridge

Project No.: EARTH D213123

Principle Investigators: Timothy C. Kenna and Frank Nitsche



Core ID: DPB2-06-09

Latitude: 41° 4.075' N

Date Opened: 05/22/06

Core Length: 53 cm

Longitude: 73° 52.263' W

Date Photographed: 05/22/06

Collection Date: 05/10/06

PDR Depth: 2.9 m

Date Described: 06/08/06

Described by: N. Anest

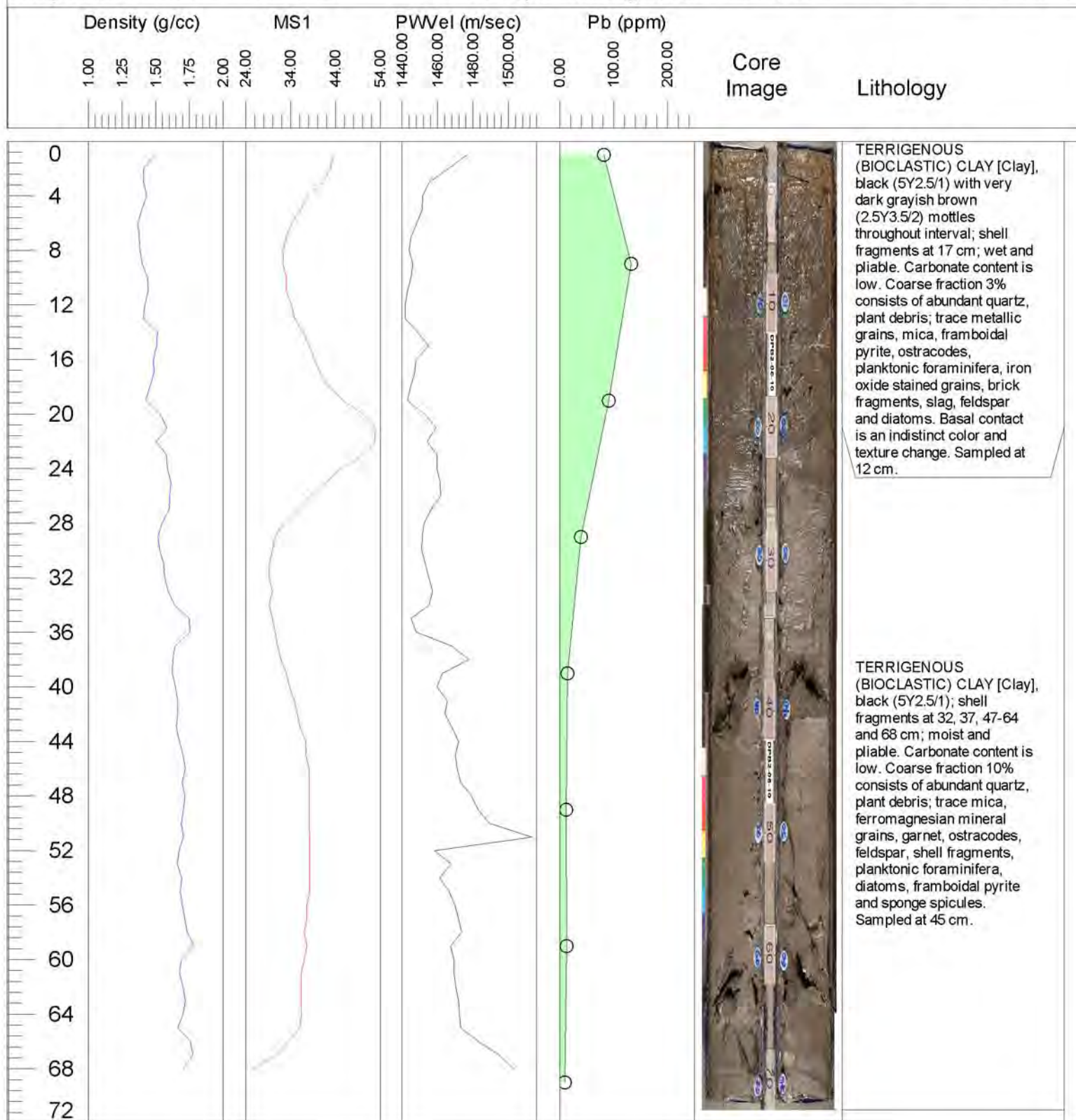
## Lamont-Doherty Earth Observatory

DPB2-06-10

Project Title: Assessment of the deposition of sediments impacted by Twentieth Century activities in the vicinity of the Tappan Zee Bridge

Project No.: EARTH D213123

Principle Investigators: Timothy C. Kenna and Frank Nitsche



Core ID: DPB2-06-10

Latitude: 41° 4.014' N

Date Opened: 05/22/06

Core Length: 71 cm

Longitude: 73° 52.179' W

Date Photographed: 05/22/06

Collection Date: 05/10/06

PDR Depth: 2.5 m

Date Described: 06/08/06

Described by: N. Anest



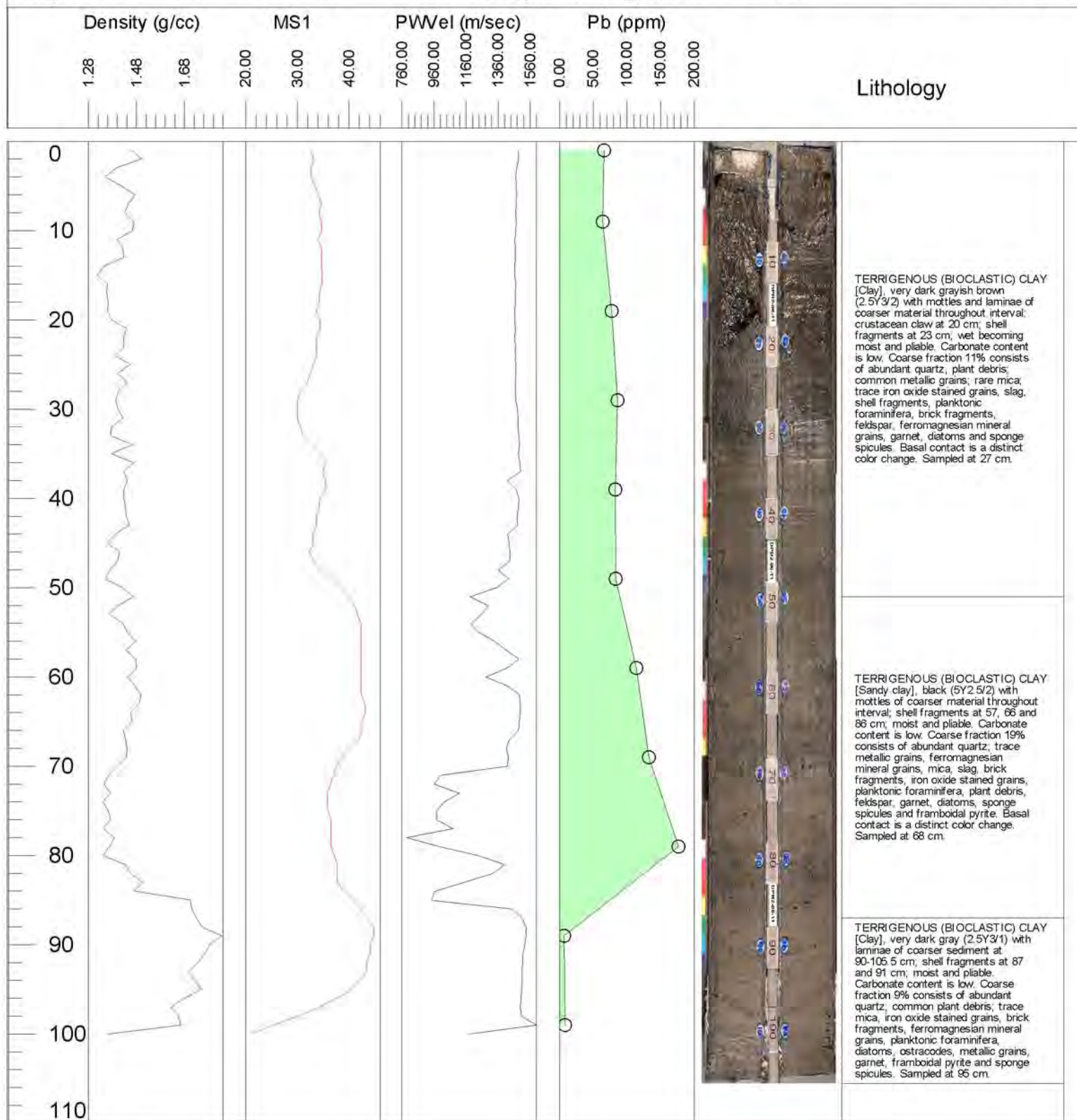
## Lamont-Doherty Earth Observatory

DPB2-06-11

Project Title: Assessment of the deposition of sediments impacted by Twentieth Century activities in the vicinity of the Tappan Zee Bridge

Project No.: EARTH D213123

Principle Investigators: Timothy C. Kenna and Frank Nitsche



Core ID: DPB2-06-11

Latitude: 41° 4.423' N

Date Opened: 05/19/06

Core Length: 105.5 cm

Longitude: 73° 52.354' W

Date Photographed: 05/19/06

Collection Date: 05/11/06

PDR Depth: 3.5 m

Date Described: 06/08/06

Described by: N. Anest

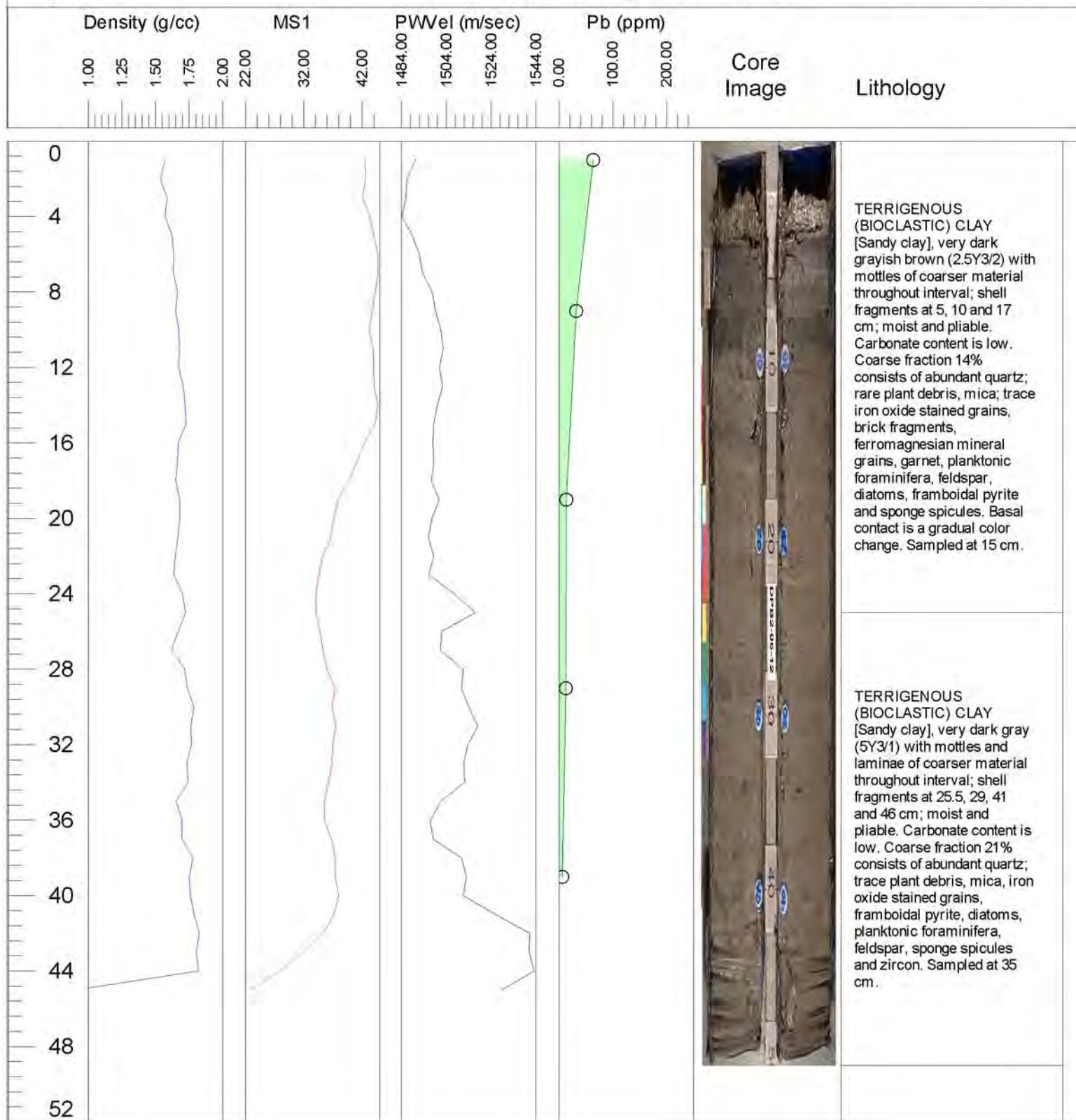
## Lamont-Doherty Earth Observatory

DPB2-06-12

Project Title: Assessment of the deposition of sediments impacted by Twentieth Century activities in the vicinity of the Tappan Zee Bridge

Project No.: EARTH D213123

Principle Investigators: Timothy C. Kenna and Frank Nitsche



Core ID: DPB2-06-12

Latitude: 41° 4.252' N

Date Opened: 05/22/06

Core Length: 49 cm

Longitude: 73° 52.253' W

Date Photographed: 05/22/06

Collection Date: 05/10/06

PDR Depth: 3.0 m

Date Described: 06/09/06

Described by: N. Anest



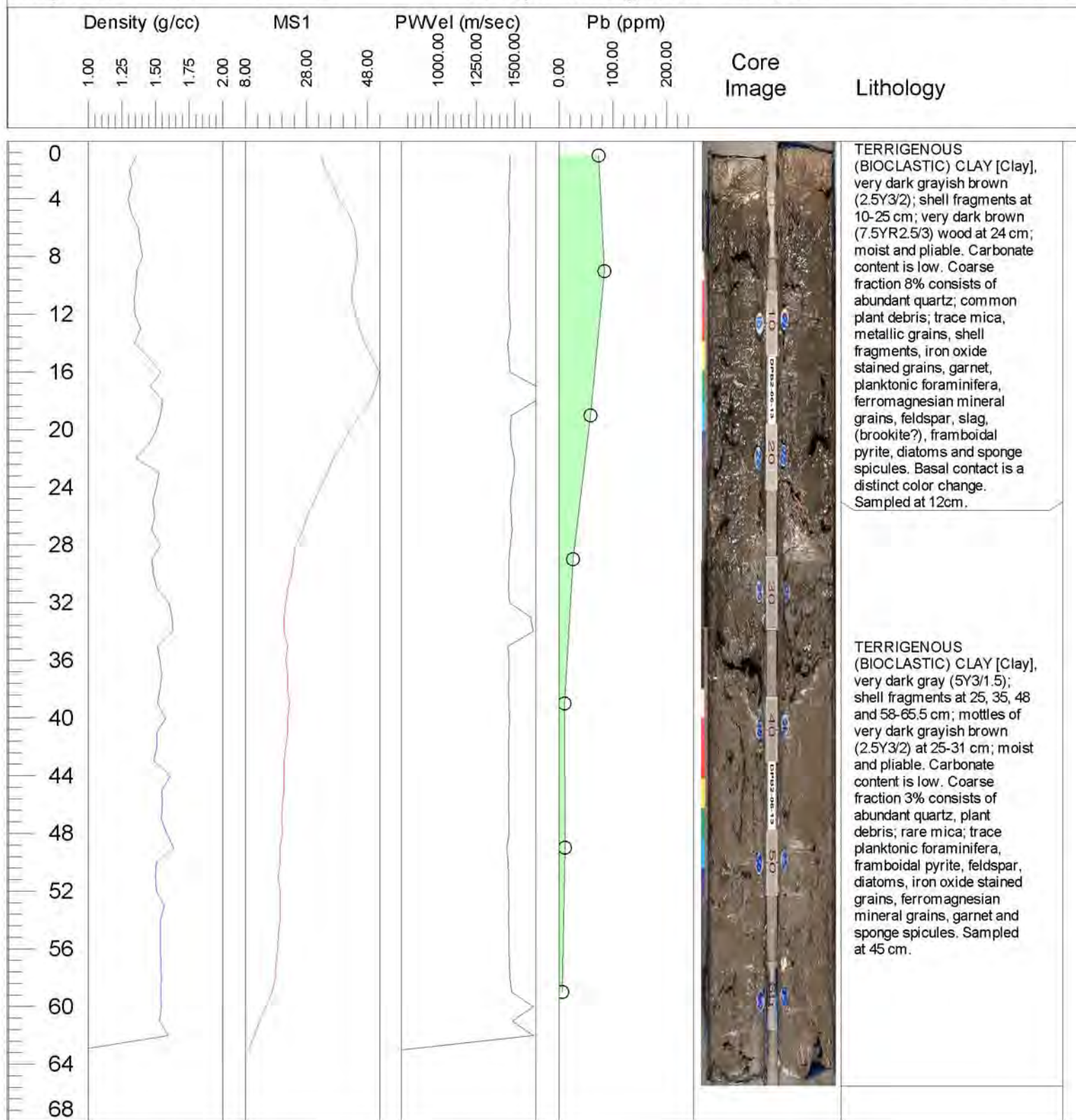
## Lamont-Doherty Earth Observatory

DPB2-06-13

Project Title: Assessment of the deposition of sediments impacted by Twentieth Century activities in the vicinity of the Tappan Zee Bridge

Project No.: EARTH D213123

Principle Investigators: Timothy C. Kenna and Frank Nitsche



Core ID: DPB2-06-13

Latitude: 41° 4.145' N

Date Opened: 05/22/06

Core Length: 65.5 cm

Longitude: 73° 52.103' W

Date Photographed: 05/22/06

Collection Date: 05/11/06

PDR Depth: 2.7 m

Date Described: 06/12/06

Described by: N. Anest

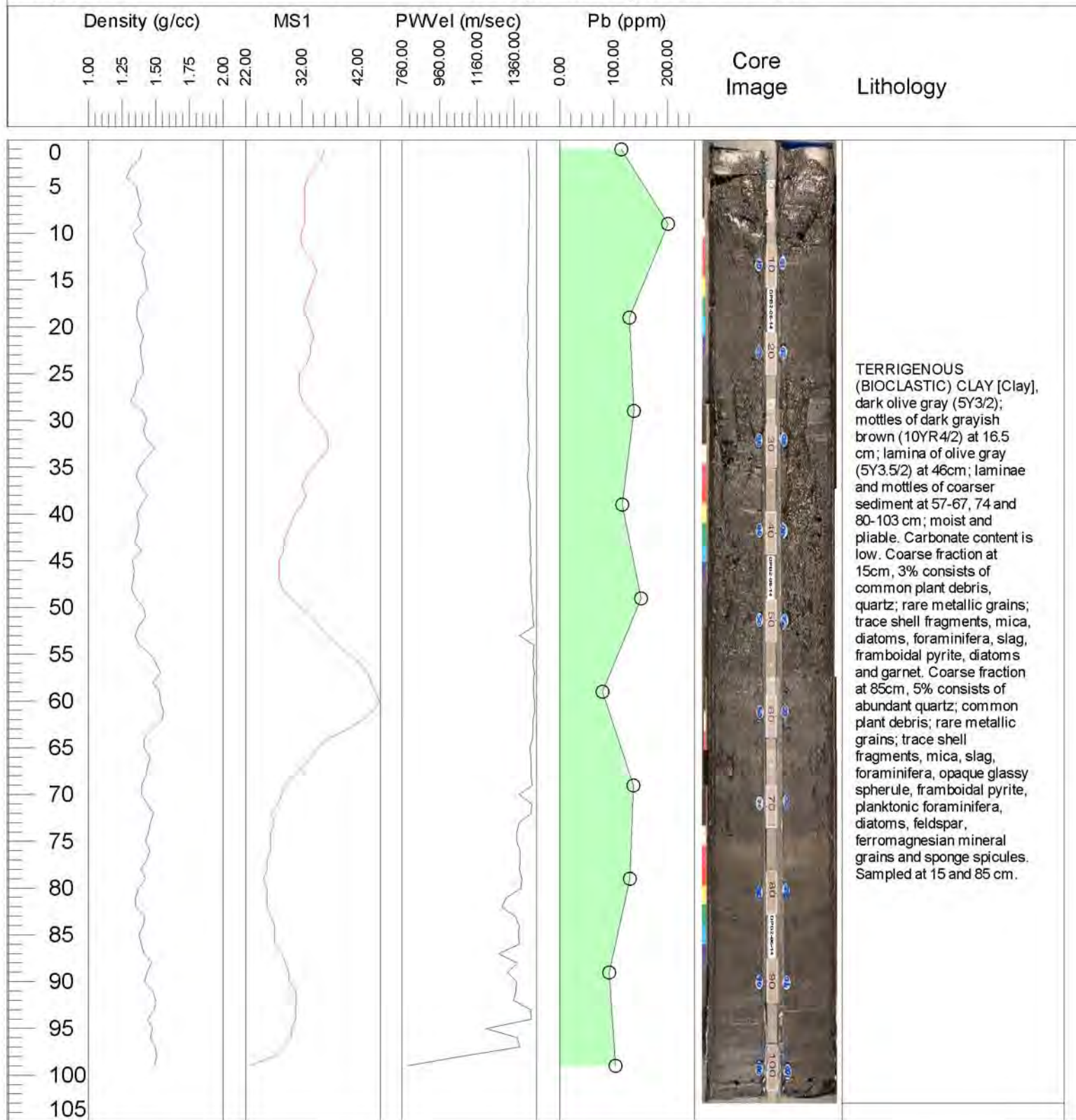
## Lamont-Doherty Earth Observatory

DPB2-06-14

Project Title: Assessment of the deposition of sediments impacted by Twentieth Century activities in the vicinity of the Tappan Zee Bridge

Project No.: EARTHT D213123

Principle Investigators: Timothy C. Kenna and Frank Nitsche



Core ID: DPB2-06-14

Latitude: 41° 3.769' N

Date Opened: 05/19/06

Core Length: 103 cm

Longitude: 73° 52.363' W

Date Photographed: 05/19/06

Collection Date: 05/10/06

PDR Depth: 3.0 m

Date Described: 06/12/06

Described by: N. Anest



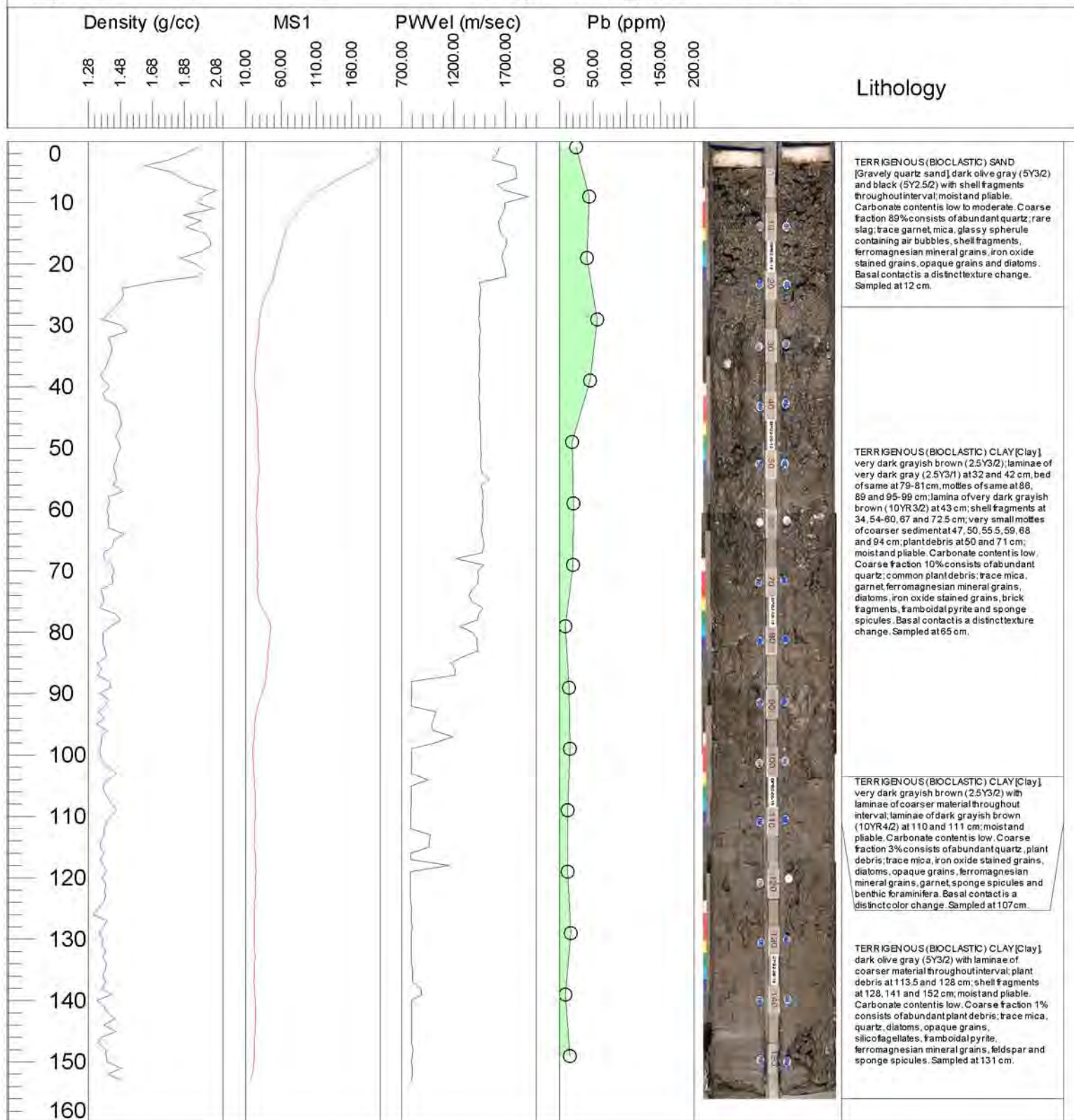
## Lamont-Doherty Earth Observatory

DPB2-06-15

Project Title: Assessment of the deposition of sediments impacted by Twentieth Century activities in the vicinity of the Tappan Zee Bridge

Project No.: EARTH D213123

Principle Investigators: Timothy C. Kenna and Frank Nitsche



Core ID: DPB2-06-15

Latitude: 41° 4.078' N

Date Opened: 05/22/06

Core Length: 156 cm

Longitude: 73° 52.732' W

Date Photographed: 05/22/06

Collection Date: 05/10/06

PDR Depth: 12.5 m

Date Described: 06/12/06

Described by: N. Anest

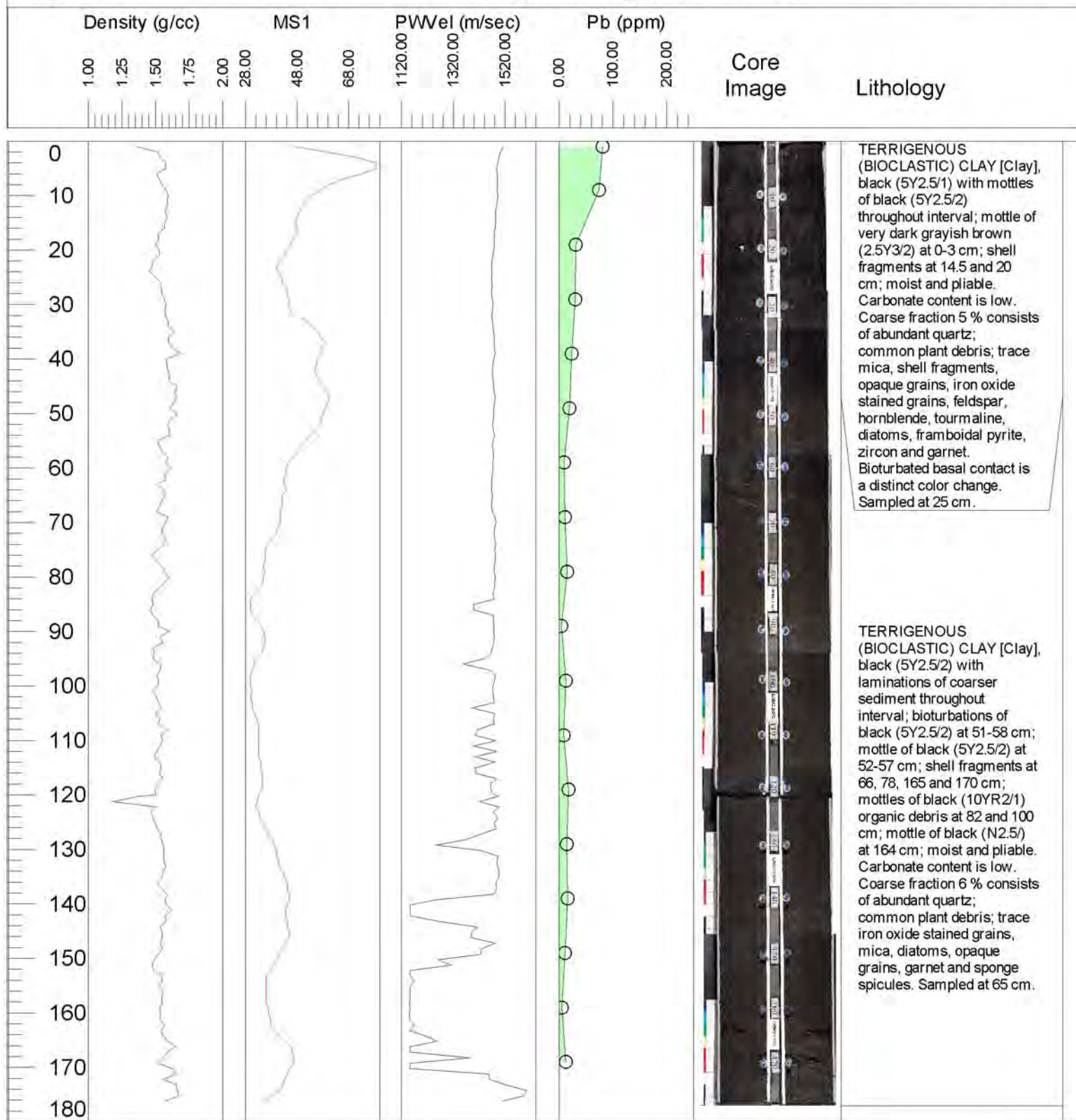
## Lamont-Doherty Earth Observatory

**LWB2-07**

Project Title: Assessment of the deposition of sediments impacted by Twentieth Century activities in the vicinity of the Tappan Zee Bridge

Project No.: EARTHT D213123

Principle Investigators: Timothy C. Kenna and Frank Nitsche



Core ID: LWB2-07

Latitude: 41° 4.313' N

Date Opened: 02/13/02

Core Length: 177 cm

Longitude: 73° 52.532' W

Date Photographed: 02/13/02

Collection Date: 09/05/01

PDR Depth: 5.5 m

Date Described: 02/13/02

Described by: N. Anest



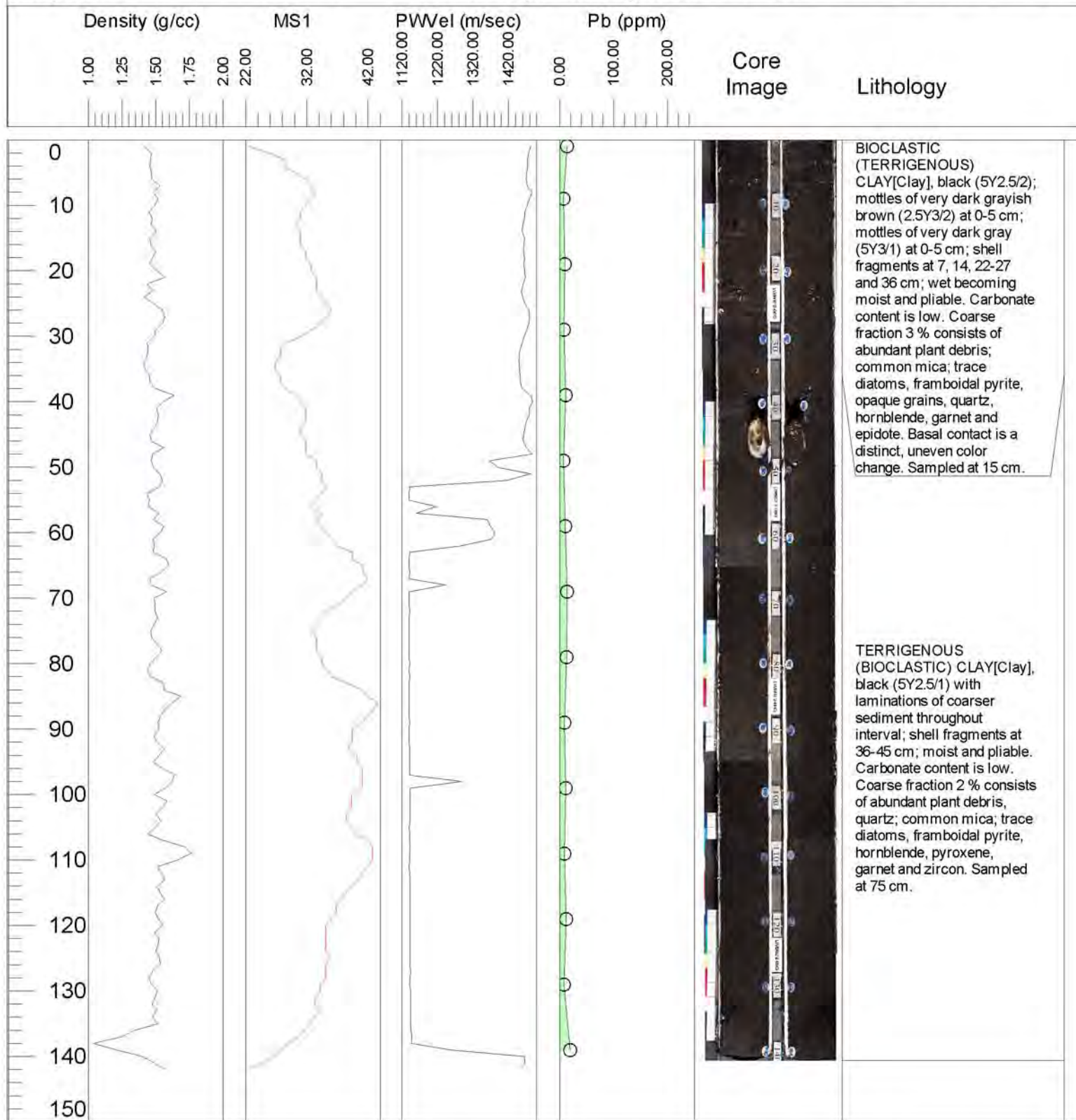
## Lamont-Doherty Earth Observatory

**LWB2-08**

Project Title: Assessment of the deposition of sediments impacted by Twentieth Century activities in the vicinity of the Tappan Zee Bridge

Project No.: EARTHT D213123

Principle Investigators: Timothy C. Kenna and Frank Nitsche



Core ID: LWB2-08

Latitude: 41° 4.308' N

Date Opened: 03/13/02

Core Length: 140.6 cm

Longitude: 73° 52.769' W

Date Photographed: 03/13/02

Collection Date: 09/05/01

PDR Depth: 12.9 m

Date Described: 03/13/02

Described by: N. Anest

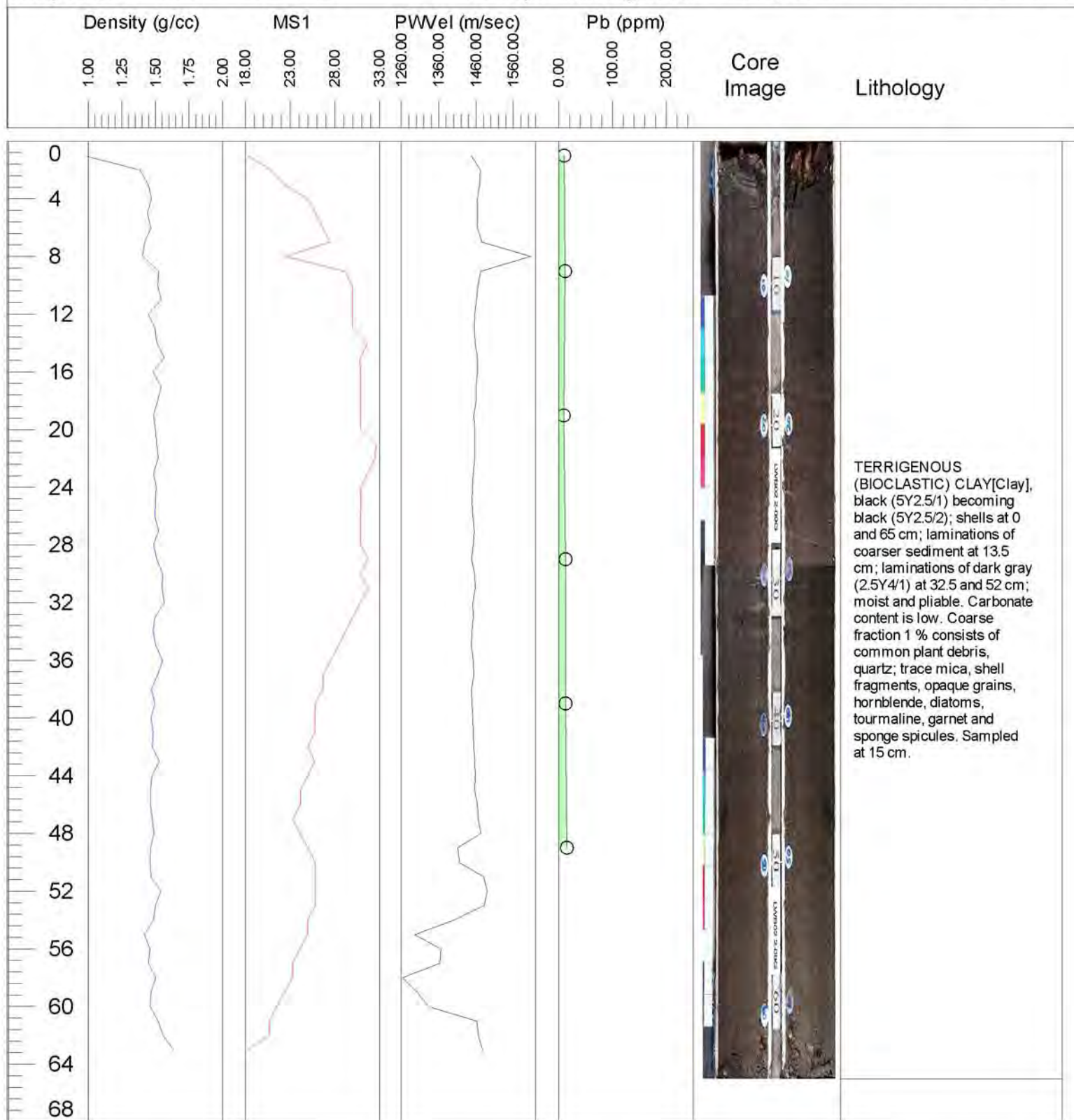
## Lamont-Doherty Earth Observatory

**LWB2-09**

Project Title: Assessment of the deposition of sediments impacted by Twentieth Century activities in the vicinity of the Tappan Zee Bridge

Project No.: EARTHT D213123

Principle Investigators: Timothy C. Kenna and Frank Nitsche



Core ID: LWB2-09

Latitude: 41° 4.314' N

Date Opened: 02/19/02

Core Length: 65 cm

Longitude: 73° 52.841' W

Date Photographed: 02/19/02

Collection Date: 09/05/01

PDR Depth: 14.3 m

Date Described: 02/19/02

Described by: N. Anest



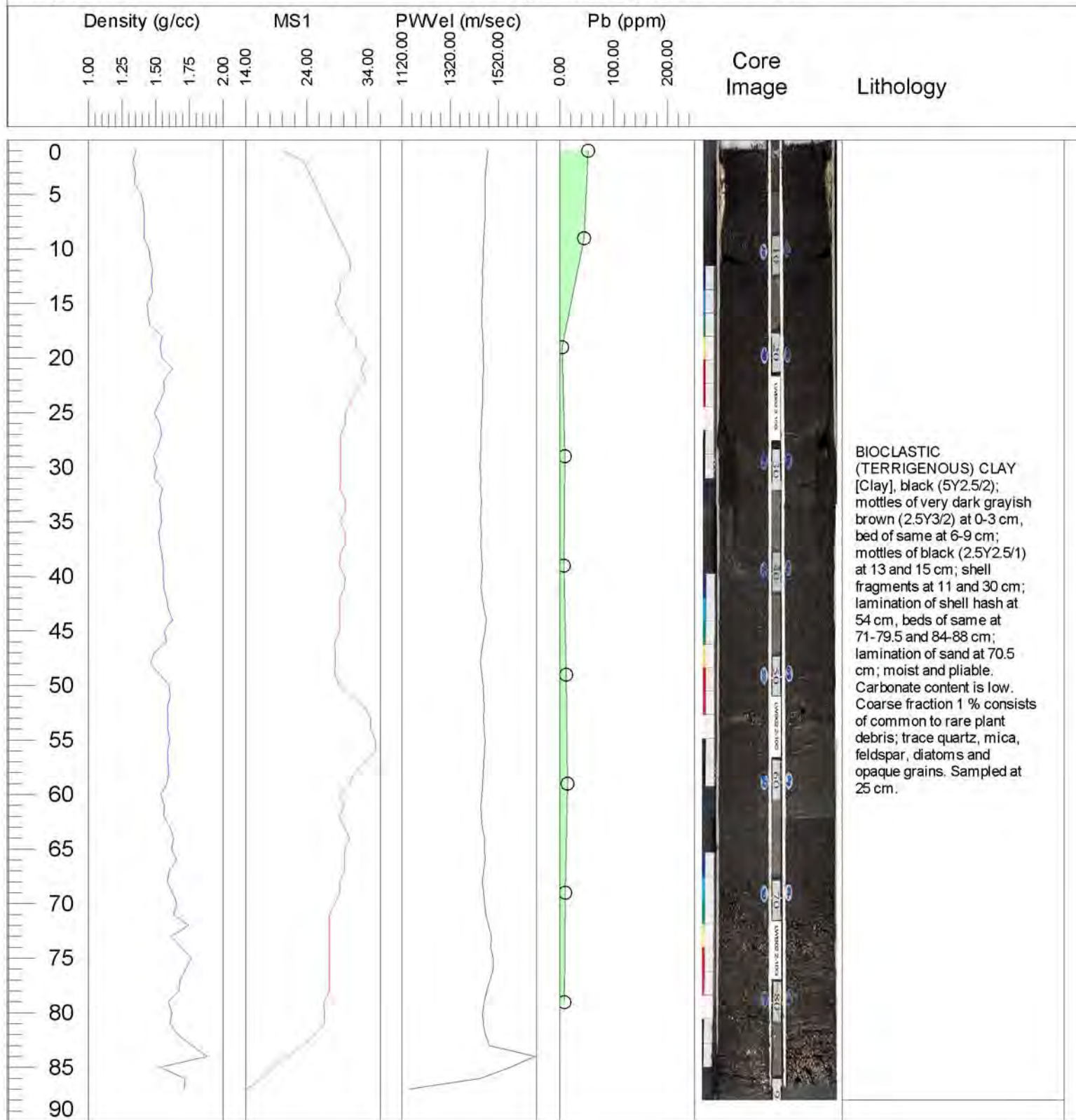
## Lamont-Doherty Earth Observatory

**LWB2-10**

Project Title: Assessment of the deposition of sediments impacted by Twentieth Century activities in the vicinity of the Tappan Zee Bridge

Project No.: EARTHT D213123

Principle Investigators: Timothy C. Kenna and Frank Nitsche



Core ID: LWB2-10

Latitude: 41° 4.323' N

Date Opened: 02/13/02

Core Length: 88 cm

Longitude: 73° 52.9' W

Date Photographed: 02/13/02

Collection Date: 09/05/01

PDR Depth: 14.0 m

Date Described: 02/13/02

Described by: N. Anest

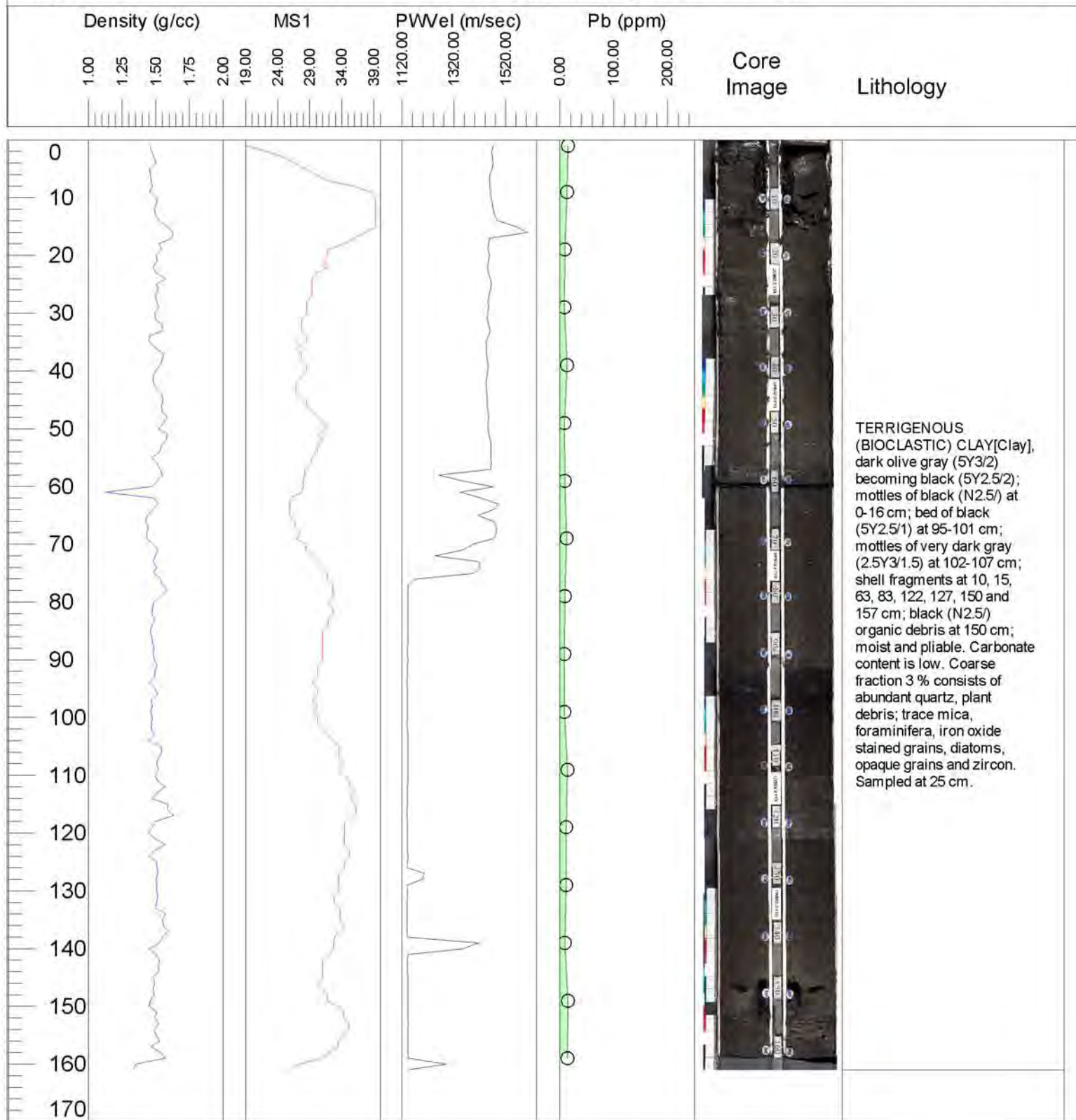
## Lamont-Doherty Earth Observatory

**LWB2-11**

Project Title: Assessment of the deposition of sediments impacted by Twentieth Century activities in the vicinity of the Tappan Zee Bridge

Project No.: EARTHT D213123

Principle Investigators: Timothy C. Kenna and Frank Nitsche



Core ID: LWB2-11

Latitude: 41° 4.316' N

Date Opened: 02/19/02

Core Length: 161 cm

Longitude: 73° 53.108' W

Date Photographed: 02/19/02

Collection Date: 09/05/01

PDR Depth: 9.6 m

Date Described: 02/19/02

Described by: N. Anest



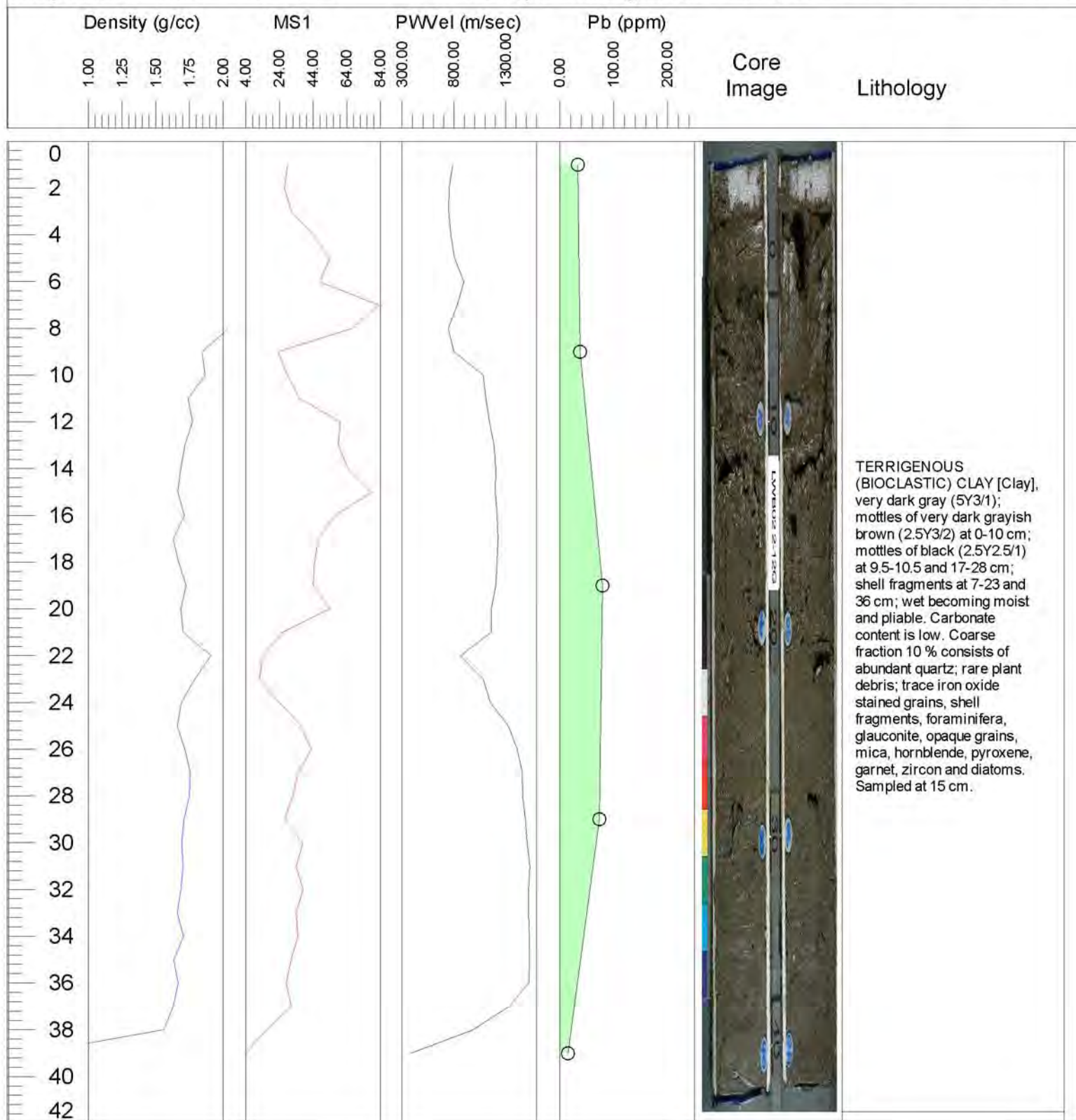
## Lamont-Doherty Earth Observatory

**LWB2-12**

Project Title: Assessment of the deposition of sediments impacted by Twentieth Century activities in the vicinity of the Tappan Zee Bridge

Project No.: EARTH D213123

Principle Investigators: Timothy C. Kenna and Frank Nitsche



Core ID: LWB2-12

Latitude: 41° 4.311' N

Date Opened: 01/25/02

Core Length: 41.5 cm

Longitude: 73° 53.657' W

Date Photographed: 01/25/02

Collection Date: 09/05/01

PDR Depth: 3.5 m

Date Described: 01/25/02

Described by: N. Anest

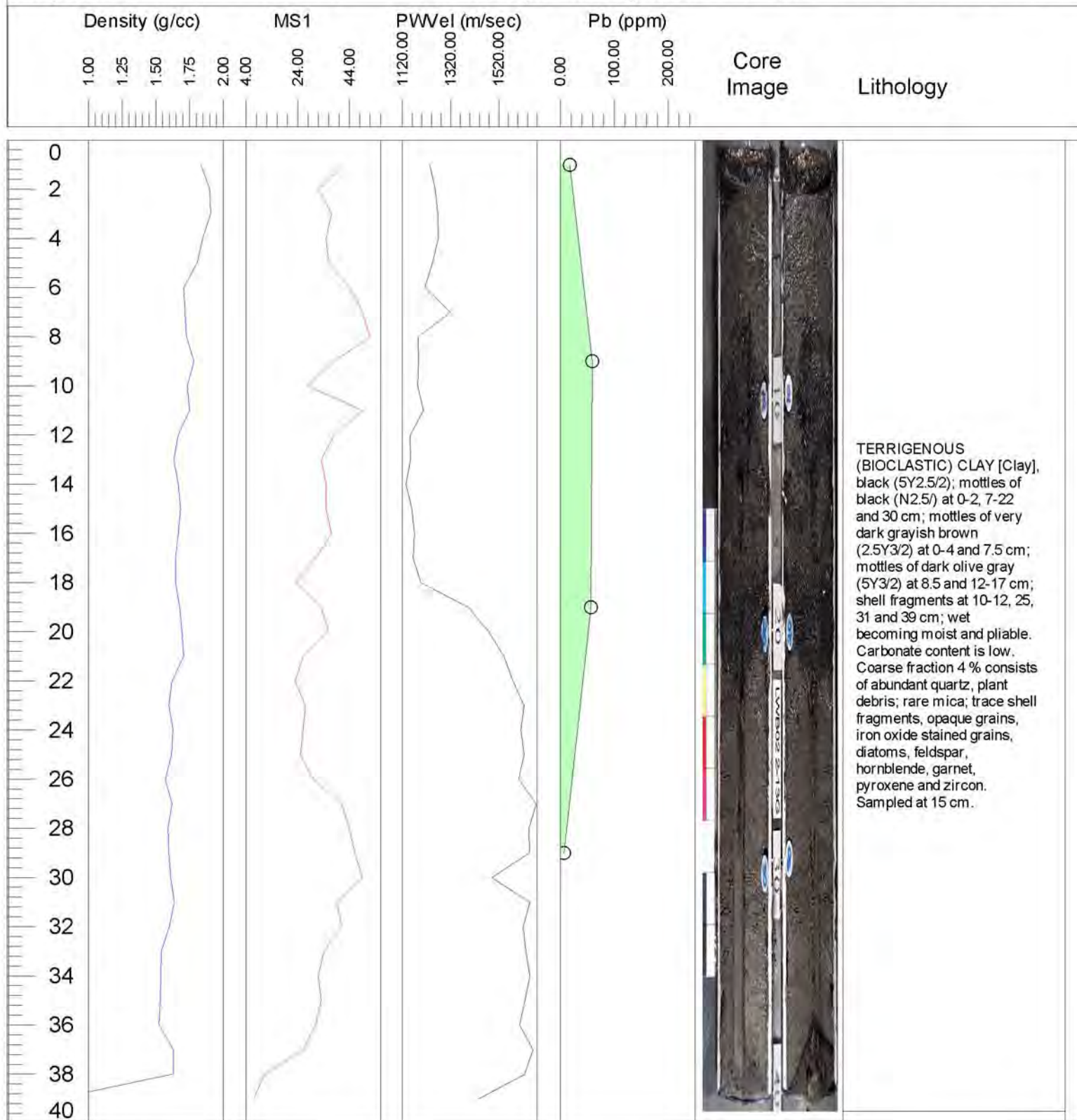
## Lamont-Doherty Earth Observatory

**LWB2-13**

Project Title: Assessment of the deposition of sediments impacted by Twentieth Century activities in the vicinity of the Tappan Zee Bridge

Project No.: EARTHT D213123

Principle Investigators: Timothy C. Kenna and Frank Nitsche



Core ID: LWB2-13

Latitude: 41° 4.318' N

Date Opened: 02/08/02

Core Length: 39.5 cm

Longitude: 73° 54.055' W

Date Photographed: 02/08/02

Collection Date: 09/05/01

PDR Depth: 3.1 m

Date Described: 02/08/02

Described by: N. Anest



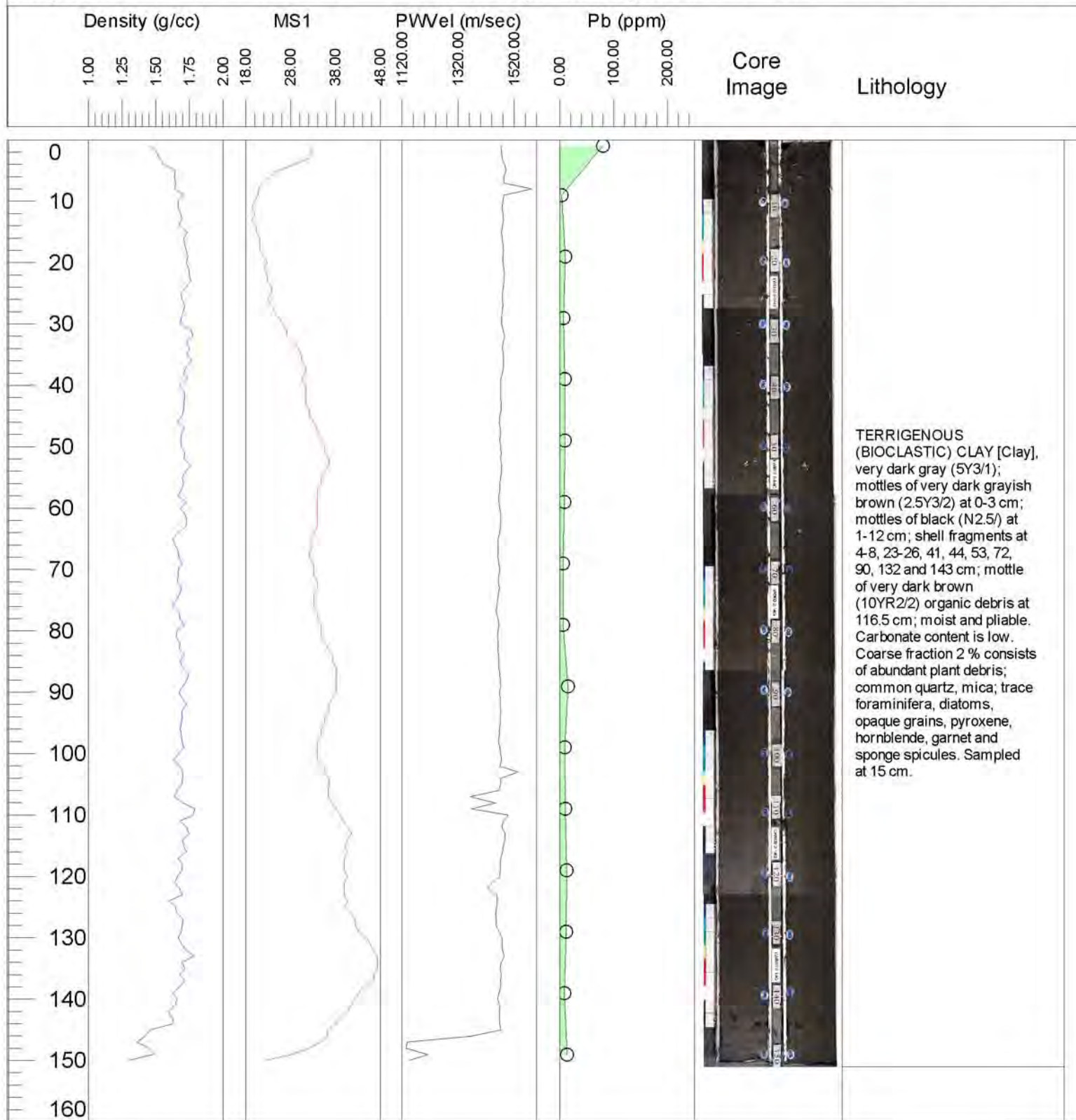
## Lamont-Doherty Earth Observatory

**LWB2-14**

Project Title: Assessment of the deposition of sediments impacted by Twentieth Century activities in the vicinity of the Tappan Zee Bridge

Project No.: EARTHT D213123

Principle Investigators: Timothy C. Kenna and Frank Nitsche



Core ID: LWB2-14

Latitude: 41° 4.314' N

Date Opened: 03/14/02

Core Length: 151 cm

Longitude: 73° 54.494' W

Date Photographed: 03/14/02

Collection Date: 09/05/01

PDR Depth:

Date Described: 03/14/02

Described by: N. Anest

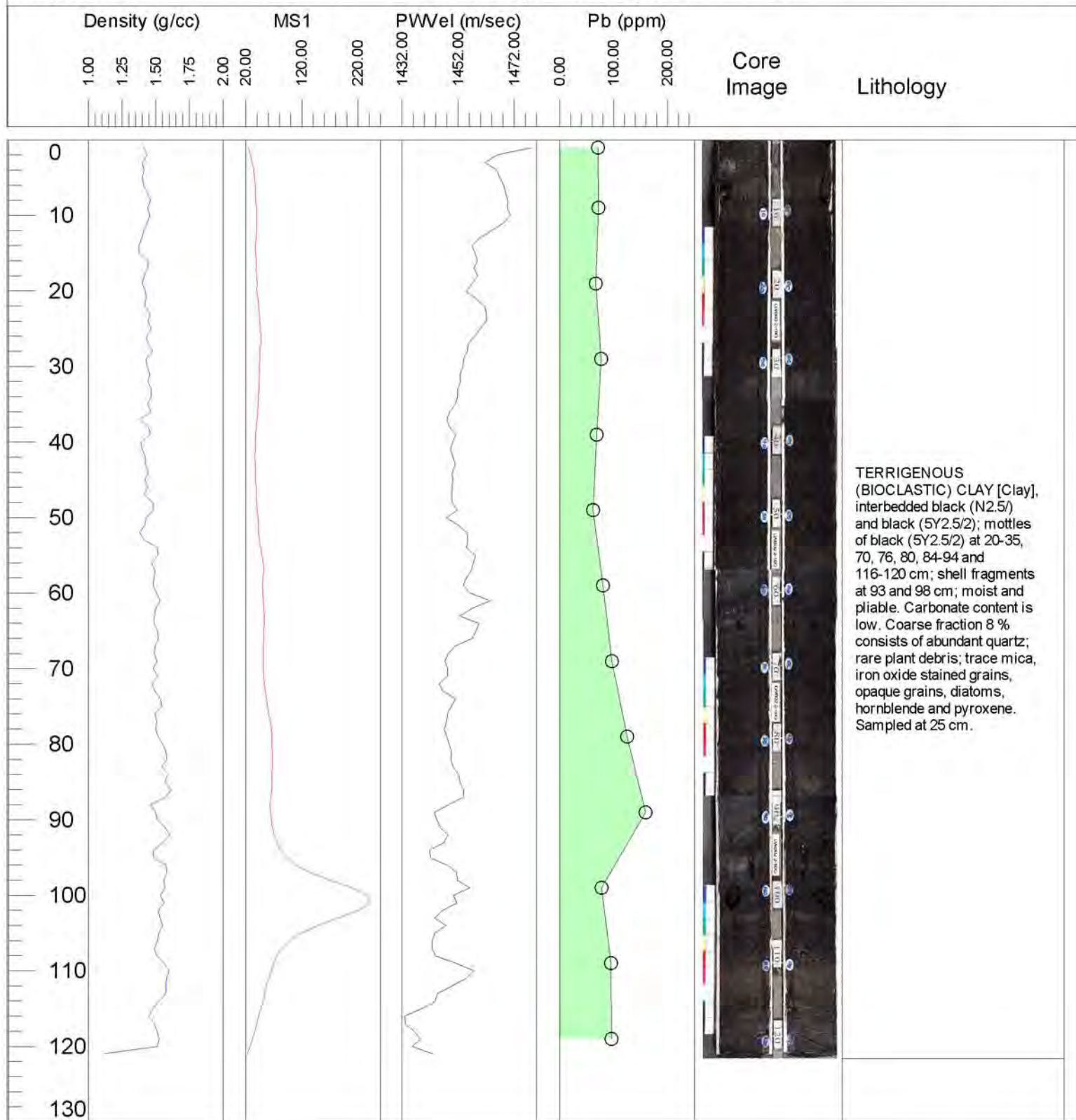
## Lamont-Doherty Earth Observatory

**LWB2-16**

Project Title: Assessment of the deposition of sediments impacted by Twentieth Century activities in the vicinity of the Tappan Zee Bridge

Project No.: EARTHT D213123

Principle Investigators: Timothy C. Kenna and Frank Nitsche



Core ID: LWB2-16

Latitude: 41° 4.121' N

Date Opened: 02/19/02

Core Length: 121.6 cm

Longitude: 73° 53.493' W

Date Photographed: 02/19/02

Collection Date: 09/05/01

PDR Depth: 3.4 m

Date Described: 02/19/02

Described by: N. Anest



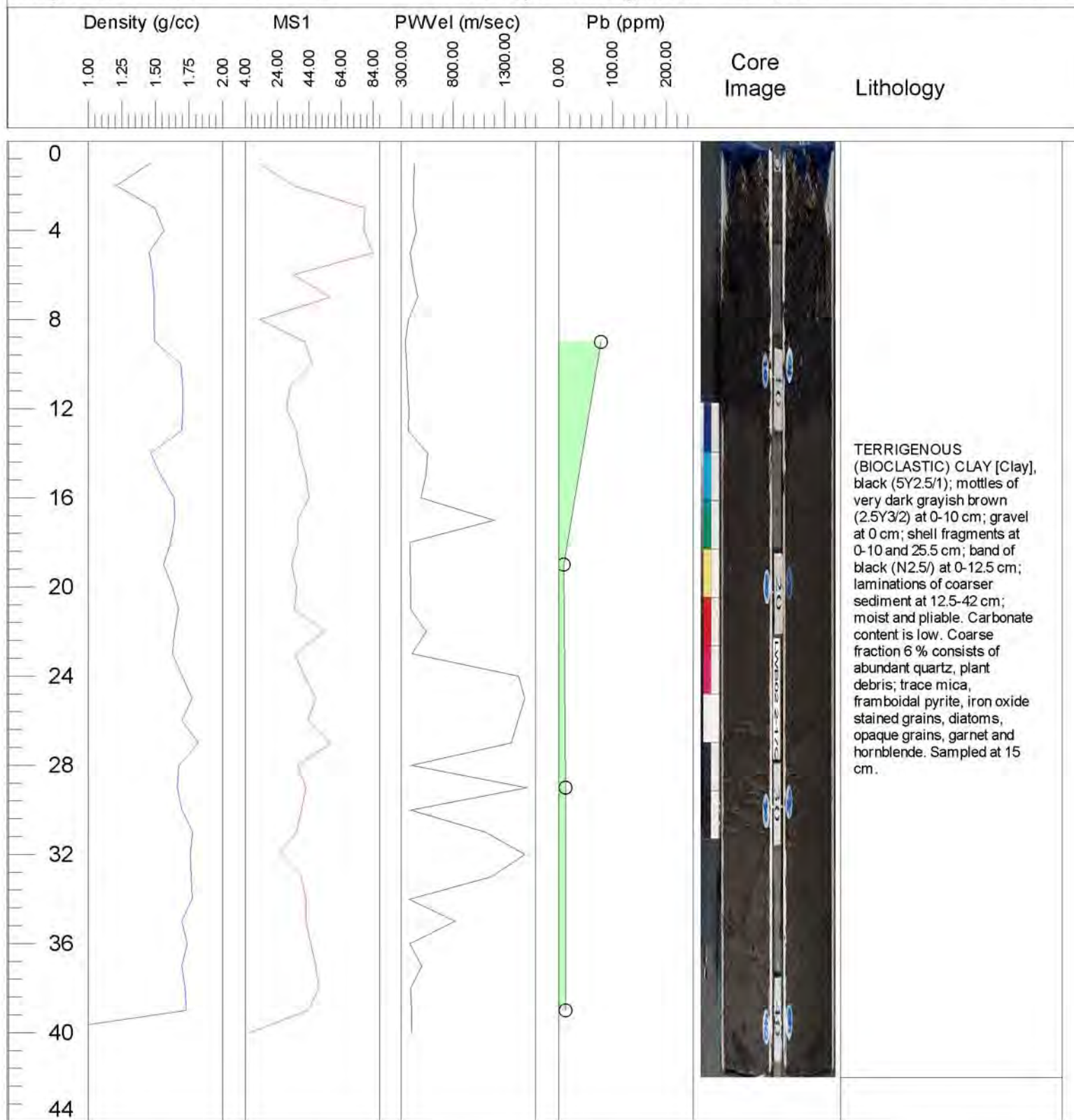
## Lamont-Doherty Earth Observatory

**LWB2-17**

Project Title: Assessment of the deposition of sediments impacted by Twentieth Century activities in the vicinity of the Tappan Zee Bridge

Project No.: EARTHT D213123

Principle Investigators: Timothy C. Kenna and Frank Nitsche



Core ID: LWB2-17

Latitude: 41° 4.134' N

Date Opened: 01/29/02

Core Length: 42 cm

Longitude: 73° 53.383' W

Date Photographed: 01/29/02

Collection Date: 09/05/01

PDR Depth: 3.1 m

Date Described: 01/29/02

Described by: N. Anest

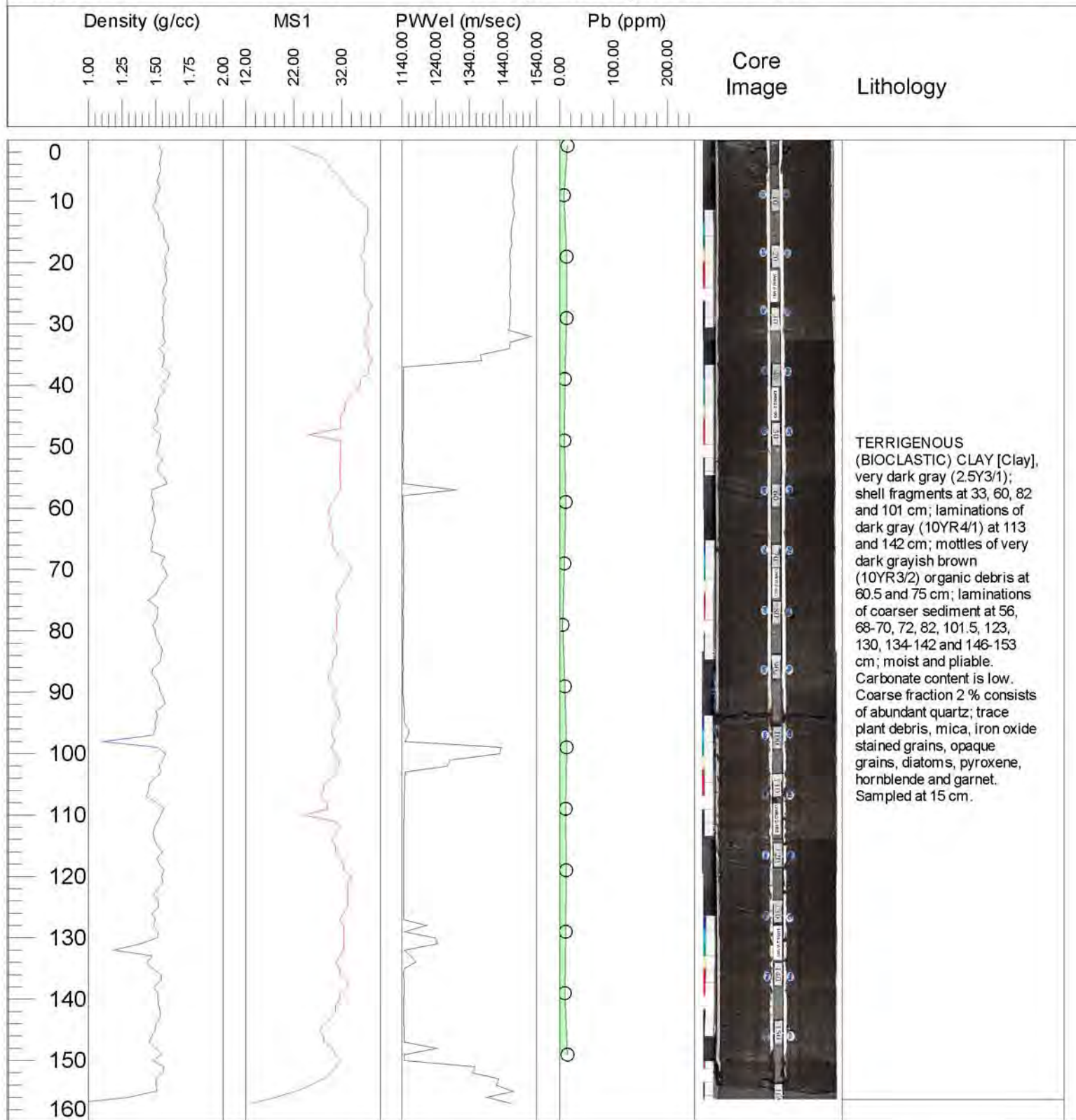
## Lamont-Doherty Earth Observatory

**LWB2-18**

Project Title: Assessment of the deposition of sediments impacted by Twentieth Century activities in the vicinity of the Tappan Zee Bridge

Project No.: EARTHT D213123

Principle Investigators: Timothy C. Kenna and Frank Nitsche



Core ID: LWB2-18

Latitude: 41° 4.122' N

Date Opened: 02/19/02

Core Length: 156.3 cm

Longitude: 73° 53.045' W

Date Photographed: 02/19/02

Collection Date: 09/05/01

PDR Depth: 10.8 m

Date Described: 02/19/02

Described by: N. Anest



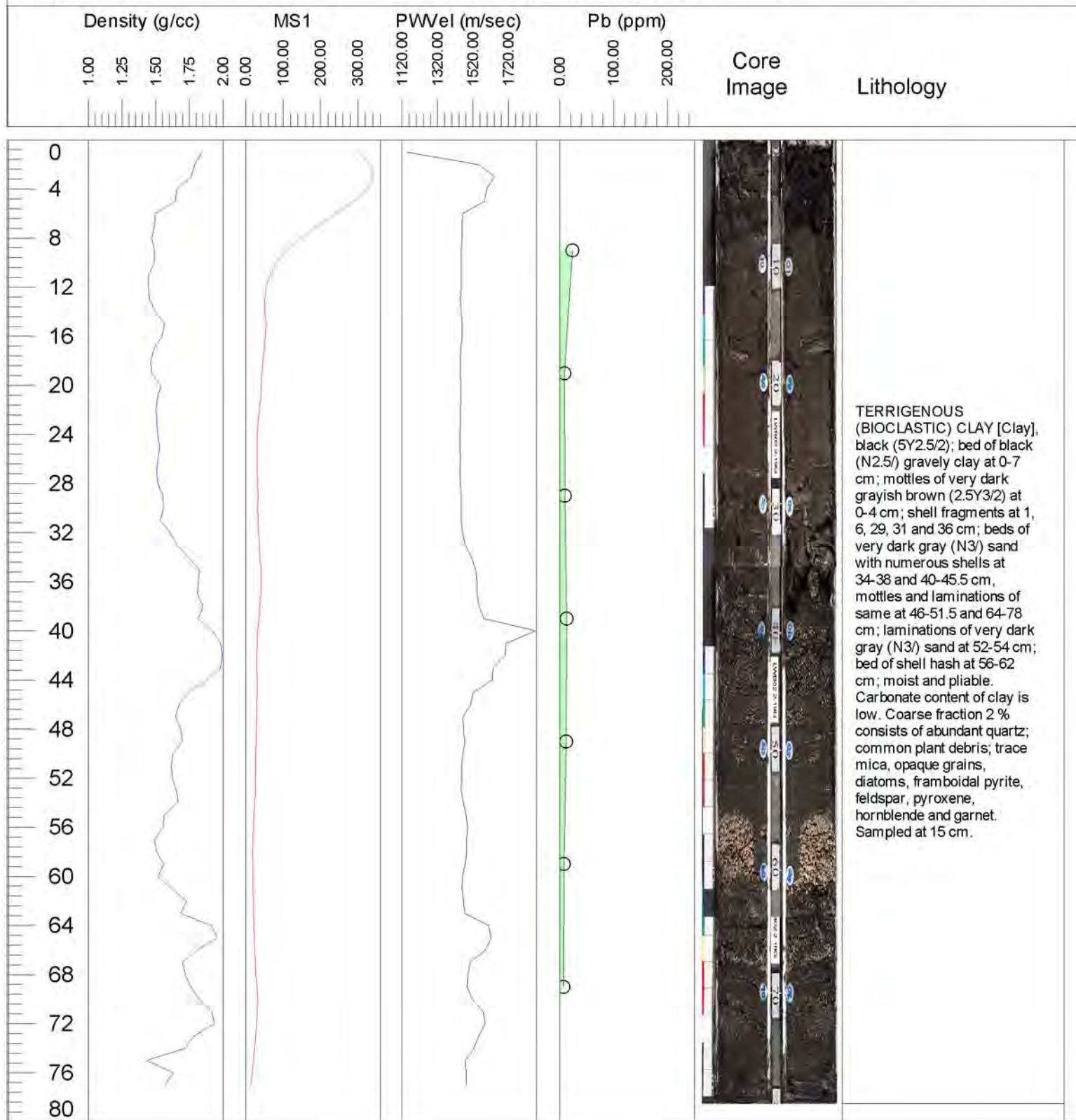
## Lamont-Doherty Earth Observatory

**LWB2-19**

Project Title: Assessment of the deposition of sediments impacted by Twentieth Century activities in the vicinity of the Tappan Zee Bridge

Project No.: EARTHT D213123

Principle Investigators: Timothy C. Kenna and Frank Nitsche



Core ID: LWB2-19

Latitude: 41° 4.126' N

Date Opened: 02/12/02

Core Length: 78.5 cm

Longitude: 73° 52.844' W

Date Photographed: 02/12/02

Collection Date: 09/05/01

PDR Depth: 13.5 m

Date Described: 02/12/02

Described by: N. Anest

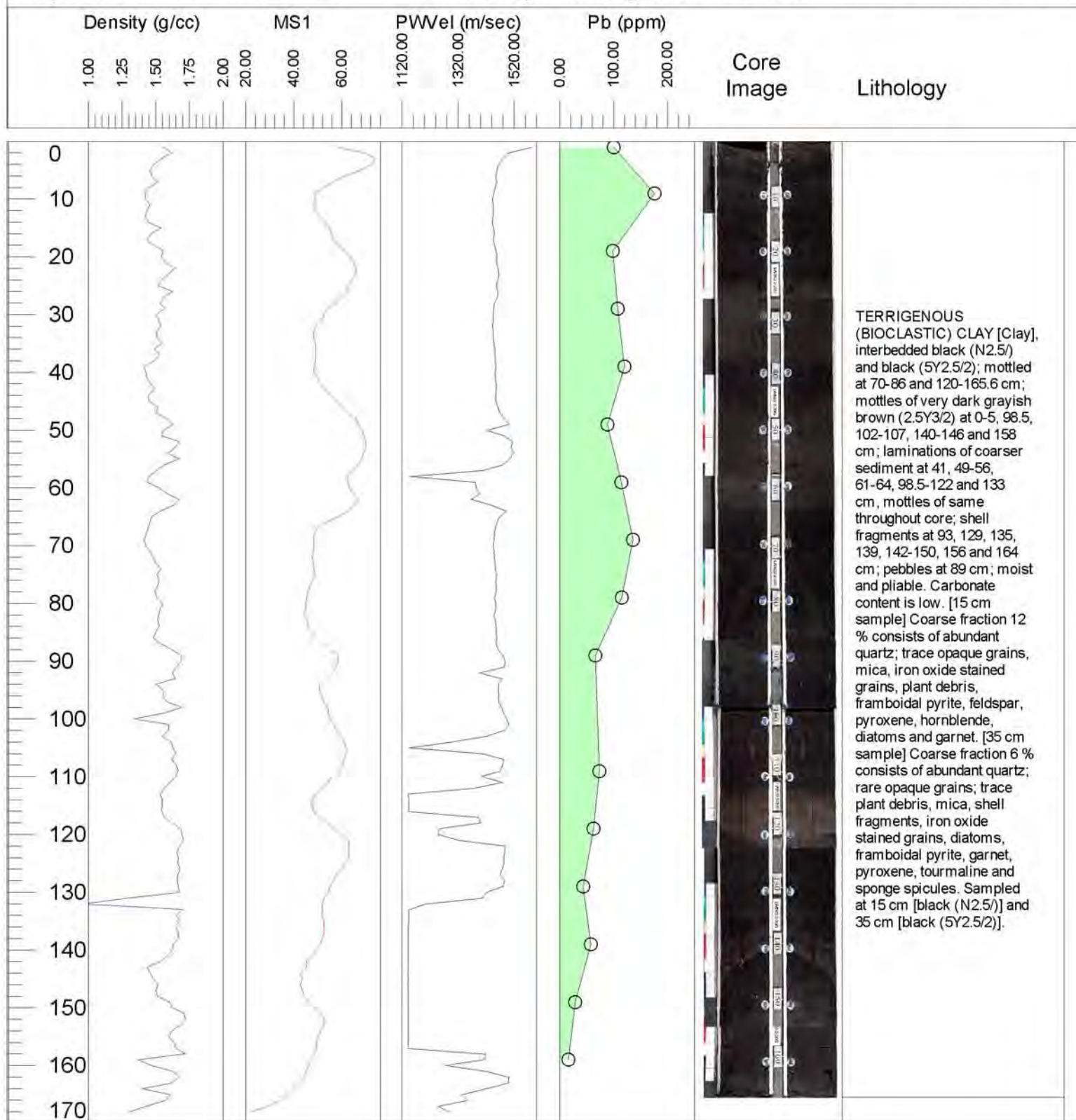
## Lamont-Doherty Earth Observatory

**LWB2-20**

Project Title: Assessment of the deposition of sediments impacted by Twentieth Century activities in the vicinity of the Tappan Zee Bridge

Project No.: EARTHT D213123

Principle Investigators: Timothy C. Kenna and Frank Nitsche



Core ID: LWB2-20

Latitude: 41° 4.124' N

Date Opened: 02/12/02

Core Length: 165.6 cm

Longitude: 73° 52.444' W

Date Photographed: 02/12/02

Collection Date: 09/05/01

PDR Depth: 2.4 m

Date Described: 02/12/02

Described by: N. Anest



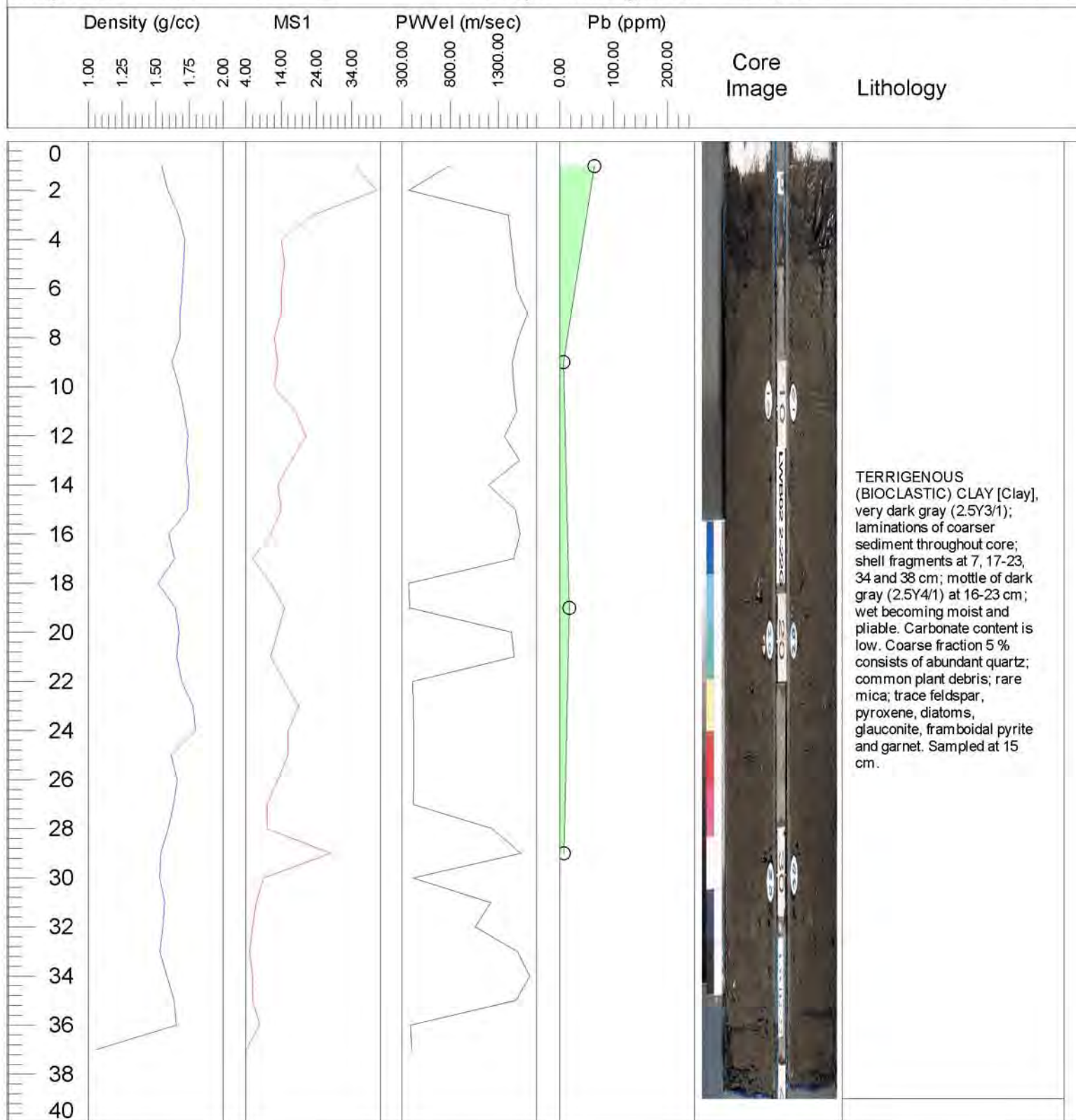
## Lamont-Doherty Earth Observatory

**LWB2-22**

Project Title: Assessment of the deposition of sediments impacted by Twentieth Century activities in the vicinity of the Tappan Zee Bridge

Project No.: EARTH D213123

Principle Investigators: Timothy C. Kenna and Frank Nitsche



Core ID: LWB2-22

Latitude: 41° 4.131' N

Date Opened: 10/23/01

Core Length: 39 cm

Longitude: 73° 53.755' W

Date Photographed: 10/23/01

Collection Date: 9/8/01

PDR Depth: 3.0 m

Date Described: 12/26/01

Described by: N. Anest



UNIVERSITY OF NEVADA, LAS VEGAS

June 9, 2012

**TO:** AECOM**FROM:** D. Hayes, Chair, Civil & Environmental Engineering and Construction**Re:** Tappan Zee Bridge SedFlume Testing and Results

*Authors Note: This memo describes the results of a funded project completed at the University of Louisiana at Lafayette in 2009 and 2010. I have since moved to the University of Nevada, Las Vegas.*

### Sediment Characteristics

Four 5-gallon composite samples of fine-grained depositional sediment were collected from surface samples at multiple locations in two general areas along the Tappan Zee bridge construction site. These samples were sealed and shipped to the University of Louisiana at Lafayette in Spring 2009. Individual samples were collected from each container and their physical properties determined. The results are summarized in Table 1.

Table 1. Physical properties of Hudson River sediment samples.

Sample	Water Content (%)	Specific Gravity	Organic Content (%)	Atterberg Limits		Sieve Analysis		
				Plastic Limit	Liquid Limit	D <sub>10</sub> (mm)	D <sub>50</sub> (mm)	D <sub>90</sub> (mm)
SF01 A	65.2	2.75	0.53%	30.2		0.11	0.17	0.25
SF01 B	61.0	2.50	3.10%	25.6		0.11	0.14	0.23
SF02 A/B	65.8	2.70	2.30%	29.3		0.11	0.14	0.25
SF02 B/C	65.1	2.70	2.29%	27.5		0.11	0.14	0.26

### SedFlume Sample Preparation

Much of the written discussion on SedFlume testing describes erosion testing of core samples taken directly from the field. In these cases, the erosion rate of in situ sediment deposits is evaluated with depth. As sediment properties and densities change, erodibility changes as well. This type of testing provides valuable information about likely scour depths for different events.

Since core samples were not available for this effort, the composite sediment samples from each general area were combined into single samples and homogenized. Sample SF01 was composed of



equal volumes from SF01A and SF01B. Sample SF02 was composed of equal volumes from SF02 A/B and SF02 B/C. The water content of composite samples SF01 and SF02 were 65.4% and 60.5%, respectively. Reconstituted core samples were constructed such that the sediment characteristics and water contents were consistent throughout the core depth. Since sediments in the wide, shallow areas of the Hudson River in the vicinity of the TZB tend to be quite homogeneous with depth, the vertical variations in erodibility should be less significant.

### SedFlume Testing

The SedFlume is a straight rectangular flume made from plexiglass sheets with an internal cross section of 50.8 mm in height by 106.7 mm in width; it is 244 cm in length. Water is pumped from a 140 gallon storage tank, through a two inch diameter pipe into the SedFlume. Flow is regulated by a three way valve, allowing a portion of the water to flow through the flume and the excess to return to the tank. A gradually widening inlet section straightens flow and assures uniform, turbulent flow as the water enters the SedFlume channel. The channel has a rectangular opening in its bottom located 120 cm from the entrance through which a sediment core can be inserted for testing. An outlet section and two-inch pipe carry the flow back to the tank for recirculation. The sediment core is housed in a rectangular tube with a 9.0 cm by 14.2 cm horizontal cross section and is 50 cm in length attached beneath the SedFlume. Top and cross section views of the Sedflume and sediment core tube are shown in Figure 1.

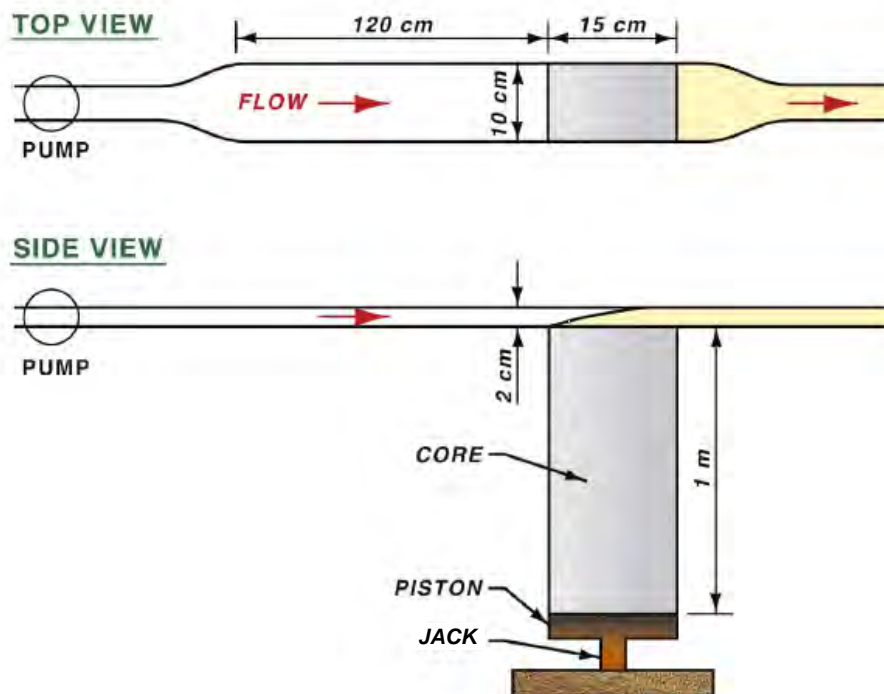


Figure 1. SedFlume schematic.

Reconstituted sediment samples from one location, either SF01 or SF02, were prepared and placed in the sediment core tube. Care was taken to ensure consistency between tests and vertically within each core sample. About 20 cm of sediment was used for each sample.

SedFlume tests were initiated with the sediment core well below the flume base until the desired flow was established. Flow meters were used to estimate flow rates, but the actual flow rate was measured based upon the time to fill a 35-gallon container. The flow for incipient erosion was determined by first establishing a flow rate less than required for erosion. Then, the piston was used to raise the sediment sample so the sediment surface was even with the bottom flow surface of the SedFlume. Flow was gradually increased until incipient erosion was noted and the flow rate measured.

Erosion rate tests were conducted by first establishing the desired flow in the SedFlume with the sediment surface below flow path. Once the proper flow was established, the sediment core was raised manually using the piston until the sediment surface was even with the bottom flow surface of the SedFlume. As flow eroded sediment from the core, it was raised to maintain the sediment surface even with the bottom flow surface. This continued until the water became too turbid to see the sediment level in the flume. Most of these tests lasted about 10 minutes in an attempt to overcome any errors that might result from either raising the sediment level too fast (resulting in increased erosion rate) or too slow (resulting in less erosion). The sediment erosion rate was recorded as the average erosion over the testing period; e.g. 10 cm of erosion over a 10 minute test would yield an erosion rate of 10 cm/minute.

A few SedFlume tests were also conducted on sediment from SF01 and SF02 at two increased water contents.

### Shear Stress Calculations

The primary purpose of the SedFlume tests is to understand the relationship between velocity and sediment erosion. Shear stress is the primary cause of erosion; thus, it is useful to estimate the shear stress experienced by the sediment during the SedFlume testing. This shear stress can be estimated as (Gailani 2001):

$$\tau = f \left( \frac{\rho_w U^2}{8} \right)$$

where  $\tau$  = wall shear stress (N/m<sup>2</sup>),  $f$  = friction factor (dimensionless),  $\rho_w$  = density of water (kg/m<sup>3</sup>), and  $U$  = average velocity (m/sec). The friction factor can be computed using the Colebrook-White formula (Walski 2003):

$$\frac{1}{\sqrt{f}} = -0.86 \ln \left[ \frac{\varepsilon}{3.7D} + \frac{2.51}{R_e \sqrt{f}} \right]$$

where  $\varepsilon$  = roughness of SedFlume surface (m),  $D$  = hydraulic diameter (m), and  $R_e$  = Reynolds number. The SedFlume is acrylic, but its surface is similar to that of PVC pipe; Walski (2003)

suggests that a reasonable value for roughness,  $\varepsilon$ , in a PVC pipe is  $1.5 \times 10^{-6}$  m. Reynolds number can be computed as:

$$R_e = \frac{UD}{\nu}$$

where  $\nu$  = kinematic viscosity ( $\text{m}^2/\text{sec}$ ). The kinematic viscosity of water at  $20^\circ\text{C}$  is  $1.004 \times 10^{-6}$   $\text{m}^2/\text{sec}$  and is reasonably representative of the conditions during the testing. The hydraulic diameter of the SedFlume's rectangular cross section is defined as:

$$D = \frac{2hw}{h + w}$$

where  $w$  = flow width(m),  $h$  = wall height(m). Internal dimensions of 50.8 mm in height by 106.7 mm in width yields a hydraulic diameter of 68.8 mm. Average velocities greater than 0.06 m/sec are adequate to produce turbulent flow ( $R_e > 4000$ ).

## SEDFLUME Results

SEDFLUME tests were conducted in the UL Hydraulics Laboratory during July and August 2009 on the two composite reconstituted Hudson River sediment samples, SF01 and SF02. Using sediment samples allowed each sample to be tested over a range of flow rates and tests to be repeated as necessary. The SedFlume results are summarized in Tables 2 and 3.

**Table 2. SedFlume results for Hudson River sediment sample SF 01**

Measured Flow Rate (GPM)	Measured Erosion Rate (cm/min)	Flow Rate ( $\text{ft}^3/\text{sec}$ )	Flow Rate (L/sec)	Velocity (ft/sec)	Velocity (m/sec)	Friction Factor (unitless)	Shear Stress (Pa)
Water content = 65.4%							
57.4	0.00	0.128	3.62	2.19	0.669	0.0218	1.21
58.2	0.19	0.130	3.68	2.22	0.678	0.0217	1.24
59.1	0.33	0.132	3.73	2.26	0.689	0.0216	1.28
60.8	0.53	0.136	3.84	2.32	0.708	0.0215	1.34
62.9	1.07	0.140	3.97	2.40	0.733	0.0213	1.43
65.2	1.62	0.145	4.18	2.49	0.760	0.0212	1.52
67.4	4.10	0.150	4.26	2.57	0.785	0.0210	1.62
Water content = 67.1%							
62.9	2.47	0.140	3.97	2.40	0.733	0.0213	1.43
Water content = 71.0%							
62.9	3.50	0.140	3.97	2.40	0.733	0.0213	1.43

**Table 3. SedFlume results for Hudson River sediment sample SF 02**

Measured Flow Rate (GPM)	Measured Erosion Rate (cm/min)	Flow Rate (ft <sup>3</sup> /sec)	Flow Rate (L/sec)	Velocity (ft/sec)	Velocity (m/sec)	Friction Factor (unitless)	Shear Stress (Pa)
Water content = 60.5%							
55.3	0.00	0.123	3.49	2.11	0.644	0.0219	1.14
57.5	0.10	0.128	3.63	2.20	0.670	0.0217	1.22
59.3	0.16	0.132	3.74	2.27	0.691	0.0216	1.29
62.0	0.46	0.138	3.92	2.37	0.722	0.0214	1.39
65.5	0.56	0.146	4.14	2.50	0.763	0.0211	1.54
67.8	0.68	0.151	4.28	2.59	0.790	0.0210	1.63
69.1	0.82	0.154	4.36	2.64	0.805	0.0209	1.69
70.8	1.08	0.158	4.47	2.70	0.825	0.0208	1.76
72.7	1.28	0.162	4.59	2.78	0.847	0.0207	1.85
73.2	1.73	0.163	4.62	2.80	0.853	0.0206	1.87
75.9	3.12	0.169	4.79	2.90	0.884	0.0205	2.00
77.7	4.07	0.173	4.91	2.97	0.905	0.0204	2.08
Water content = 63.0%							
70.8	2.14	0.1578	4.471	2.70	0.825	0.0208	1.76
Water content = 65.3%							
70.8	3.40	0.1578	4.471	2.70	0.825	0.0208	1.76

### Analysis of SedFlume Results

*Critical Velocity and Critical Shear Stress.* SedFlume results allow direct observation of the critical velocities and critical shear stresses required to induce incipient erosion in the two samples tested. Those are:

	<u>Sample SF01</u>	<u>Sample SF02</u>
Critical Velocity, $V^*$ (m/s)	0.669	0.644
Critical Shear Stress, $\tau^*$ (Pa)	1.21	1.14

Given the accuracy of the testing approach and potential variability in sediment characteristics, it seems wise to take the critical velocity of the sediments to be 0.64 m/s and the critical shear stress to be 1.1 Pa.

*Erosion Rate versus Shear Stress.* Most previous analyses of SedFlume results used linear regression to fit the data to a curve of the form:

$$E = a\tau^n$$

where  $E$  = erosion rate (cm/min);  $a$  and  $n$  are regression coefficients. Figure 2 shows the regression results for the data in Tables 2 and 3.

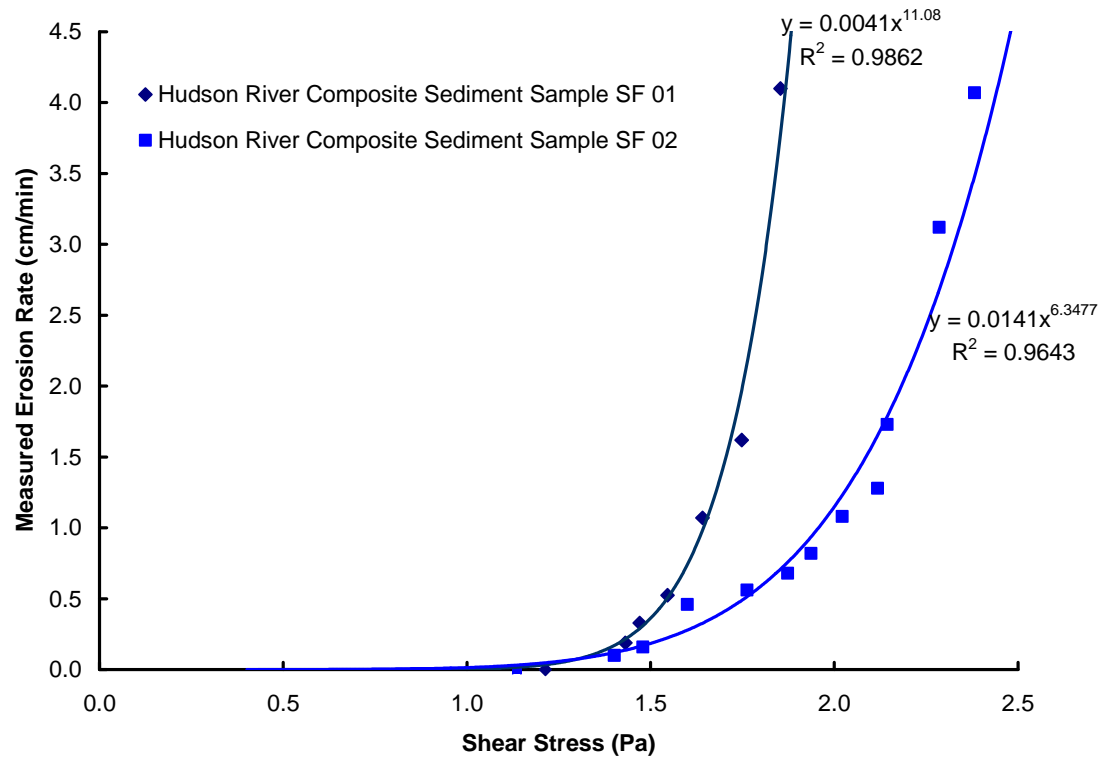


Figure 2. Measured erosion rate versus shear stress from SedFlume testing on two Hudson River sediments.

The regression results in Figure 2 show strong correlation coefficients. The resulting equations also fit the data well. However, the large exponents in the resulting equations require caution not to apply them outside of the range of available data. Care should especially be taken not to use the equations for shear stresses less than the critical shear stress since the equations will errantly give a small amount of erosion at any shear stress.

Gailani (2001) indicated that it is also possible to fit data for moderate shear stresses ( $< 1.5$  Pa) to the equation:

$$E = a \left( \frac{\tau - \tau^*}{\tau^*} \right)^n$$

Figure 3 shows the data that fit the criteria and the resulting regression results.

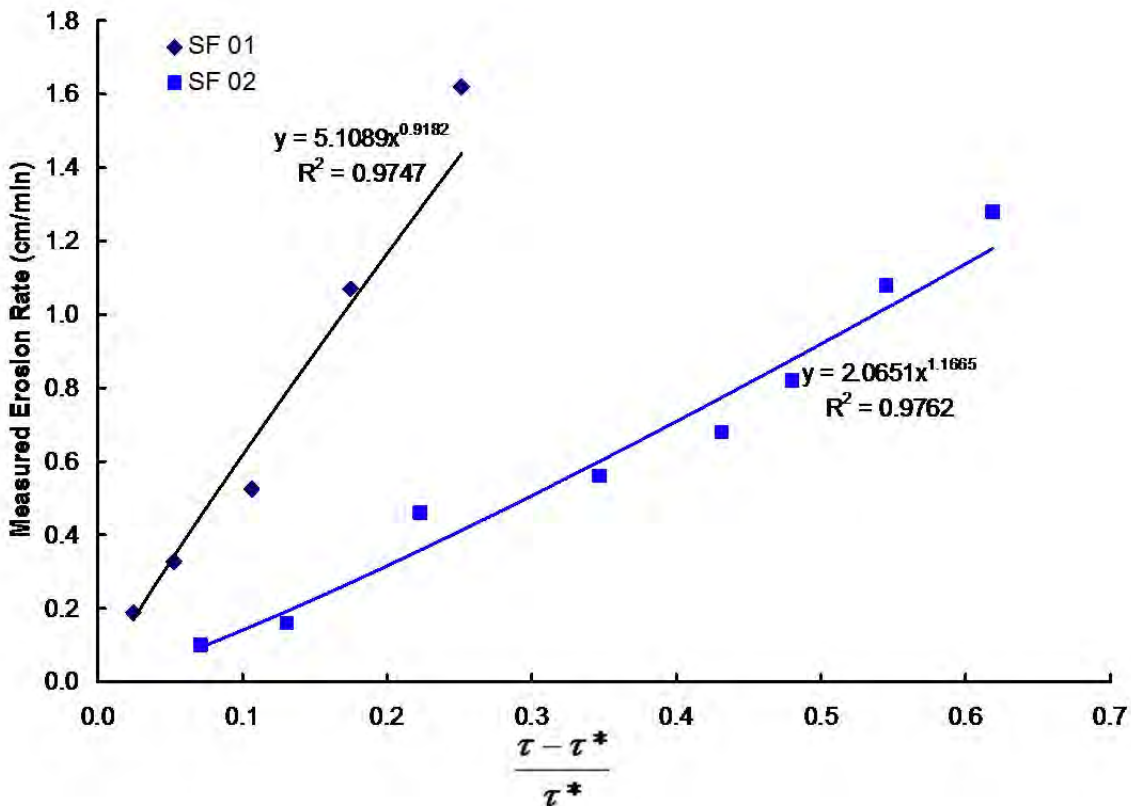


Figure 3. Erosion rate versus relative shear stress.

## References

Borrowman, T.D.; Smith, E.R.; Gailani, J.Z., and Caviness, L. 2006. "Erodibility Study Of Passaic River Sediments Using USACE Sedflume," US Army Engineer Research and Development Center, Vicksburg, MS, June 2006.

Gailani, J. Z., Kiehl, A., McNeil, J., Jin, L. and Lick, W. (2001). "Erosion rates and bulk properties of dredged sediments from Mobile, Alabama," *DOER Technical Notes Collection* (ERDC TN-DOER-N10), U.S. Army Engineer Research and Development Center, Vicksburg, MS. [www.wes.army.mil/el/dots/doer](http://www.wes.army.mil/el/dots/doer)



UNIVERSITY OF NEVADA, LAS VEGAS

June 18, 2012

**TO:** AECOM

**FROM:** D. Hayes, Chair, Civil & Environmental Engineering and Construction

**Re:** Estimating water quality impacts from construction vessel traffic

---

*Authors Note: This memo describes the results of a funded project completed at the University of Louisiana at Lafayette in 2009 and 2010. I have since moved to the University of Nevada, Las Vegas.*

Previous bridge construction projects have noted construction vessel traffic as a significantly contributor to water quality impacts. This is a concern since a new Tappan Zee Bridge (TZB) will involve extensive on-water construction activity. Personnel, equipment, and materials will be moved using barges and tugs from shoreline docks and the navigation channel side to construction locations along the bridge alignment.

The Hudson River bathymetry in the anticipated construction area is relatively shallow outside of the navigation channel, gradually rising from about 12 to 14 ft near the banks of the navigation channel to 2 to 3 feet at the shoreline, with most of the area west of the channel being 10 to 12 ft deep. The bottom sediments are primarily soft silts. SedFlume testing of these sediments showed they begin to erode at shear stress of 1.14 Pa which occurred at a velocity of 0.64 m/s.

This memo utilizes the SedFlume results and models of propeller-induced shear stress to assess the potential for sediment scour and resulting water quality impacts. Additional information on the shear stress-erosion rate relationship can be found a companion memo that describes the SedFlume testing and results.

### **Prop-wash Models**

*Bottom Shear Stress.* Maynord (2000) indicated that the bed shear stress should be calculated as:

$$\tau = 0.5 \rho_w C_{fs} V_{prop}^2$$

where

$\tau$  = bed shear stress (Pa)

$\rho_w$  = density of water (kg/m<sup>3</sup>)

$C_{fs}$  = bottom friction factor for propeller wash (dimensionless)

$V_{prop}$  = bottom velocity due to propeller wash, as calculated previously.



Shear stress and bottom friction factor should consider both propeller velocity and vessel wake velocity. However, tugs and barges associated with the construction project should be maneuvering at low speeds resulting in minimal wake effects. Ignoring wake effects, the bottom friction factor for propeller wash can be computed as (Maynard 2000):

$$C_{fs} = 0.01 \left( \frac{D_p}{H_p} \right)$$

where,

$D_p$  = propeller diameter (m)

$H_p$  = distance from propeller centerline to the sediment surface (m)

*Propeller-induced Velocities at Sediment Surface.* While other models of propeller-induced velocities exist, those presented in Maynard (2000) seem most applicable to the TZB project. Many tugs have two engines and propellers, located equidistant on either side of the tug centerline. The velocity fields immediately behind the propellers act independently, but eventually join to create a single flow field.

Maynard designated the region nearest the propeller where each engine creates its own velocity field as Zone 1. The empirical equation for spatial velocity distribution in Zone 1 is provided in Figure 1. Maynard indicated that this equation is applicable from just beyond the propeller to a distance of about ten propeller diameters ( $X_p \leq 10 D_p$ ). The model develops the 2D flow field for both propellers and the total power of both engines should be used in the model application.

Somewhere beyond Zone 1, the independent velocity fields of the two propellers begin to merge. Maynard (2000) presents the model shown in Figure 2 for this region, denoting it as Zone 2. Maynard notes that the models are the weakest in the vicinity of the transition which occurs at about  $X_p = 10 D_p$ . Again, the total power of both engines should be used in the model application.

### Model Application

The models were applied using the basic physical characteristics of Weeks Marine's tug Elizabeth and SedFlume data on composite sediment samples collected from the Hudson River in the vicinity of the TZB construction. The Elizabeth is one of the tugs provided by ARUP as an example of what might be used during the TZB project. Although smaller tugs may end up being used in the actual vicinity of the construction, the Elizabeth will serve to illustrate the model application.

Figure 3 shows maximum propeller-induced velocities along the sediment surface at a range of applied powers and distance between the propeller centerline and sediment surface ( $H_p$ ). The resulting curves show that the maximum induced velocity along the sediment surface in Zone 1 varies little with  $H_p$ , but reduce significantly as the applied power reduces.

$$z^1 V(X_p, Y_{cl}) = 1.45 V_2 \left( \frac{X_p}{D_p} \right)^{-0.524} \left( \exp \left( -15.4 \frac{R_1^2}{X_p^2} \right) + \exp \left( -15.4 \frac{R_2^2}{X_p^2} \right) \right)$$

where

$$V_2 = \frac{1.13}{D_0} \sqrt{\frac{T}{\rho_w}}$$

$$R_1^2 = (Y_{cl} - 0.5W_p)^2 + (H_p - C_j)^2$$

$$R_2^2 = (Y_{cl} + 0.5W_p)^2 + (H_p - C_j)^2$$

$$C_j = - \left[ 0.213 - 1.05 \left( \frac{C_p g}{V_2^2} \right) (X_p - 0.5L_{set}) \right] (X_p - 0.5L_{set})$$

### Kort Nozzle Propeller

$$C_p = 0.04$$

$$D_0 = D_p$$

$$EP = 31.82 P_{hp}^{0.974} - 5.4 V_w^2 P_{hp}^{0.5}$$

### Open Nozzle Propeller

$$C_p = 0.12 \left( \frac{D_p}{H_p} \right)^{0.67}$$

$$D_0 = 0.71 D_p$$

$$EP = 23.57 P_{hp}^{0.974} - 2.3 V_w^2 P_{hp}^{0.5}$$

$X_p$  = Distance behind the propeller (m)

$D_p$  = Propeller diameter (m)

$W_p$  = Distance between propellers (m)

$L_{set}$  = Distance from ship stern to propeller (m)

$H_p$  = Distance from center of propeller axis to channel bottom (m)

$Y_{cl}$  = Lateral distance from ship centerline (m)

$C_j$  = vertical distance from propeller shaft to location of maximum velocity within the jet (m)

$g$  = acceleration of gravity ( $m/s^2$ )

$T$  = Thrust (N)

$\rho_w$  = Density of water ( $kg/m^3$ )

$EP$  = Effective Push (equivalent to thrust) from both propellers (N)

$P_{hp}$  = Total ship power (hp)

$V_w$  = Ship speed relative to water, 0 for stationary vessels (m/s)

Figure 1. Maynard (2000) model for propeller-induced flow at the sediment surface within Zone 1 ( $\leq 10 D_p$ ) of the propeller.

$${}^{z1}V(X_p, Y_d) = 0.34V_2 \left( \frac{D_p}{H_p} \right)^{0.93} \left( \frac{X_p}{D_p} \right)^{0.24} C_1 \exp \left[ -0.0178 \frac{X_p}{D_p} - \frac{Y_d^2}{2C_{z2}^2 X_p^2} \right]$$

Where:

$C_1 = 0.66$  for open-wheeled propeller;  $0.85$  for Kort nozzle propeller

$C_{z2} = 0.84 (X_p/D_p)^{-0.62}$

Figure 2. Maynard (2000) model for propeller-induced flow at the sediment surface within Zone 2 ( $\geq 10 D_p$ ) of the propeller.

**Table 1. Properties of assumed tug operations, taken primarily from Weeks Marine's tug Elizabeth**

Description	Notation	Value	Comment
<u>Available specifications</u>			
Tugboat Length	$L_{tb}$ (m)	23.50	
Engines		2	
Engine Power (per engine)	HP (horsepower)	900	
Diameter of Propellers	$D_p$ (m)	1.83	
Propeller Type	Open/Kort	Kort	
Tug Draft Depth	$H_d$ (m)	3.23	
Boat Width/Beam	$W_b$ (m)	7.93	
<u>Assumed or calculated specifications</u>			
Propeller Axis Depth	$Z_p$ (m)	4.15	Estimated as $H_d + 0.5D_p$
Distance Between Propellers	$W_p$ (m)	2.64	Estimated as $W_b/3$
Distance From Stern to Propeller	$L_{set}$ (m)	2.35	Assumed
Boat Speed	$V_w$ (m/s)	1.00	Assumed

Zone 2 velocities vary less with distance and power. However, they also show a significant variation with variations in  $H_p$ . This variation seems to be in contradiction to the Zone 1 model.

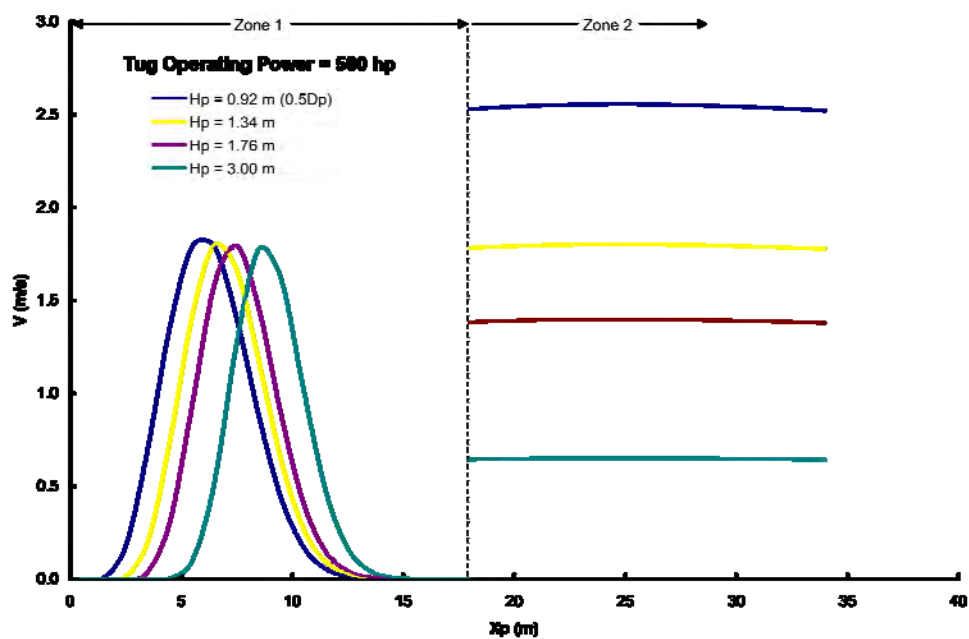


Figure 3. Maximum propeller-induced velocities along the sediment surface as they vary with applied power and height of the propeller shaft above the sediment ( $H_d$ ).

### Model Application

Erosion begins when sediment experiences the critical shear stress,  $\tau_c$ , at the surface due to water movement at the interface. Keeping the shear stress associated with the peak velocity (see Figure 3) less than the critical shear stress will ensure that erosion does not occur. Thus, the application of the models described above should focus on determining minimum water depth and maximum applied power necessary to maintain peak velocities below that associated with the critical shear stress. This section describes the approach to generate a simple graphical representation of this relationship.

The downstream location of the peak velocity,  $X_p^*$ , can be determined by solving for  $X_p$  at

$$\frac{\partial V}{\partial X_p} = 0$$

The resulting equations are shown in Figure 4. Although cumbersome, these equations they are readily solvable with EXCEL or other computational software for known values of  $T$  and  $H_b$ .

$$\frac{\partial V_1}{\partial X_p} = -0.524AX_p^{-1.524} \left( e^{\frac{-15.4R_1^2}{X_p^2}} + e^{\frac{-15.4R_2^2}{X_p^2}} \right) +$$

$$\left( AX_p^{-0.524} \right) \left( \frac{-15.4 \left( \frac{\partial R_1^2}{\partial X_p} X_p - 2R_1^2 \right)}{X_p^3} e^{\frac{-15.4R_1^2}{X_p^2}} + \frac{-15.4 \left( \frac{\partial R_2^2}{\partial X_p} X_p - 2R_2^2 \right)}{X_p^3} e^{\frac{-15.4R_2^2}{X_p^2}} \right)$$

where

$$A = 1.45V_2D_p^{0.524}$$

$$\frac{\partial R_i^2}{\partial X_p} = -2(H_p - C_i) \left[ \frac{8.1\rho_w D_o^2 C_p}{T} (X_p - 0.5L_{set}) - \left( 0.213 - \frac{8.1\rho_w D_o^2 C_p}{T} (X_p - 0.5L_{set}) \right) \right]$$

$$\frac{\partial C_i}{\partial X_p} = \left( \frac{8.1\rho_w D_o^2 C_p}{T} \right) (X_p - 0.5L_{set}) - \left( 0.213 - 8.1 \frac{\rho_w D_o^2 C_p}{T} (X_p - 0.5L_{set}) \right)$$

Figure 4. First derivative of the velocity equation with respect to  $X_p$  used to compute  $X_p^*$ .



In this case, we are interested in the velocity that will generate the critical shear at the sediment surface. The equation presented previously can be rearranged to yield the critical velocity:

$$V_c = \sqrt{\frac{\tau_c}{0.5\rho_w C_{fs}}}$$

For this velocity, unique combinations of applied power and  $H_p$  that satisfy the equations for  $V$  (provided in Figure 1) and  $\partial V/\partial X_p = 0$  represent operational conditions that produce the critical shear stress. Thus, any values above this function represent scour conditions while values beneath the function represent acceptable operational conditions. Figure 5 shows the results of this analysis in the form of minimum water depth versus applied horsepower necessary.

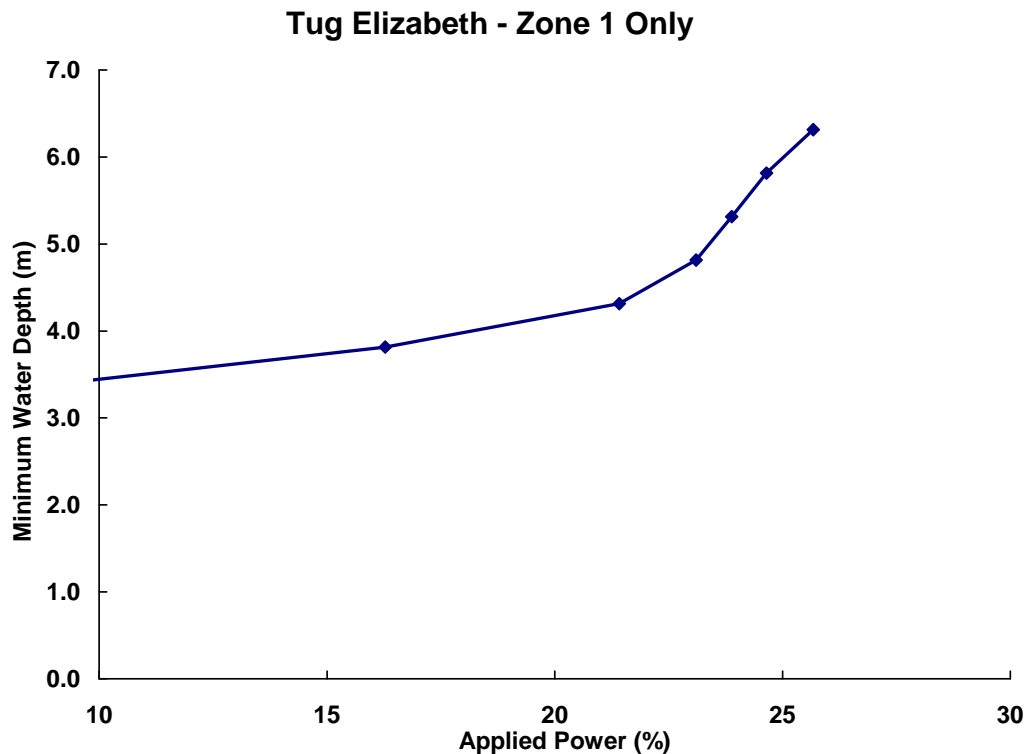


Figure 5. Minimum water depth versus horsepower to avoid sediment erosion.

### Site Characteristics

The models were applied to a simplified, hypothetical site to facilitate comparisons between vessels. The site was assumed to consist of a perfectly flat bathymetry extending infinitely in all directions. Water depths from 2 to 10 m were used to evaluate the effect of water depth on scour. The bottom sediment was assumed to be infinitely thick soft silty clay with an in situ water content of 62.5%, specific gravity of 2.75, and 0.53% organic content.

SEDFLUME tests were conducted on two sediments and relationships between shear stress and erosion rate developed based upon the results. For these computations, the relationships for the most erodible sediment (SF 01) were selected:

$$\varepsilon = 0 \quad \text{for } \tau < 1.21 \text{ Pa} \quad (25)$$

$$\varepsilon = 5.1089 \left( \frac{\tau}{1.21} - 1 \right)^{0.9182} \quad \text{for } 1.52 \text{ Pa} \geq \tau \geq 1.21 \text{ Pa} \quad (26)$$

The rate at which erosion rates could be accurately measured in the SEDFLUME was exceeded at about 1.52 Pa. Since the prop-wash models may generate shear stresses in excess of 1.52 Pa, it was necessary to establish a relationship to extrapolate the results beyond the laboratory data. The power curve relationship above generates excessively large erosion rates at small increases in shear stress. The resulting extrapolation was thought to likely overestimate resuspension flux. Thus, the following linear relationship was used to extrapolate the results for shear stresses greater than 1.52 Pa:

$$\varepsilon = 1.46 + 24.8(\tau - 1.52) \quad \text{for } \tau \geq 1.52 \text{ Pa} \quad (27)$$

This relationship was chosen because it should not produce excessive erosion rates, i.e. the resulting resuspension flux should not be overstated. This approach has not been proven to be accurate and this work should not be taken as proving its viability.

### Vessel Selection and Operation

Dredging and other marine construction operations use a wide range of vessels. A range of representative vessels was selected for comparison. Table 2 provides the physical characteristics of those vessels.

**Table 2. Representative vessels used in dredging and other marine construction activities. Note that all vessels have dual engines and propellers.**

Vessel	Length (m)	Beam (m)	Draft (m)	Depth to Center of Prop Shaft (m)	Width Between Props (m)	Distance from Prop to Stern (m)	Total HP (both engines)	Prop Dia. (m)
1800 HP Tug	22.1	7.4	3.2	2.3	3.0	1.5	1800	1.8
600 HP Pushboat	7.7	4.2	1.5	1.05	1.3	0.7	600	0.9
180 HP Pushboat	7.6	3.1	0.6	0.6 <sup>a</sup>	1.0	0.7	180	0.4

<sup>a</sup>Depth to Center of Prop. Shaft is approximate because jack-plates can adjust prop depth.

**Computational Details**

A uniform computational grid was used with 0.152 m cells in both the X and Y direction. Each vessel was allowed to move forward until a steady-state resuspension flux rate was achieved. The forward speed was varied from 1 to 10 knots while applied horsepower was varied from 0 to the maximum horsepower. Computations were made at 0.1 second time steps to minimize error when the computations produced excessive scour rates. Steady-state was reached within the first few minutes of movement in most cases.

**RESULTS**

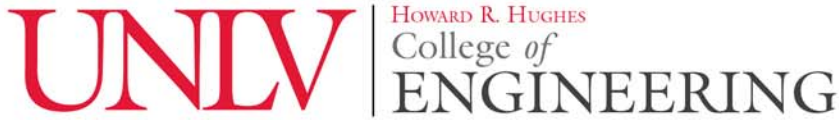
Table 3 summarizes approximate dimensions of the areas scoured and the steady-state suspended sediment fluxes computed for the vessels described in Table 2 and the hypothetical site conditions used. Most importantly, these results are based upon highly erodible sediment conditions of unlimited depth. The results follow expected patterns, suggesting that they are comparable, i.e. the trends shown are likely accurate even if the computed flux values vary.

The results show that an 1800 HP tug operating at 25% power and moving forward at 1 knot over a range of depths could potentially resuspend almost 14,000 kg/sec at 4.0 m water depth to 8,300 kg/sec at 10.0 m water depth. A 600 HP pushboat operating similarly (25% power) could potentially resuspend 4,300 kg/sec at 2.0 m water depth, but that drops to 10 kg/sec at 10.0 m. Finally, a small pushboat (180 HP) could potentially resuspend 1000 kg/sec to 5000 kg/sec at 2.0 m water depth depending upon the power applied. However, the resuspension rates are much less at a depth of 4.0 m, requiring 75% power to achieve 70 kg/sec.

**Table 3. Predicted steady-state sediment resuspension flux from a range of vessels and operating conditions. All vessels are moving forward at 1 knot.**

Applied Horsepower	Water Depth (m)	Prop Clearance (m)	Suspended Sediment Flux (kg/sec)	Scour Length (m)	Scour Width (m)
<b><u>1800 HP Tug</u></b>					
450	4.0	1.7	13893	25.9	5.9
450	6.0	3.7	12464	20.1	6.9
450	8.0	5.7	10360	17.7	7.2
450	10.0	7.7	8279	15.2	7.5
<b><u>600 HP Pushboat</u></b>					
150	2.0	1.3	4294	21.6	4.1
150	4.0	3.3	3557	15.4	5.3
300	4.0	3.3	7989	30.2	8.7
150	6.0	5.3	1944	11.1	5.6
300	6.0	5.3	5302	24.1	9.6
150	8.0	7.3	536	6.5	5.0
300	8.0	7.3	2619	17.7	9.0
150	10.0	9.3	10	2.1	2.3
300	10.0	9.3	556	10.7	7.2
<b><u>180 HP Pushboat</u></b>					
45	2.0	1.4	998	16.3	5.6
90	2.0	1.4	2345	31.1	10.2
135	2.0	1.4	3505	43.6	12.4
180	2.0	1.4	5119	56.7	18.4
90	4.0	3.4	0	0.0	0.0
135	4.0	3.4	71	13.3	5.0
180	4.0	3.4	220	21.8	8.1





UNIVERSITY OF NEVADA, LAS VEGAS

June 9, 2012

**TO:** AECOM

**FROM:** D. Hayes, Chair, Civil & Environmental Engineering and Construction

**Re:** Overview of Tappan Zee Bridge Sediment Resuspension Rate Findings

---

*Authors Note: This memo describes the results of a funded project completed at the University of Louisiana at Lafayette in 2009 and 2010. I have since moved to the University of Nevada, Las Vegas.*

This memo provides preliminary estimates of water quality impacts associated with reconstruction of the Tappan Zee Bridge for use in the Environmental Impact Statement (EIS) Analyses. The primary water quality concerns result from suspending bottom sediments during dredging, driving piles, sheet pile installation, vessel movement, and cofferdam dewatering for pier construction. This document summarizes our best estimates of sediment suspension rates associated with these activities.

#### Bottom Sediment Characteristics

Hudson River bottom sediments in the vicinity of the Tappan Zee Bridge are mostly clayey silts. Soil tests showed an average water content of 64%, specific gravity of 2.66, and 2% organic content. SedFlume tests showed the sediments are highly erodible and most areas do not have a distinguishable bedrock layer near the sediment surface.

#### Resuspension Due to Dredging

Bridge construction and demolition will involve an array of vessels with drafts significantly greater than available water depth. Anticipated characteristics of the access channel are stated in *Replacement Bridge: Hudson River Construction* include:

- Construction access channel will be dredged to an elevation of -17.89 feet NAVD88.
- Demolition access channel will be dredged to an elevation of -14.89 feet NAVD88.
- Sediment volume to be dredged is approximately 1.77 million cubic yard
- Clamshell dredges will be used with environmental (closed) buckets.
- Each dredge will remove an average of 7,500 cubic yards/day.
- Two dredges will operate concurrently during portions of the operation to expedite construction yielding a typical daily sediment removal rate of 15,000 cubic yards.

Sediment resuspension during dredging has been a topic of substantial interest. Hayes and Wu (2001) summarized loss rates from environmental clamshell buckets. Based upon that data, loss rates for clamshell bucket dredges have been observed to range between 0.16% and 0.88%. The highest values are associated with open clamshell buckets with substantial overflow from adjacent barges. This suggests that the resuspension for this project should be on the lower side since environmental clamshell buckets will be used and barge overflow will not be allowed. However, SedFlume results of these sediments in the channel areas showed that they are more susceptible to resuspension than most. Synthesizing all of these factors, an estimate of 1% sediment resuspension loss is recommended to provide an adequate degree of conservatism in estimated impacts. Thus, the average sediment resuspension rate for each dredge is estimated as:

$$(g_d)_{avg} = (7,500 \text{ yd}^3/\text{day}) (1 \text{ m}^3/1.3 \text{ yd}^3)(980 \text{ kg/m}^3)(0.01)(1 \text{ d}/1440 \text{ min}) = 39 \text{ kg/min}$$

Short-term production rate estimate:

Assuming a 25 cy bucket @ 2 minute cycle = 12.5 cy/min

$$(g_d)_{max} = (12.5 \text{ cy/min}) (1 \text{ m}^3/1.3 \text{ yd}^3)(980 \text{ kg/m}^3)(0.01) = 94 \text{ kg/min}$$

### Vessel Movement

Bridge construction and demolition activities will require frequent tug operations and barge movements along the dredged channels throughout the construction period. Larger tugs than usual are being planned for because of potential safety concerns working upstream of the existing bridge. Weeks Marine recommended tugs similar to their 1,400 HP Virginia tug and the 1,800 HP Shelby tug for prop scour analyses. Scour modeling results for these vessels showed the potential for substantial sediment scour while operating over the soft bed sediments of the site. Thus, the channel design was modified to accommodate armoring of the channel bed and the side slopes. This armor will prevent bottom sediments scour during vessel operations. Thus, the only sediment available for scour will be freshly deposited from upstream currents.

Current sediment accumulation in the area is very limited, i.e. the streambed is near equilibrium depth. However, the dredged channel will act as a sediment trap increasing the deposition rate. Several water sampling efforts were undertaken in 2007 and 2008 in the construction area. Grab samples ranged in TSS from 13 mg/L to 111 mg/L with an average of 30 mg/L.

A trap efficiency of 5% is recommended based upon an analysis using the work of van Rijn (1986). Since the channel lays normal to the flow and resuspension is expected along the length of the channel, the source rate per unit length can be estimated as:

$$g_{scour} = \epsilon V_{avg} h_0 c_{avg} = 0.05(0.4 \text{ m/s})(2 \text{ m})(30 \text{ g/m}^3)(1 \text{ kg}/1000 \text{ g})(86400 \text{ s/d}) = 104 \text{ kg/m/d}$$

where  $g$  = sediment resuspension rate, kg/m/sec;  $\varepsilon$  = trap efficiency, dimensionless;  $V_{avg}$  = depth averaged velocity upstream of the channel, m/sec;  $h_0$  = upstream water depth, m; and  $c_{avg}$  = depth-averaged TSS concentration upstream of the channel.

Since the rate of scour is based upon daily sedimentation rate, it should be proportioned according to anticipated work day. For example, if vessel movement is anticipated only over a 12 hour work day, the hourly scour rate would be:

$$g_{scour} = 104 \text{ kg/m/d (1 d/12 hr)} = 8.7 \text{ kg/hr}$$

Similar proportions should be used for other workday schedules.

### Bridge Construction Activities

In-water specific bridge construction activities also have the potential to resuspend sediments and impair water quality. The primary construction activities of concern are sheet pile installation, dewatering of cofferdams during pier construction, and pile driving activities. An extensive literature search was undertaken to identify previous estimates for sediment resuspension rates associated with these activities or available data to develop estimates. No previous estimates were identified, but data from several bridge construction projects were found. The most comprehensive and applicable data set was from the San Francisco-Oakland Bay Bridge East Span Seismic Safety Project. Thousands of water quality measurements – mostly turbidity – were taken during various aspects of this project including dredging, sheet pile installation, cofferdam dewatering, and pile driving. These were reported in routine water quality monitoring reports<sup>1</sup>. Unfortunately, velocity data were not collected in conjunction with these measurements, so they cannot be immediately converted to resuspension rates.

After a number of approaches were considered, the best approach is thought to be a comparison of these activities to dredging. The average suspended sediment concentrations above ambient observed were:

Activity	Avg TSS, mg/L	Relative to Dredging
Dredging	5.1 mg/L	1.0
Sheet Pile Installation	1.3 mg/L	0.3
Pier Installation (pile driving and dewatering)	2.0 mg/L	0.4

Since these are based upon average values of numerous water quality observations, it is most appropriate to apply these values to the average daily dredged production rate. The resulting estimates are:

<sup>1</sup> San Francisco-Oakland Bay Bridge, 2002-2008 Water Quality Report, found online at ([http://biomitigation.org/reports/default.asp?page\\_size=10&page\\_no=2&sort\\_field=@publishdate&sort\\_order=descending&date=&subject=&location=&type=OTD Westbound Water Quality November 2008.pdf](http://biomitigation.org/reports/default.asp?page_size=10&page_no=2&sort_field=@publishdate&sort_order=descending&date=&subject=&location=&type=OTD Westbound Water Quality November 2008.pdf))

$$g_{sp} = 39 \text{ kg/min (0.3)} = 12 \text{ kg/min}$$

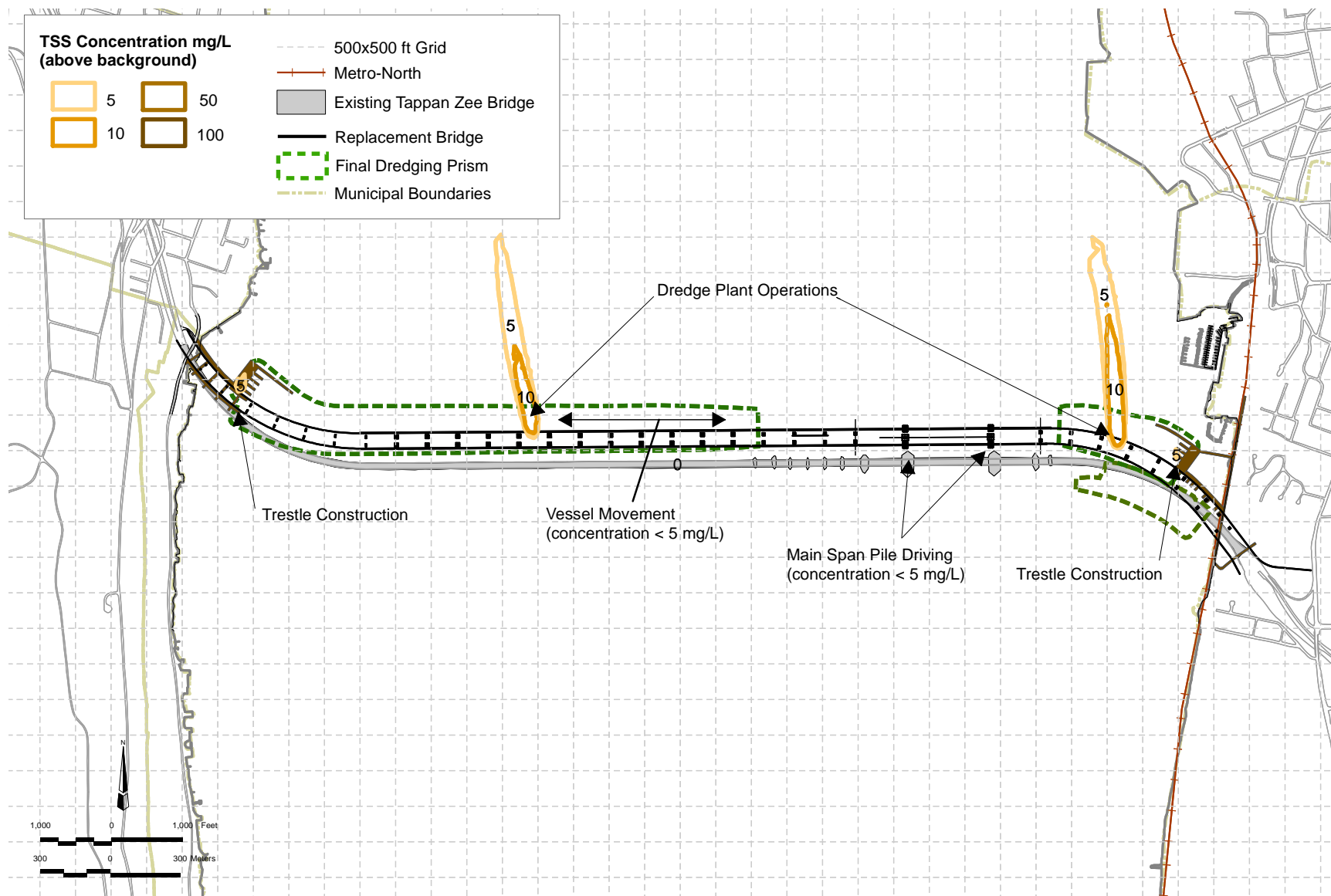
$$g_{pier} = 39 \text{ kg/min (0.4)} = 16 \text{ kg/min}$$

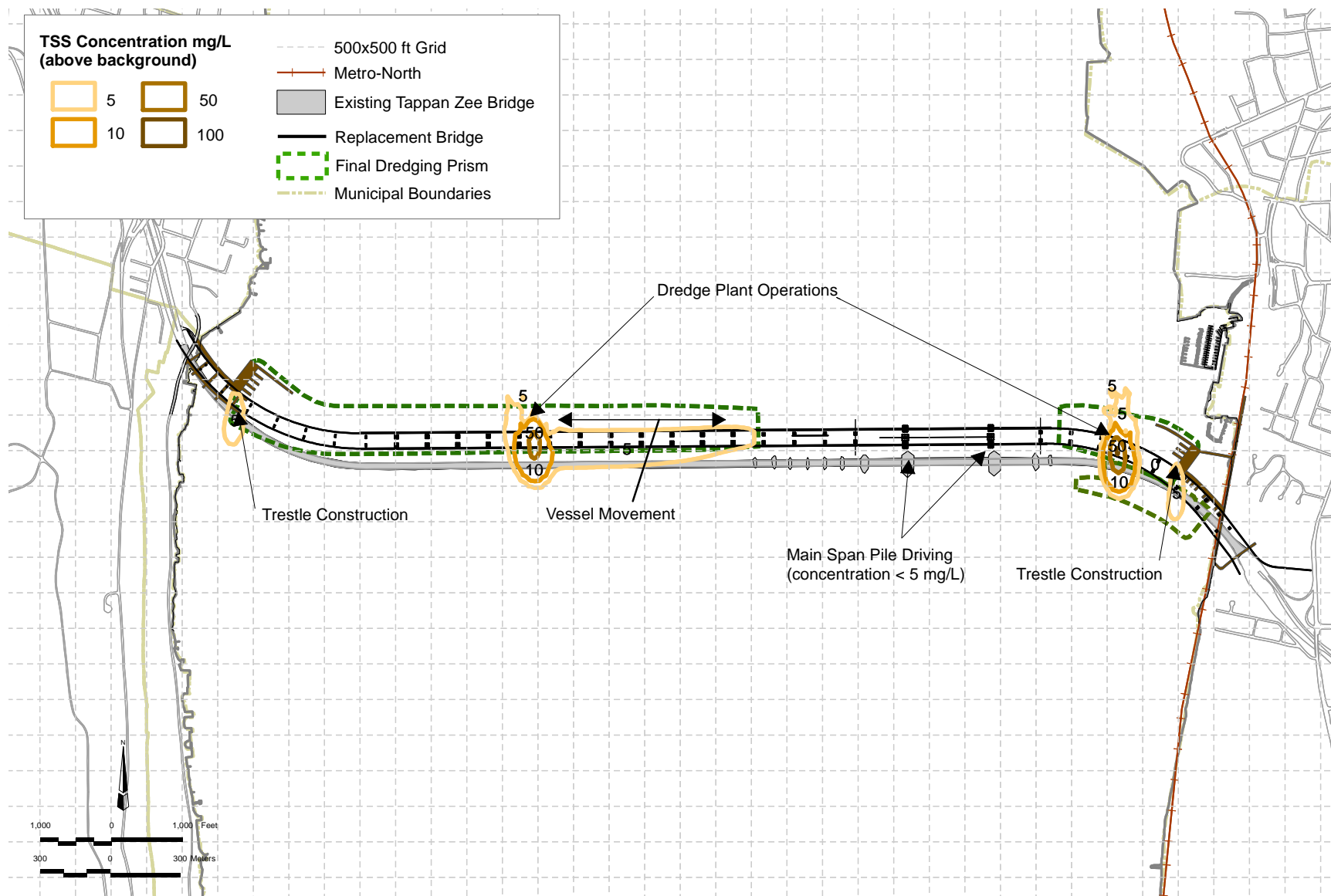
**References**

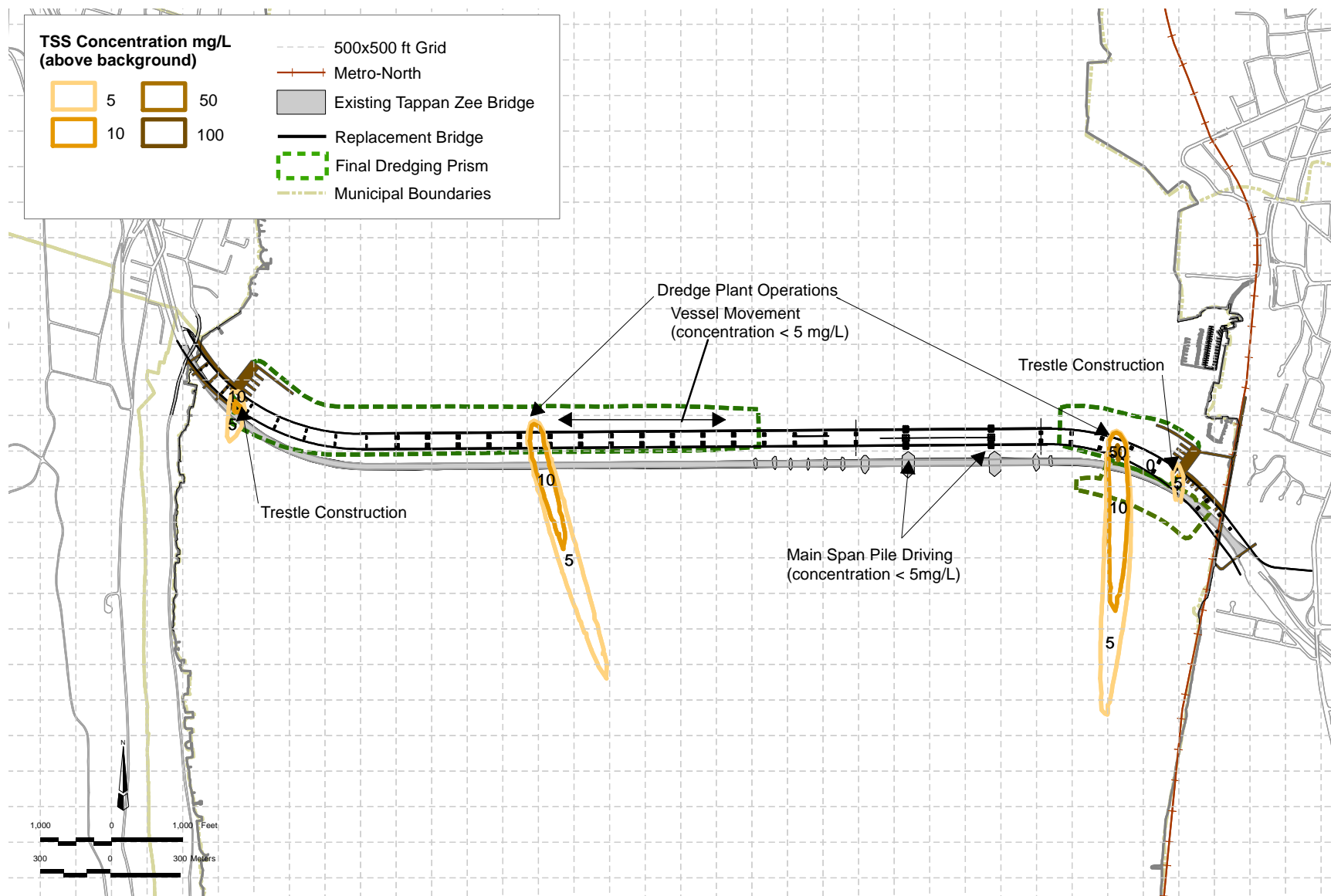
Hayes, Donald and Wu, Pei-Yao (2001). "Simple Approach to TSS Source Strength Estimates," *Proceedings of the WEDA XXI Conference*, Houston, TX, June 25-27, 2001.

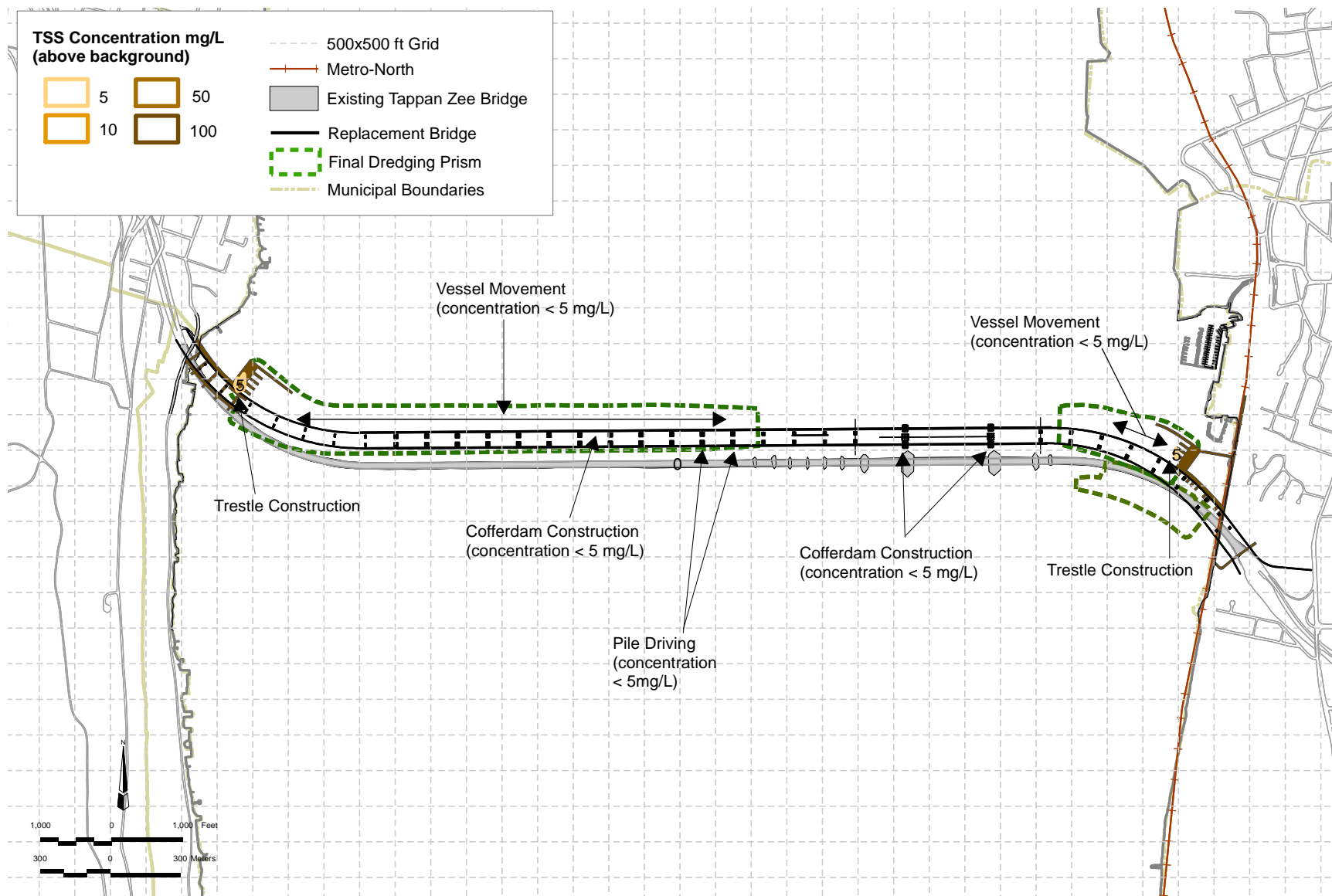
van Rijn, Leo C. 1986. "Sedimentation of Dredged Channels by Currents and Waves," *Journal of Waterway, Port, Coastal, and Ocean Engineering*, Vol. 112, No. 5, September, 1986.



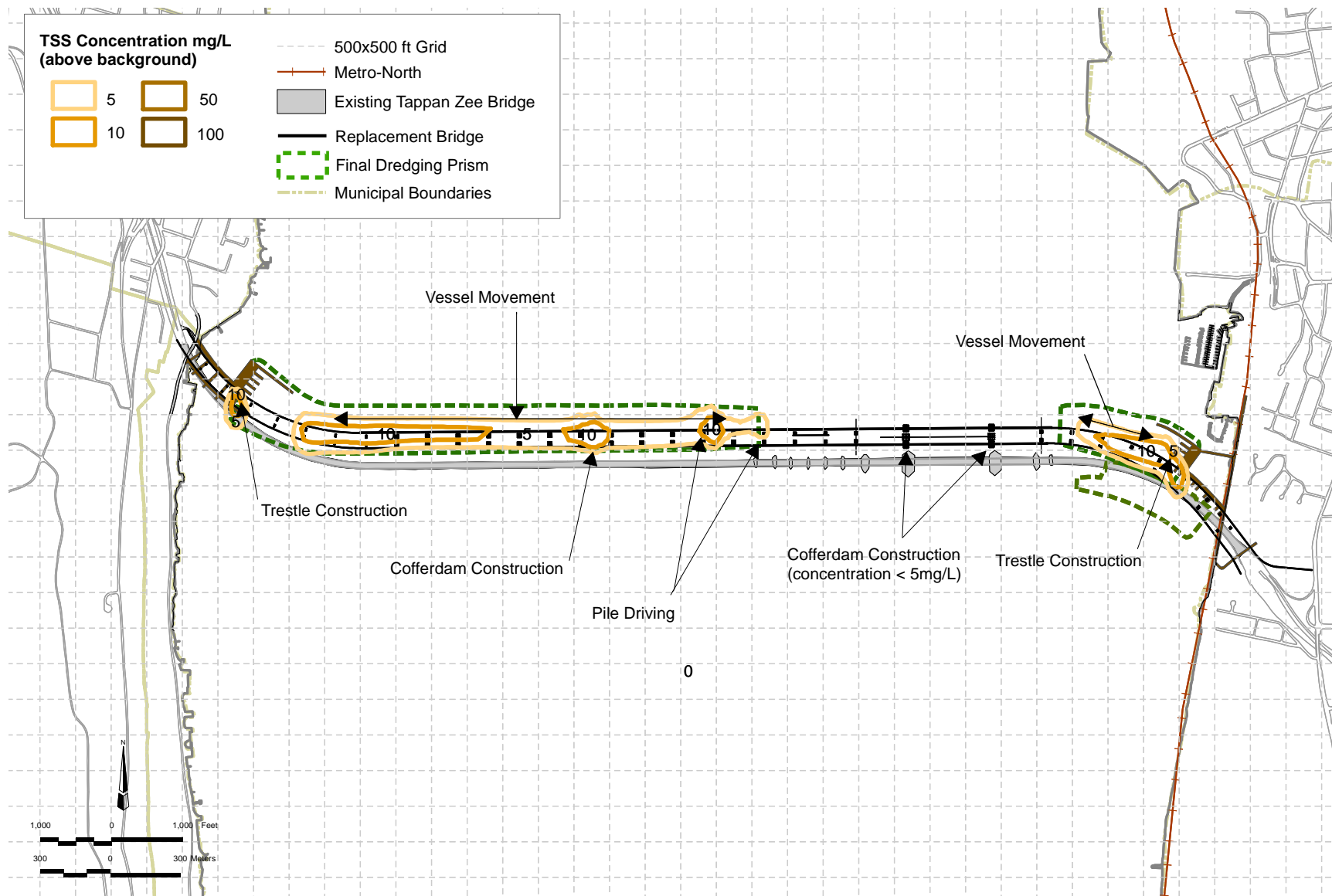


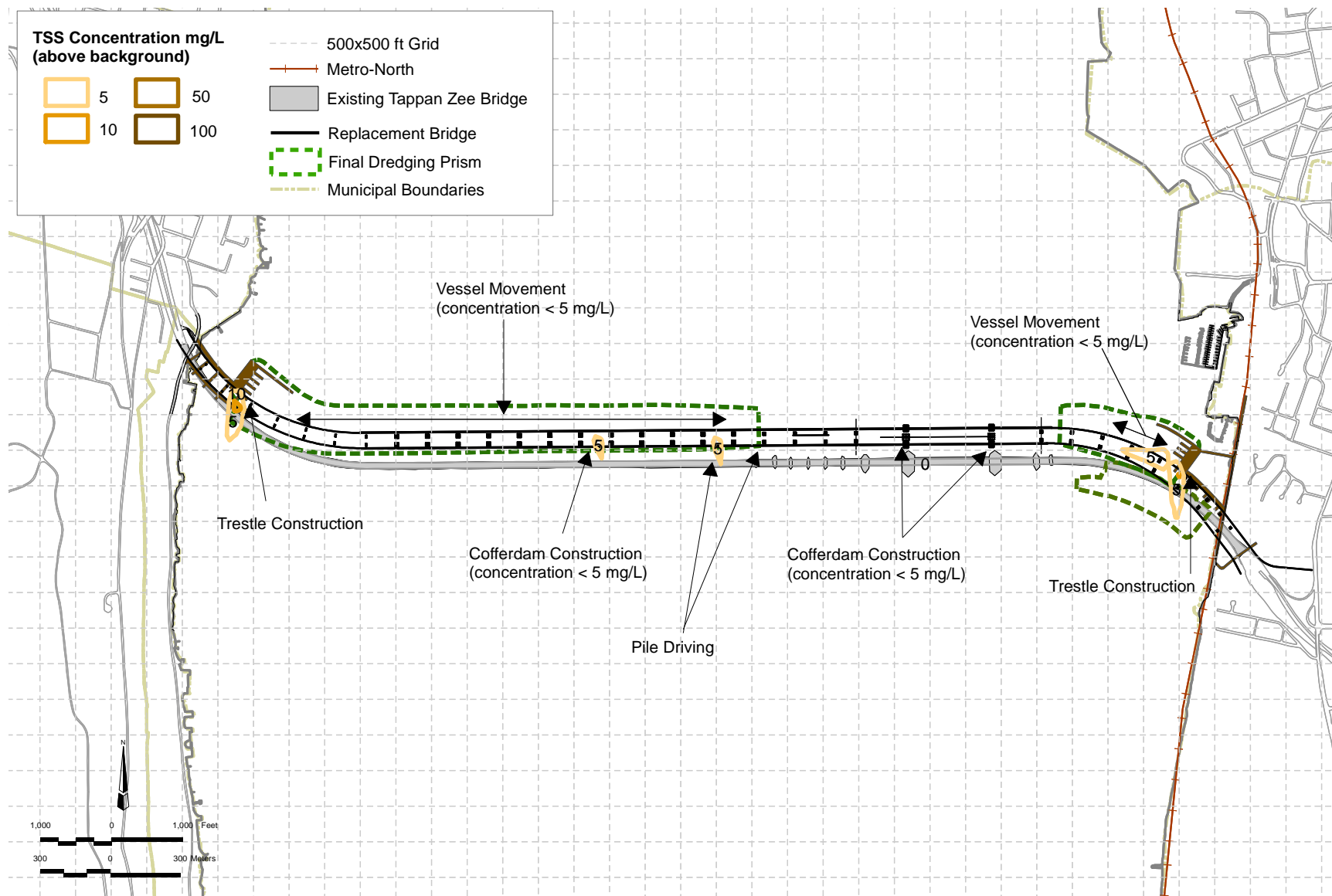


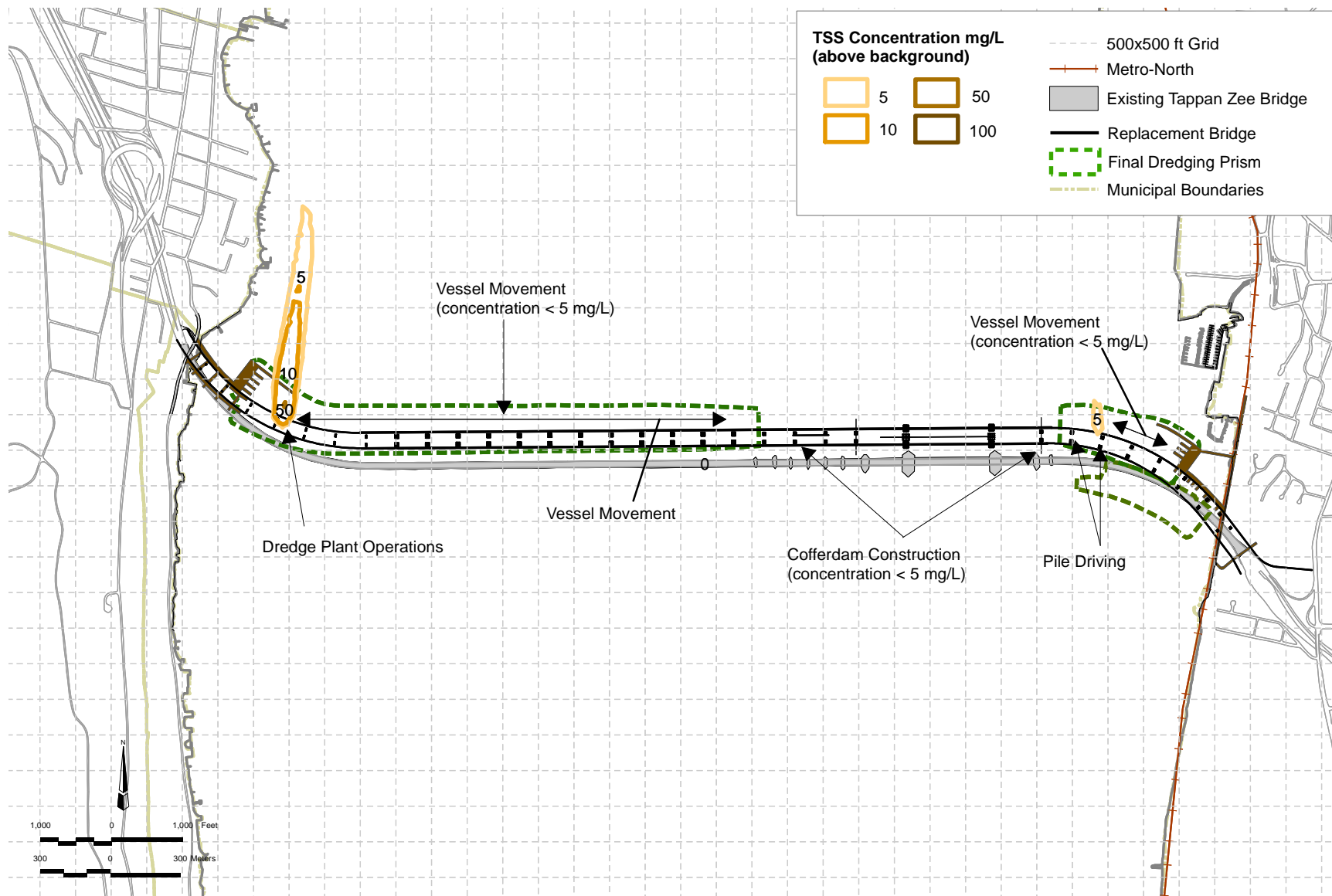


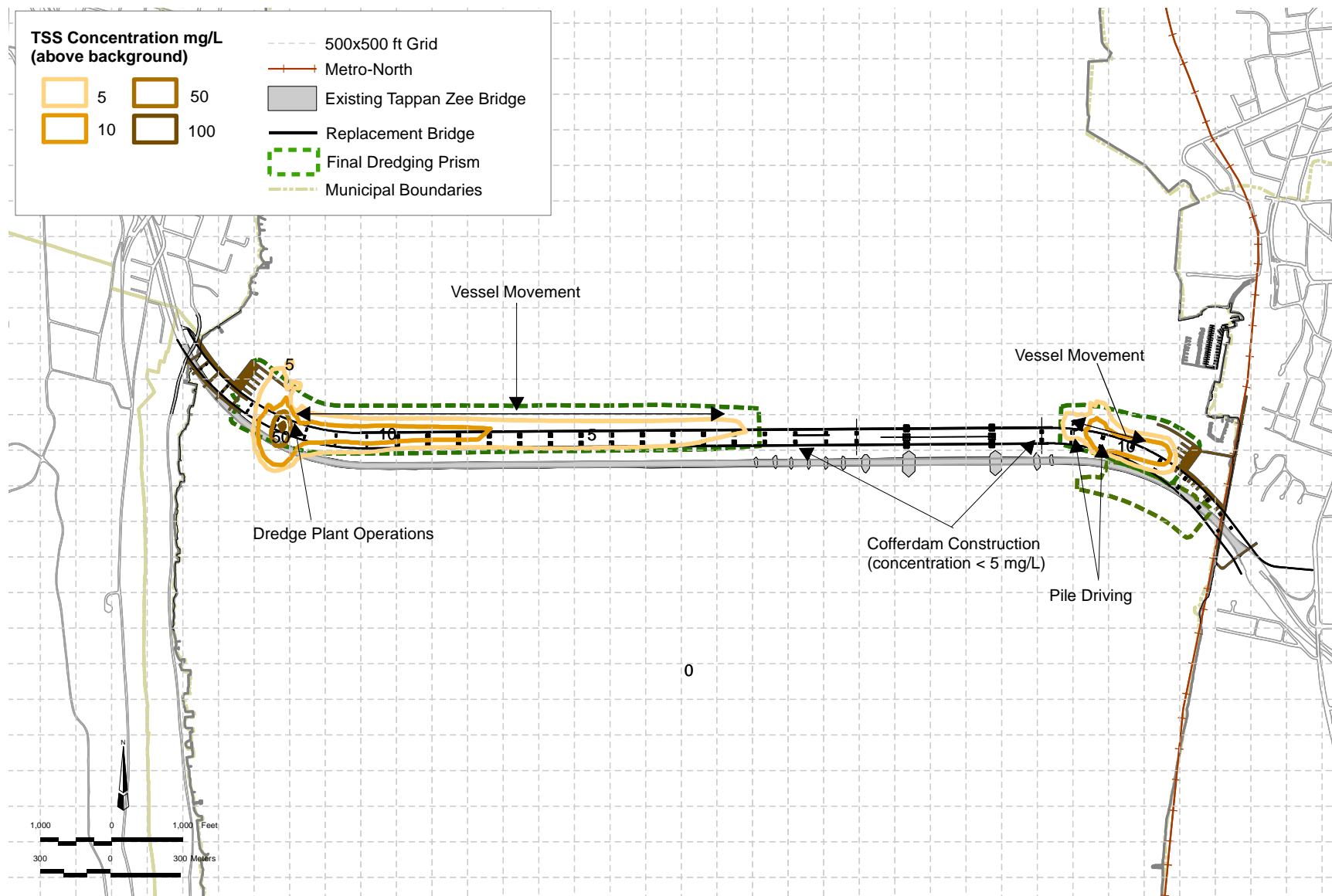




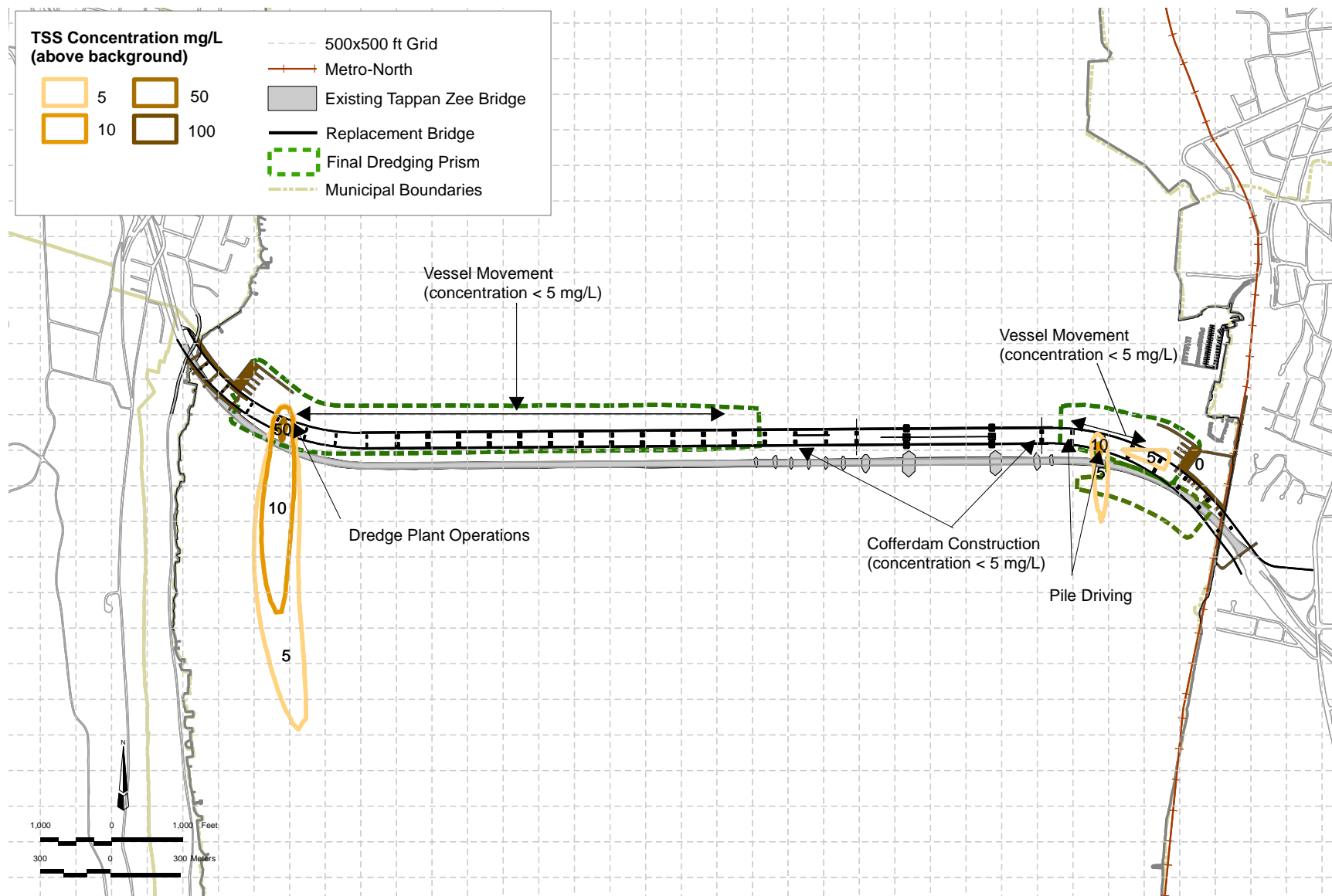














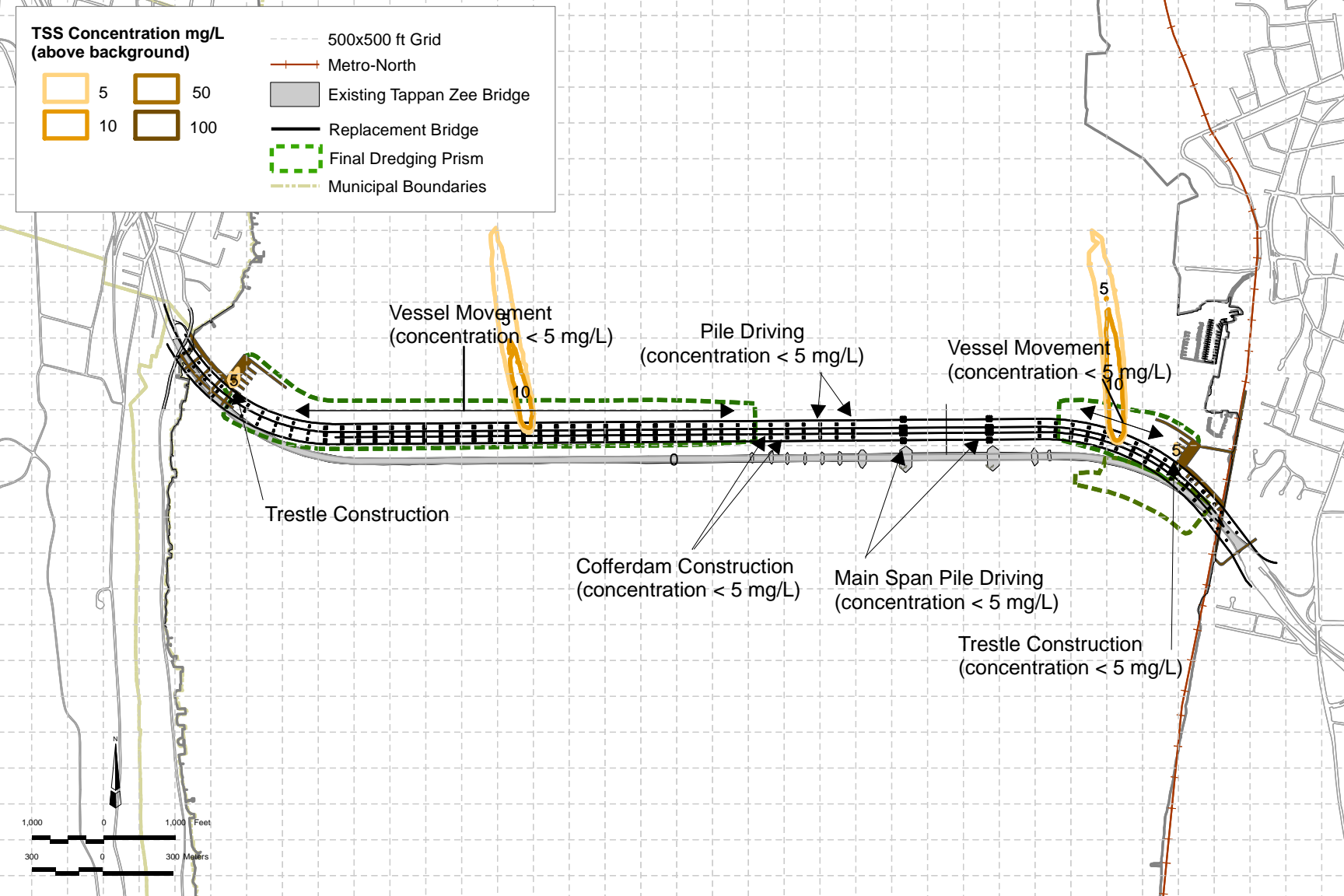


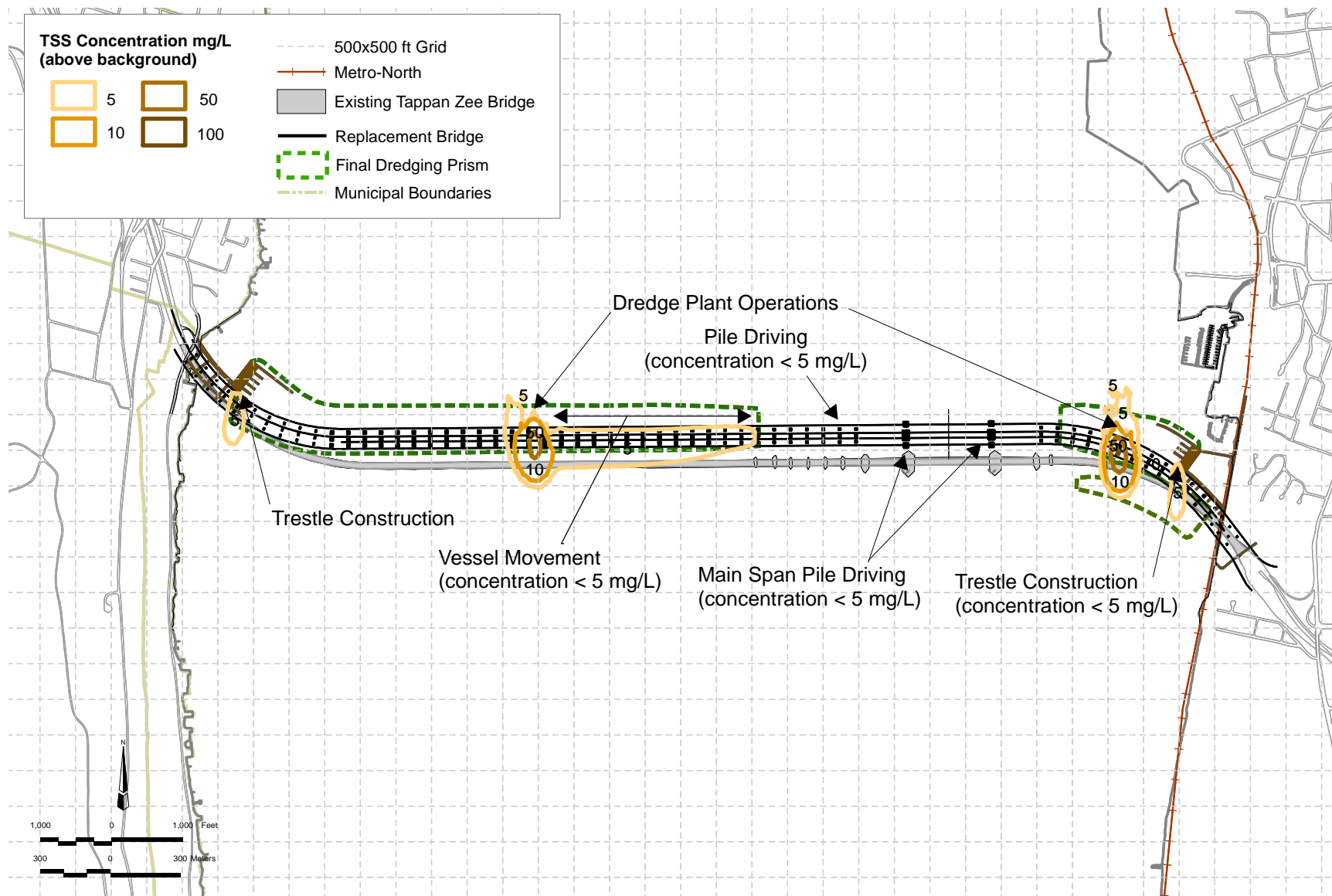


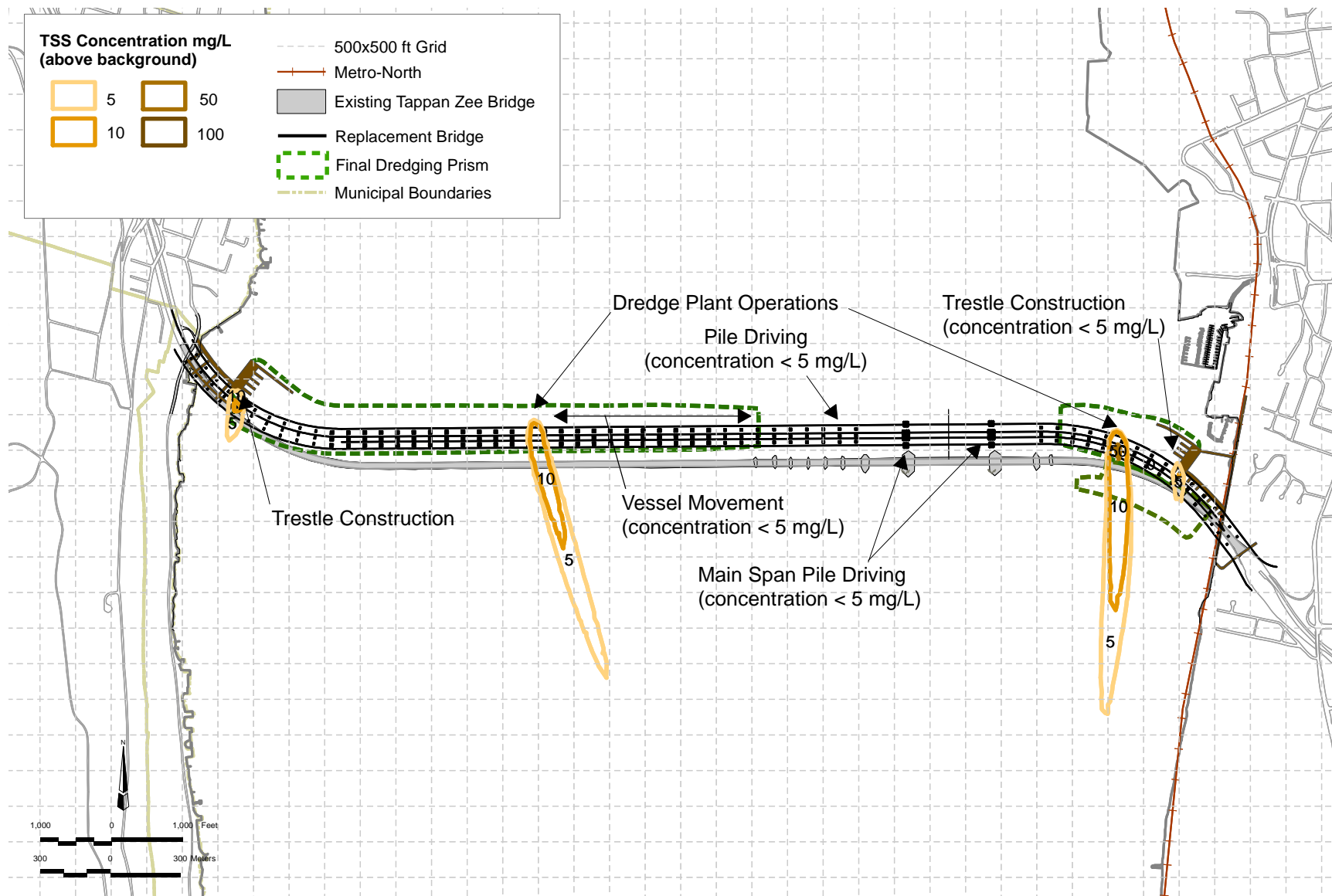
**TSS Concentration mg/L  
(above background)**



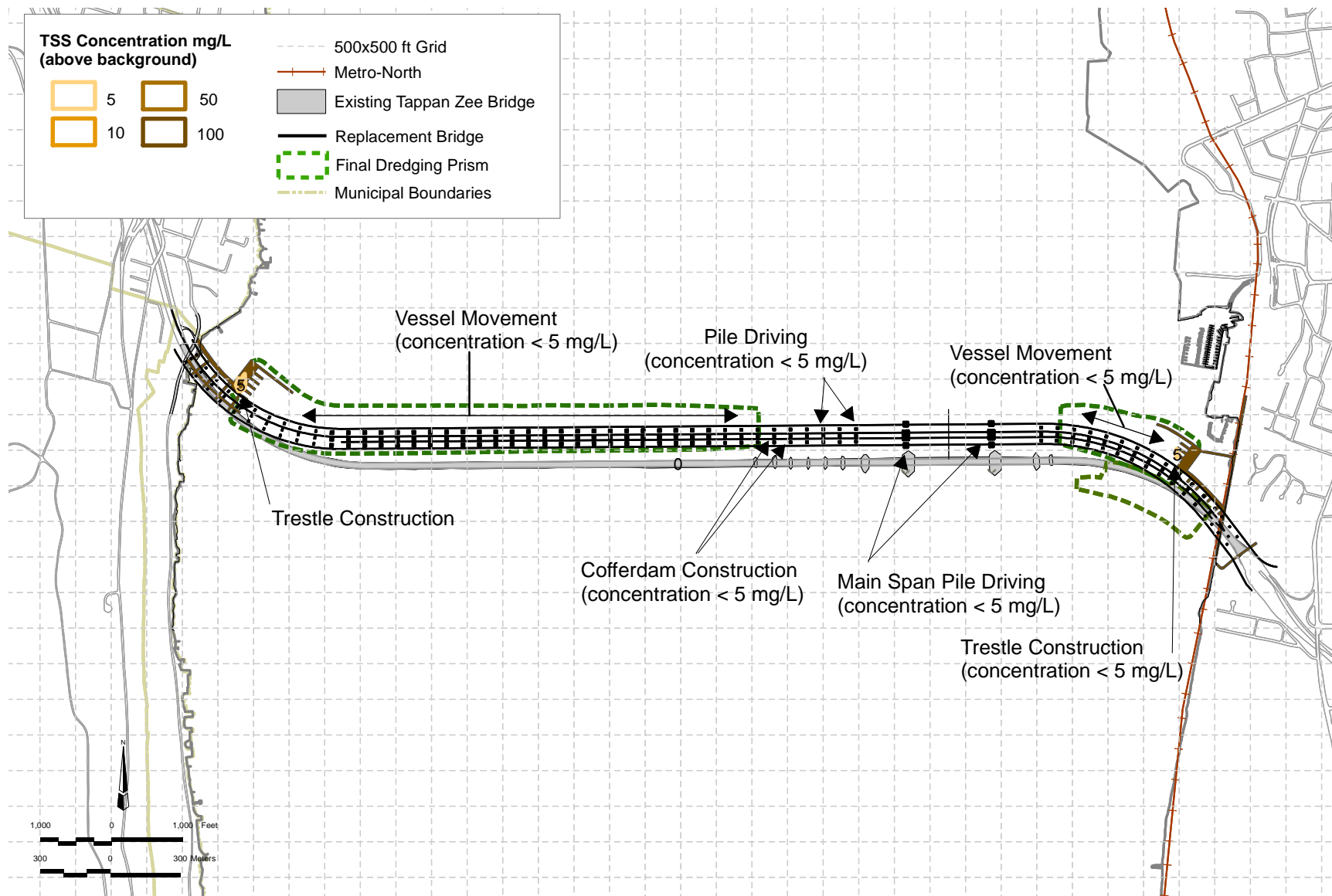
-  500x500 ft Grid
-  Metro-North
-  Existing Tappan Zee Bridge
-  Replacement Bridge
-  Final Dredging Prism
-  Municipal Boundaries













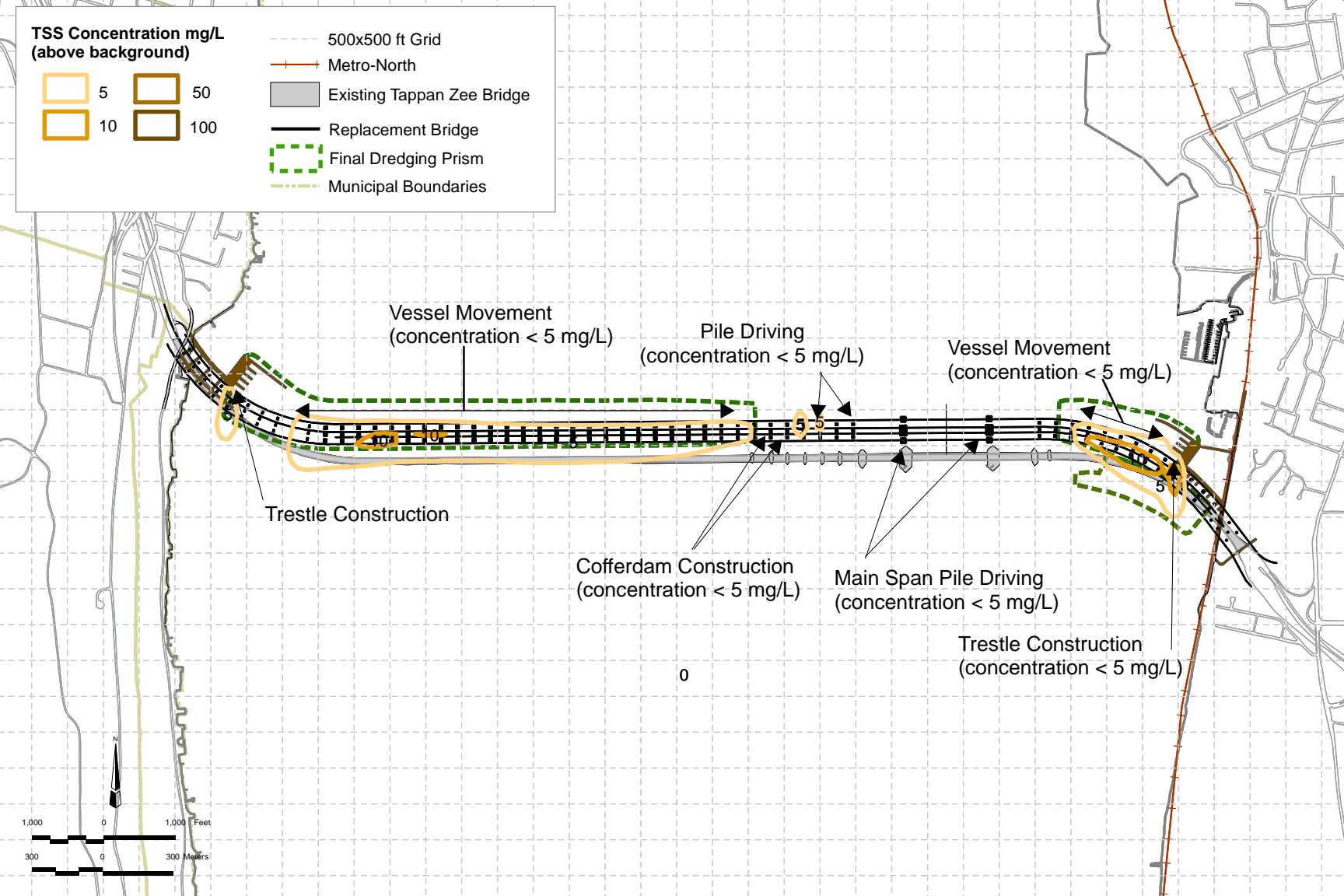




**TSS Concentration mg/L  
(above background)**









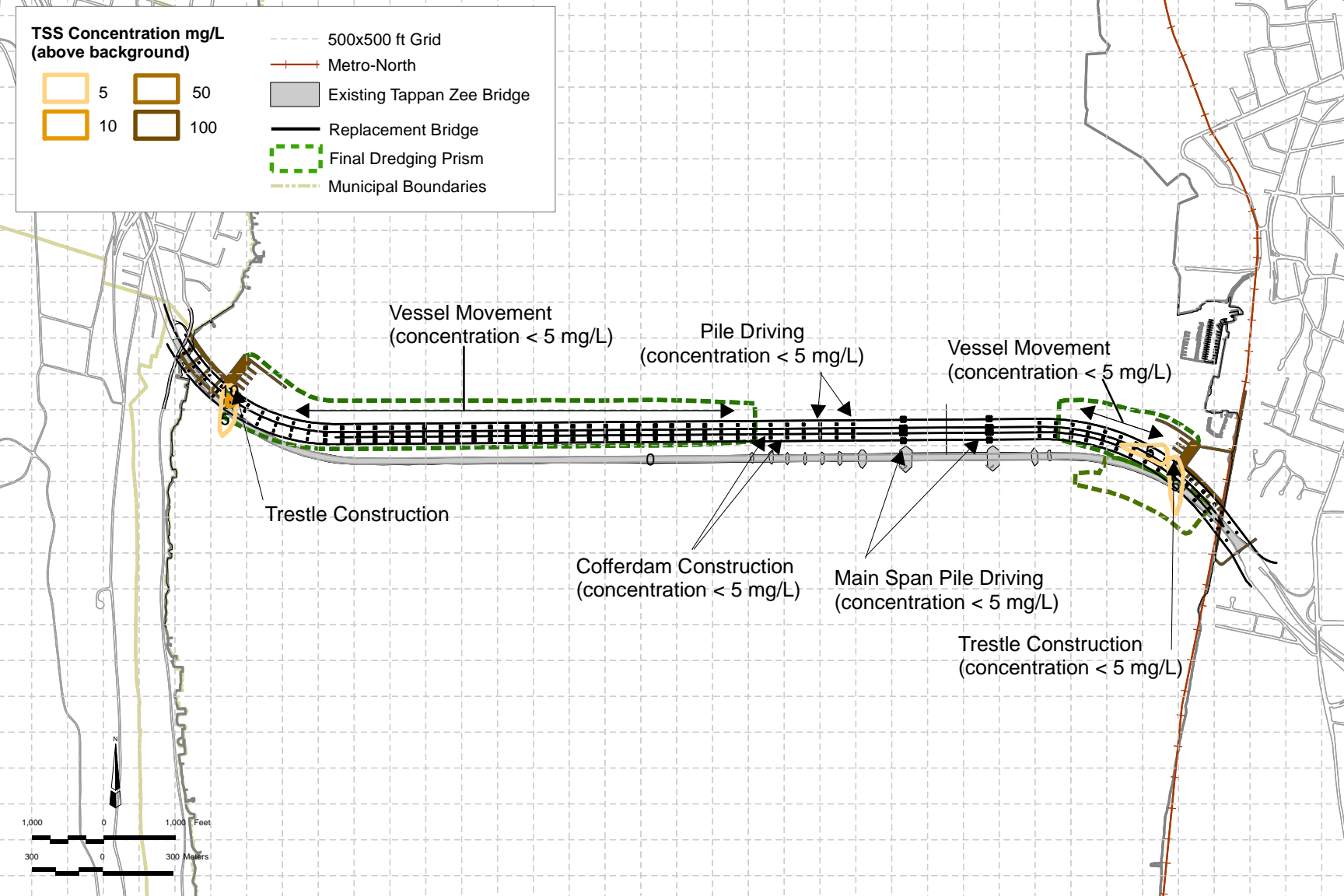
-  500x500 ft Grid
-  Metro-North
-  Existing Tappan Zee Bridge
-  Replacement Bridge
-  Final Dredging Prism
-  Municipal Boundaries



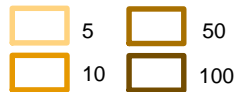
**TSS Concentration mg/L  
(above background)**









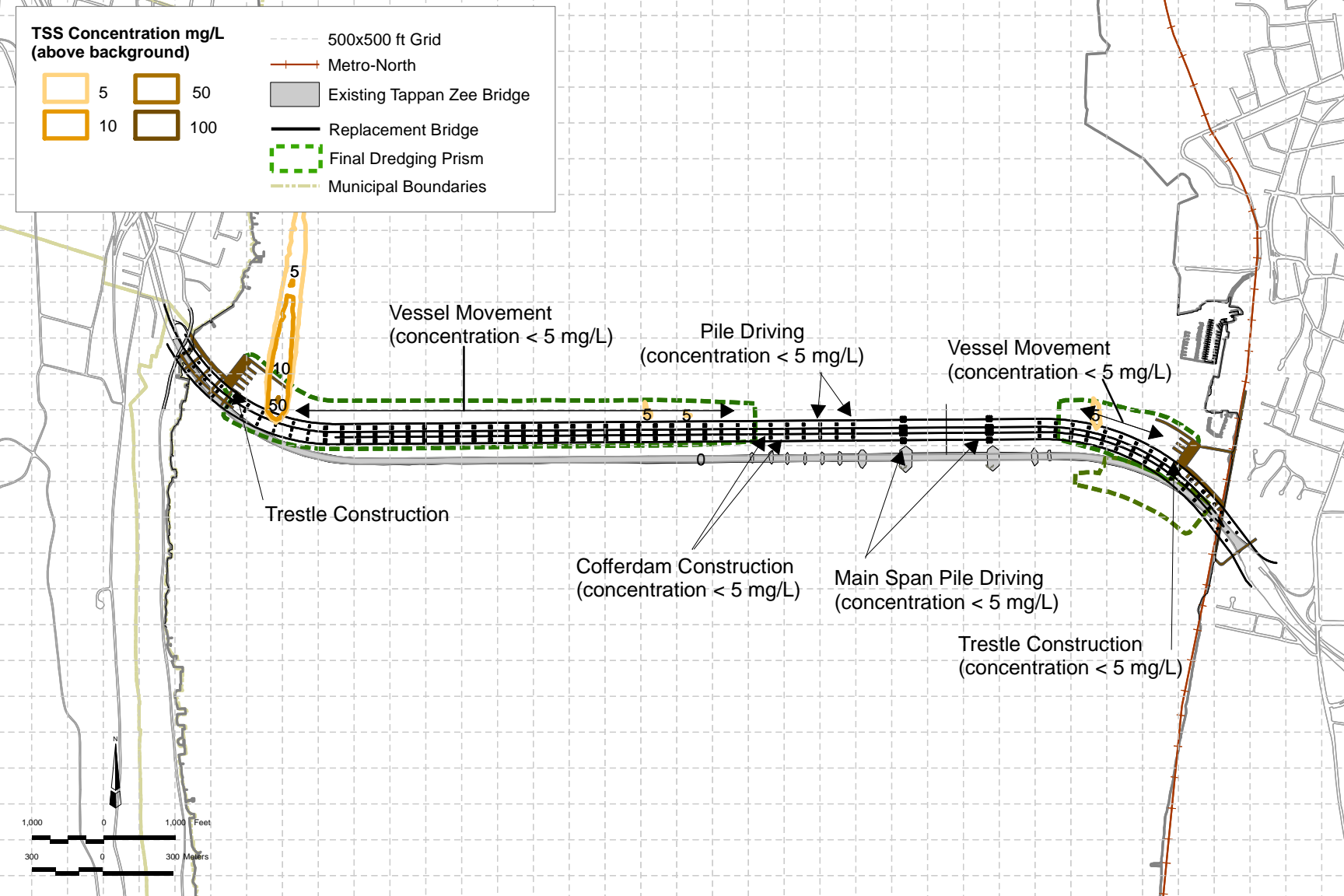
-  500x500 ft Grid
-  Metro-North
-  Existing Tappan Zee Bridge
-  Replacement Bridge
-  Final Dredging Prism
-  Municipal Boundaries



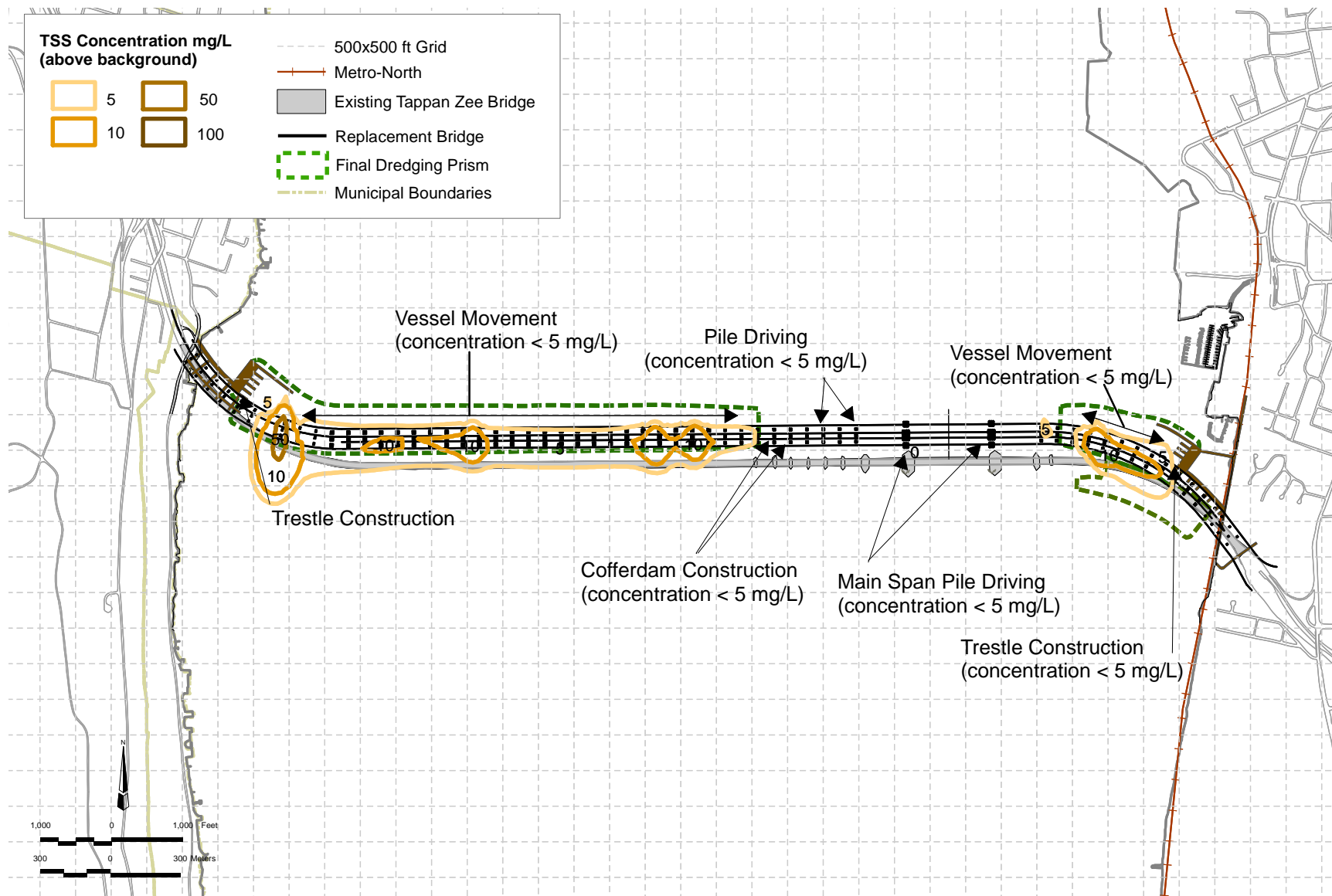
**TSS Concentration mg/L  
(above background)**



-  500x500 ft Grid
-  Metro-North
-  Existing Tappan Zee Bridge
-  Replacement Bridge
-  Final Dredging Prism
-  Municipal Boundaries









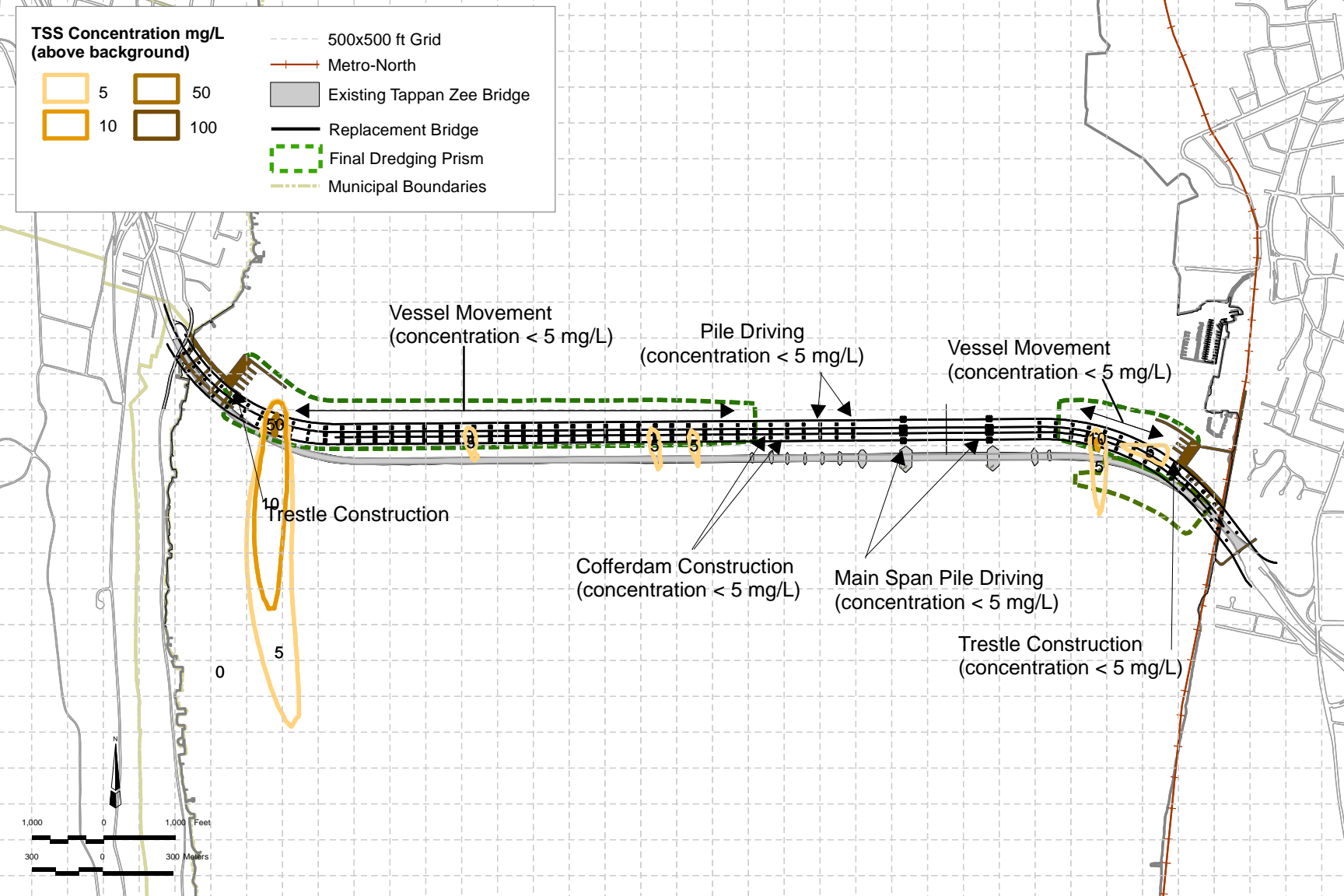




**TSS Concentration mg/L  
(above background)**



-  500x500 ft Grid
-  Metro-North
-  Existing Tappan Zee Bridge
-  Replacement Bridge
-  Final Dredging Prism
-  Municipal Boundaries



**Attachment 6, Table 1**  
**Pollutant Loading Calculations for Landings and Bridge with Treatment of Only the Landings**

	Rockland Side		Bridge		Westchester Side				Pollutant Loading Rates		Pollutant Loading		Pollutant Loading Rate with Treatment*		Percent Change	
Description	Area		Area		Area		Total Area		Total Phosphorus (TP)	Total Suspended Solids (TSS)	TP	TSS	TP	TSS	TP	TSS
Existing Condition	SF	Acres	SF	Acres	SF	Acres	SF	Acres	lbs/acre/year	lbs/acre/year	lbs/year	lbs/year	lbs/year	lbs/year	%	%
Total Area	1,183,118	27	1,511,630	35	751,169	17	3,445,917	79.1	0.6	883	47.5	69,852	N/A	N/A		
Grass Area	324,879	7	0	0	77,855	2	402,734	9.2	0.6	883	5.5	8,164	-	-		
Impervious Area	858,239	20	1,511,630	35	673,314	15	3,043,183	69.9	0.6	883	41.9	61,688	-	-		
Proposed Condition																
Total Area	1,183,118	27	2,618,327	60	751,169	17	4,552,614	104.5	0.6	883	62.7	92,286	52.1	60,918	10%	(0)
Grass Area	265,274	6	0	0	0	0	265,274	6.1	0.6	883	3.7	5,377	-	-		
Impervious Area	917,844	21	2,618,327	60	751,169	17	4,287,340	98.4	0.6	883	59.1	86,908	-	-		

Notes

SF - square feet

lbs/year - pounds per year

Bridge area was assumed proposed abutment to proposed abutment.

The area on the east side between east and west traffic at the toll plaza is assumed paved.

The proposed maintenance facility is assumed fully paved.

Source of TSS and TP loading rates are Wanielista, MP and Yousef, YA 1992.

\* Assumes 80% reduction of TSS and 40% reduction of TP for landing areas. Excludes treatment of bridge surfaces.

**Attachment 6, Table 2**  
**Pollutant Loading Calculations for Landings Only**

Description	Rockland Side				Westchester Side				TOTAL					
											Pollutant Loading		Pollutant Loading with Treatment*	
	Area		TP	TSS	Area		TP	TSS	Total Area without Bridge		TP	TSS	TP	TSS
	SF	Acres	lbs/year	lbs/year	SF	Acres	lbs/year	lbs/year	SF	Acres	lbs/year	lbs/year	lbs/year	lbs/year
Existing Total Area	1,183,118	27	16	23,983	751,169	17	10	15,227	1,934,287	44.4	26.6	39,210	N/A	N/A
Grass Area	324,879	7	4	6,586	77,855	2	1	1578.19	402,734	9.2	5.5	8,164	-	-
Impervious	858,239	20	12	17,397	673,314	15	9	13648.67	1,531,553	35.2	21.1	31,046	-	-
Long Span Total Area	1,183,118	27	16	23,983	751,169	17	10	15226.86	1,934,287	44.4	26.6	39,210	16.0	7,842
Grass Area	265,274	6	4	5,377	0	0	0	0	265,274	6.1	3.7	5,377	2.2	1,075
Impervious	917,844	21	13	18,606	751,169	17	10	15226.86	1,669,013	38.3	23.0	33,832	13.8	6,766

Notes

SF - square feet

lbs/year - pound per year

Bridge area was assumed proposed abutment to proposed abutment.

The area on the east side between east and west traffic at the toll plaza is assumed paved.

The proposed maintenance facility is assumed fully paved.

TSS loading rate used was 833 lbs/acre/year; TP loading rate used was 0.6 lbs/acre/year.

Source of TSS and TP loading rates are Wanielista, MP and Yousef, YA 1992.

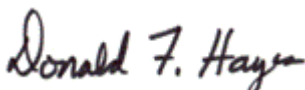
\* Assumes 80% reduction of TSS and 40% reduction of TP.

**Donald F. Hayes, Ph.D., P.E., BCEE**

2433 E. Tropicana Avenue #120 • Las Vegas, NV 89121

**MEMO**

April 24, 2012

**TO:** AECOM**FROM:** Don Hayes**RE:** Tappan Zee Hudson River Crossing Project, Dredging Water Quality Assessment

This memo contains an assessment of potential water quality impacts associated with dredging sediments from Hudson River as part of the Tappan Zee Bridge project. Dredging is necessary to create access channels from the navigation channel to both shorelines to allow delivery of construction equipment and supplies along the bridge alignment. Sediment losses occur during dredging and some of these sediments remain suspended in the water column and may be transported downstream.

Regulatory agencies requested information regarding potential water column concentrations of constituents due to the resuspension of river sediments during dredging operations. Constituent concentrations in the water column due to sediment resuspension during construction were previously estimated using a qualitative approach that indicated relatively low concentrations of suspended sediments. The regulatory agencies requested more extensive modeling in order to confirm this conclusion.

This memo describes the use of analytical tools to estimate water column concentrations of suspended sediment and associated constituents during anticipated dredging operations. This analysis uses sediment constituent concentrations typical for this reach of the Hudson River based upon the results of sediment chemistry analyses previously performed. The analysis focuses specifically on suspended sediment, lead, mercury, total PCBs and total PAHs.

**Sediment Characteristics**

The predominant sediment textures in the vicinity of the Tappan Zee Bridge are silt and clay. These finer-grained materials represent the majority of sediment samples collected throughout the study area and comprise in excess of 80% of the sediments contained within the proposed dredge prism, as shown in Table 1. Accumulations of a combined sand, silt and clay material are observed along the causeway section of the existing bridge. Gravelly sediments are also found near the eastern shore of the Hudson River and across a large swath of the mud flats north of the existing causeway section.

Particle settling velocities affect the size and extent of the suspended sediment plume associated with dredging and water column concentrations of sediment-bound constituents. Settling velocities of non-cohesive sediments were estimated using the methodology presented by van Rijn L.C. (1984) for non-cohesive sediments when the total sediment concentration is less than 25,000 mg/liter. The settling velocity for cohesive sediments was estimated at  $5 \times 10^{-4}$  m/s based on recent estimates by Maa and Kwo (2007).



Table 1. Sediment size classification used in the EFDC model

Wentworth Size Class	Diameter (mm)	Phi Value	Percentage in Dredge Prism	Sediment Class	Settling Velocity (m/s)
Medium Sand and Larger	0.250 to $\infty$	2 to $-\infty$	4.40%	#1	0.01
Fine Sand	0.125 to 0.250	3 to 2	5.10%		
Very Fine Sand	0.0625 to 0.125	4 to 3	8.80%		
Coarse Silt	0.031 to 0.0625	5 to 4	9.80%	#2	0.0008
Medium Silt	0.016 to 0.031	6 to 5	12.30%		
Fine Silt	0.008 to 0.016	7 to 6	16.50%	#3	0.0005
Very Fine Silt	0.0039 to 0.008	8 to 7	12.80%		
Clay	$\sim 0$ to 0.0039	$\sim \infty$ to 8	30.20%	#4	0.0005

The mass-weighted average settling velocity for the sediment size distribution in Table 1 is 0.0023 m/s. However, over 80% of the sediment mass has a significantly lower settling velocity. Since almost 60% of the sediment has an estimated settling velocity of 0.0005 m/sec, this value will be used in subsequent computations to provide conservative results.

As described in Chapter 15 of the DEIS, depth averaged water-column sediment samples in the vicinity of the Tappan Zee Bridge appear to range from 15 to 50 (mg/L) under normal conditions, and may exceed 100 mg/L during large freshwater events. These suspended sediment particles are not of the same distribution as the sediment being dredged because of the sedimentation process and, thus, have different settling velocities and contaminant concentrations. The analyses below focus on “above ambient” concentrations by ignoring the input of the upstream particles. The results should further increase the conservative nature of the results.

### Anticipated Dredging Operations

The final channel geometry and associated sediment volume have not been determined. However, it is expected that dredging will occur using a bucket dredging operation with an environmental clamshell bucket (e.g. CableArm® Clamshell). Dredging is anticipated to require 2 dredges working simultaneously (in different areas of the channel), using 25 yd<sup>3</sup> buckets, and removing 30 buckets/hour with 20 hours of effective production each day (dredges of this size normally operate 24 hrs/day and 7 days/week). Net production must account for non-effective dredging time such as downtime, dredge movement, debris, equipment repair, and scow availability; the net efficiency of the Tappan Zee Bridge dredging operations is estimated to be 50% with a net production rate of 7,500 yd<sup>3</sup>/day per dredge or 15,000 yd<sup>3</sup>/day combined.

Once a final sediment volume is determined, the minimum dredging time can be estimated by using this production rate. The actual dredging operation may take a bit longer if there is an unusual amount of

debris or other reasons for more downtime than normal. It is also possible that sediment disposal or barge availability could be a limiting factor extending the dredging time even further.

Sediment resuspension during dredging has been a topic of substantial interest. As a result, a number of publications are available that include both field data and empirical models based upon those data. However, at this stage it is adequate to simply estimate loss based upon other similar operations. Wu and Hayes (1999) suggested that an environmental clamshell bucket typically resuspends about 0.5% of the total dredged mass if proper best management practices are applied and barge overflow does not occur. Given the river environment and soft sediments, this analysis has conservatively assumes a resuspended sediment loss rate of 1 percent for an environmental clamshell bucket.

Appendix E, Attachment 4 of the DEIS noted that although two dredges are expected to be operating on site, they will be sufficiently far apart for safety reasons that any suspended sediment or contaminant plumes from their operations should not interact. It was also noted that the average production rate is not necessarily representative of all dredging operations, i.e. there are times when dredges are very effective for short durations. Based upon these two factors, Appendix D, Attachment D recommended the evaluation of two source estimates. The first estimate, described herein as  $M_R(\text{avg})$  is 39 kg/min and represents a single dredge removing 7,500 yd<sup>3</sup>/day of sediment with a density of 980 kg/m<sup>3</sup> at a 1% loss rate. The second estimate, described herein as  $M_R(\text{max})$  is 94 kg/min and represents a single dredge with a 25-cy bucket and 2 minute cycle times removing sediment with a density of 980 kg/m<sup>3</sup> at a 1% loss rate without any downtime. The latter scenario is likely to occur only for a few hours at a time. The remainder of this memo generates computations for both scenarios.

### Water Quality Criteria

NYS Division of Water Technical and Operational Guidance Series 1.1.1 (TOGS 1.1) dated June 1998 provides ambient water quality standards and guidance values for New York State waters including the Hudson River. Because of the short-term nature of the dredging operation, the appropriate water quality criteria are acute aquatic exposure. The Hudson River is Class SB in this reach. Class B values were used when Class SB values were not available. Table 2 summarizes the water quality criteria for the constituents of concern. The water quality criterion for Cadmium is based upon water hardness; several internet sites reported hardness values of about 85 mg/L as CaCO<sub>3</sub>. Acute water quality criteria were not found for PCBs or PAHs, but the constituents are included because of they are common in many regions of the Hudson River.

**Table 2. Water quality criteria for project site**

Constituent	Acute WQ Criteria (µg/L)		Basis
Arsenic (As)	340	Dissolved	Class B; acute
Cadmium (Cd)	3.2*	Dissolved	Class B; acute
Copper (Cu)	4.8	Dissolved	Class SB; acute
Lead (Pb)	204	Dissolved	Class SB; acute
Mercury (Hg)	1.4	Dissolved	Class B; acute
Total PCBs	Acute WQ standard for aquatic exposure not specified		
Total PAHs	Acute WQ standard for aquatic exposure not specified		
*Using the equation specified in the TOGS 1.1.1 for hardness of 85 mg/L as CaCO <sub>3</sub> ; [(0.85) exp(1.128 [ln(ppm hardness)] - 3.6867)]			

TOGS 5.1.9 provides mixing zone criteria for dredging operations. This section of the Hudson River is assumed to be a “river-like” section of an estuary for the purposes of this analysis. This provides the shortest mixing zone – the lesser of one-third the waterway’s width or a total length of 500 ft; because of the width of the river, 500 ft (150m) is the applicable length for this project. The slack tide in this tidal system has a very short duration, so directional flow is the primary. Currents are highest during Ebb tide and will result in the longest plume. Thus, the plume analysis that follows is applied to ebb tide currents.

Suspended sediment plumes resulting from dredging operations tend to be short-lived and the simple transport model used to estimate water column concentrations is based upon one-directional flow. Thus, water quality criteria are compared to model predictions at a distance of 500 ft (150m) downstream of the dredging operation.

### **Near-Field Models and Application**

#### Suspended Sediment

Two distinct zones of mixing and transport exist with common bucket dredging operations. The active dredging area can reasonably be characterized as well mixed since bucket-induced turbulence dominates the ambient current. Once the suspended sediment escape from the immediate vicinity of the dredging operations, ambient currents dominate transport downstream and away from the dredging area. This section deals exclusively with the well-mixed area in the immediate vicinity of the dredging operation.

The size of the well-mixed near-field zone depends upon the bucket operation and the strength of ambient currents. For purposes of this analysis, the near-field zone is assumed to be a cylindrical area 20 meters in diameter. Using an ideal completely mixed reactor model at steady state, the suspended sediment concentration in the immediate vicinity of the dredging operation can be estimated using the equation:

$$m = \frac{m_{in}Q + M_R}{\lambda_m V_{nf}}$$

and

$$\lambda_m = \frac{1}{\theta_{nf}} + \frac{v_s}{H}$$

where  $m$  = average suspended sediment concentration ( $\text{g}/\text{m}^3$ ),  $m_{in}$  = suspended sediment concentrations in upstream flow ( $\text{g}/\text{m}^3$ ),  $Q$  = flow into the near-field area from upstream ( $\text{m}^3/\text{sec}$ ),  $M_R$  = sediment resuspension rate associated with the dredging operation ( $\text{g}/\text{sec}$ ),  $V_{nf}$  = volume of the well-mixed near-field area ( $\text{m}^3$ ),  $H$  = average water depth (m),  $v_s$  = average particle settling velocity (m/sec), and  $\theta_{nf}$  = hydraulic retention time of the near-field volume (sec).

Water velocities, sediment characteristics, and water depths of the river vary considerably between the shorelines and with flow conditions. Previous efforts associated with the EIS considered the site conditions along the Tappan Zee Bridge construction corridor and concluded that the following values were most representative for use in modeling efforts (Appendix D 5.8):

Ambient Current Velocity =  $u = 0.5 \text{ ft/s}$

Water Depth =  $h = 10 \text{ ft}$

Particle Settling Velocity for silt =  $w = 0.0005 \text{ m/s}$

Based upon these values, the near-field volume is 964 m<sup>3</sup> with an inflow of 9.4 m<sup>3</sup>/sec and a theoretical retention time of about 102 seconds. Ambient suspended sediment concentrations in the Tappan Zee Bridge reach of the Hudson River tend to be relatively low; thus, for the purposes of this analysis, the upstream suspended sediment concentration will not be considered and the values presented as “above ambient.”

Appendix E, Attachment 4 of the DEIS anticipated estimated average and maximum sediment resuspension rates,  $M_R$ , from Tappan Zee dredging operations as 39 kg/min and 94 kg/min respectively. Modeling the near-field area as a 20-m diameter well-mixed zone predicts water column concentrations of 68 mg/L and 164 mg/L respectively.

### Constituent Concentrations

This same approach can be used to compute dissolved and particulate constituent concentrations at steady-state. Assuming volatilization of these constituents and additional constituent flux from residual sediment during dredging is negligible, the total constituent concentration can be computed as:

$$c = \frac{Qc_{in} + qM_R}{\lambda_c V_{nf}}$$

where

$$\lambda_c = \frac{1}{\theta_{nf}} + \left(\frac{v_s}{H}\right) F_p$$

$$F_p = \frac{K_d m}{1 + K_d m}$$

where  $c_{in}$  = total upstream constituent concentration (µg/L),  $q$  = sediment constituent concentration (mg/kg),  $F_p$  = particulate fraction of constituent (dimensionless), and  $K_d$  = equilibrium partitioning coefficient (L/kg).

Table 3 shows sediment constituent concentrations and partitioning coefficient values used for estimating water column concentrations along with references for their source. Tables 4 and 5 show modeled near-field concentrations for average release rate or the maximum release rate. It is notable that all of the estimates are below the water quality criteria for which values were identified.

## **Far-Field Models and Application**

### Suspended Sediment

Once the suspended sediment exits the well-mixed near-field volume, its transport can be modeled using the 2-D, depth averaged analytical solution presented by Kuo and Hayes (1991) for bucket dredging operations. Kuo and Hayes (1991) proposed the following steady-state Gaussian plume model to compute depth averaged TSS concentrations downstream from bucket dredging operations in areas with a sustained unidirectional flow:

<b>Table 3. Sediment constituent concentrations and partitioning coefficients for suspended matter in water.</b>				
<u>Constituent</u>	<u>Sediment Concentration (mg/kg)</u>			
	<u>Value</u>	<u>Source</u>	<u>Log(K<sub>d</sub>)</u>	<u>Source</u>
Arsenic	8.06	Tables 15-3, 15-4 and 15-5 in the DEIS.	4.0	Allison and Allison 2005
Cadmium	1.9		4.7	Allison and Allison 2005
Copper	32		4.7	Allison and Allison 2005
Lead (Pb)	36		5.6	Allison and Allison 2005
Mercury (Hg)	0.89		5.3	Allison and Allison 2005
PCBs	0.169		5.46	Henry and DeVito 2003
PAHs	1.673		3.56	Khodadoust <i>et. al</i> 2005

**Table 4. Near-field constituent concentrations\* for M<sub>R</sub>(avg)**

<u>Constituent</u>	<u>Particulate Fraction</u>	<u>Total</u>	<u>Particulate</u>	<u>Dissolved</u>
<u>Units of Measure</u>	(%)	(µg/L)	(µg/L)	(µg/L)
Arsenic (As)	40.5	0.553	0.224	0.329
Cadmium (Cd)	77.3	0.130	0.100	0.029
Copper (Cu)	77.3	2.18	1.69	0.50
Lead (Pb)	96.4	2.45	2.36	0.09
Mercury (Hg)	93.1	0.061	0.056	0.004
Total PCBs	95.1	0.012	0.011	0.001
Total PAHs	19.8	0.115	0.023	0.092
*These constituent concentrations are in the immediate vicinity for the dredge and, thus, should not be compared to the water quality criteria				

**Table 5. Near-field constituent concentrations\* for M<sub>R</sub>(max)**

<u>Constituent</u>	<u>Particulate Fraction</u>	<u>Total</u>	<u>Particulate</u>	<u>Dissolved</u>
<u>Units of Measure</u>	(%)	(µg/L)	(µg/L)	(µg/L)
Arsenic (As)	62.1	1.33	0.82	0.50
Cadmium (Cd)	89.1	0.312	0.278	0.034
Copper (Cu)	89.1	5.25	4.68	0.57
Lead (Pb)	98.5	5.90	5.81	0.09
Mercury (Hg)	97.0	0.146	0.141	0.004
Total PCBs	97.9	0.0277	0.0271	0.0006
Total PAHs	37.3	0.277	0.103	0.174
*These constituent concentrations are in the immediate vicinity for the dredge and, thus, should not be compared to the water quality criteria				



$$c(x, y) = \frac{M_R}{uh\sqrt{4\pi k_y\left(\frac{x-x'}{u}\right)}} e^{\left[-\frac{(y-y')^2}{4k_y\left(\frac{x-x'}{u}\right)} - \frac{w(x-x')}{hu}\right]}$$

where the x-dimension is along the flow path, y-dimension is normal to the flow path, and

$c(x, y)$  = depth average concentration (mg/L)

$u$  = ambient flow velocity (m/sec)

$h$  = water depth (m)

$k_y$  = lateral (normal to the direction of flow) turbulent diffusion coefficient ( $m^2/sec$ )

$w$  = particle settling velocity (m/sec)

$x', y'$  = position of vertical line source of suspended sediment (m)

$x, y$  = position of interest (m)

This model is the basis of far-field transport computations in the COE's DREDGE model. It assumes that advection in the direction of flow significantly exceeds turbulent diffusion in that direction. Although the hydrodynamic regime in the vicinity of the Tappan Zee Bridge varies significantly from bank-to-bank, the majority of the river is consistent with definition. Downstream TSS concentrations were estimated for anticipated dredging operations within the Hudson River using both the average and maximum dredging rates previously identified and the site conditions described in Table 1. These computations utilized the site and sediment characteristics shown in Table 6.

**Table 6. Site and sediment characteristics used in TSS modeling**

<u>Site Condition</u>	<u>Variable</u>	<u>Value</u>	<u>Units</u>	<u>Source</u>
Water Depth	H	3.1	m	Appendix D (Page 112)
Ambient Current	u	0.15	m/sec	Appendix D (Page 112)
Particle Settling Velocity	$v_s$	0.0005	m/sec	Appendix D (D5.2.2.9 and D5.2.2.10)
Upstream TSS	$m_{in}$	5.1	mg/L	Table D-1 (Page 5)
Sediment Density	$\gamma_s$	982	kg/m <sup>3</sup>	4 sample average
Water Content	$\omega$	64.3	%	4 sample average
Specific Gravity	$G_s$	2.66		4 sample average
Viscosity of Water at 20°C	$\mu$	0.0010	Ns/m <sup>2</sup>	
Density of Water at 20°C	$\rho$	998.2	kg/m <sup>3</sup>	
Dispersion Co-efficient	$K_y$	0.2787	m <sup>2</sup> /sec	Appendix D (Page 112)

Figure 1 shows a contour plot of predicted downstream TSS concentrations using the estimated maximum flux rate of 94 kg/min (Hayes 2009). These results are similar to those estimated in the draft EIS.

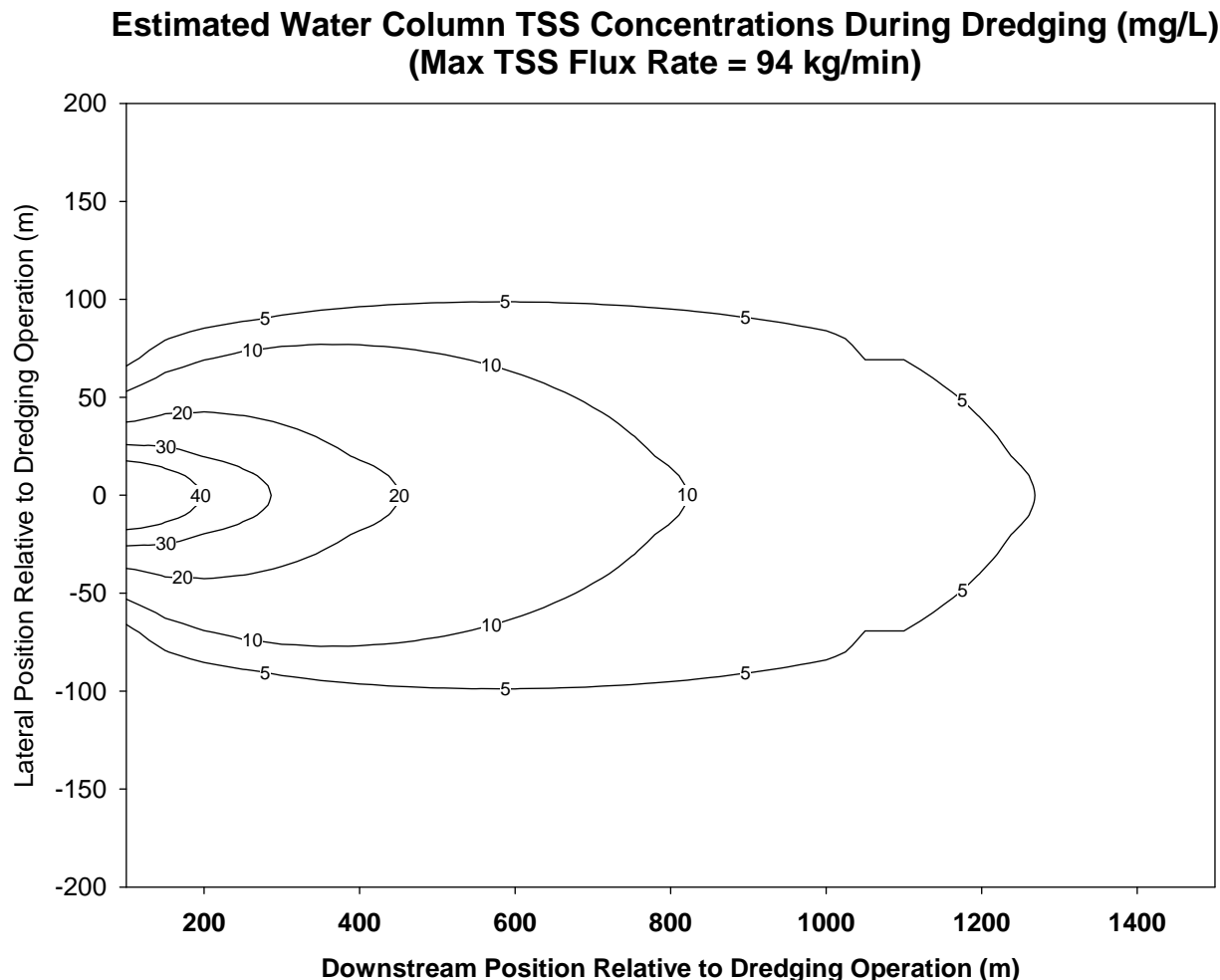


**Figure 1. Estimated Water Column TSS Concentrations above ambient during Dredging (mg/L) using max TSS Flux Rate = 94 kg/min).**

#### Constituent Concentrations

Constituents are transported downstream from the well-mixed near-field region attached to the suspended sediment. In fact, particulate constituents are transported along with the suspended sediment particles. In contrast, dissolved constituents move with the ambient current becoming more dilute as the dissolved plume spreads.

Comprehensive modeling of the physical transport processes that govern downstream transport of multiple constituents is a very complex undertaking and beyond the scope of this effort. The simple modeling approach utilized here provides conservative results by simplifying some of the transport processes. One significant simplification is that total constituent concentrations are distributed between particulate and dissolved concentrations applied at all locations based upon water column TSS concentrations. This approach does not consider the continuous decrease in particulate constituent concentrations due to the continual “washing” of particulate constituents into the dissolved phase. Thus, the resulting water constituent concentrations estimates are conservative (higher than actual).

Table 7 compares modeled dissolved constituent concentrations 500 ft (150 m) downstream from the dredging operation for the average and maximum suspended sediment flux rate.

### Comparison to Water Quality Criteria

Table 7 shows that the dissolved water column concentrations of all constituents predicted by the DREDGE model are all substantially less than their corresponding acute water quality criterion for aquatic exposure.

**Table 7. Dissolved Constituent Concentrations along the X axis using  $M_R(\text{avg})$ ; all concentration values are in  $\mu\text{g/L}$ .**

	WQ Criteria ( $\mu\text{g/L}$ )	Modeled Dissolved Concentrations ( $\mu\text{g/L}$ ) at 500 ft (150 m)	
		$M_R(\text{avg})$	$M_R(\text{max})$
TSS (mg/L)		19.8	47.7
Arsenic (As)	340	0.133	0.260
Cadmium (Cd)	3.2	0.0189	0.0267
Copper (Cu)	4.8	0.318	0.450
Lead (Pb)	204	0.0802	0.0859
Mercury (Hg)	1.4	$3.56 \times 10^{-3}$	$4.04 \times 10^{-3}$
Total PCBs		$4.99 \times 10^{-4}$	$5.46 \times 10^{-4}$
Total PAHs		0.0309	0.0680

### References

Allison, J.D. and Allison, T.L. 2005. *Partition Coefficients for Metals in Surface Water, Soil, and Waste*, EPA/600/R-05/074, July 2005.

Chapra, S.1999. *Surface Water Quality Modeling*, McGraw-Hill.

Hayes, D., Borrowman, T., and Welp, T. 2000. "Near-Field Turbidity Observations During Boston Harbor Bucket Comparison Study," *Proceedings of WEDA XX and TAMU 32nd Annual Conference*, Providence, RI, June 2000.

Henry, T.R. and DeVito, 2003. *M. J. Non-Dioxin-Like PCBs: Effects And Consideration In Ecological Risk Assessment*, NCEA-C-1340 ERASC-003, June 2003.

Khodadoust, A.P.; Lei, L.; Antia, J.E.; Bagchi, R.; Suidan, M.T.; and Tabak, H.H. 2005. *Adsorption of Polycyclic Aromatic Hydrocarbons in Aged Harbor Sediments*, Journal of Environmental Engineering, Vol. 131, No. 3.

Kuo, A. Y.; and D. F. Hayes. 1991. A Model for Turbidity Plume Induced by Bucket Dredge. *Journal of Waterways, Port, Coastal, and Ocean Engineering* **1991**, 117 (6), 610-623.

Maa and Kwon, "Using ADV for cohesive sediment settling velocity measurements." *Estuarine Coastal and Shelf Science*. 2007.

National Research Council. 2007. *Sediment Dredging at Superfund Megasites: Assessing the Effectiveness*, National Academies Press, 2007.

Van Rijn, Leo C. "Sediment Transport, Part II: Suspended load transport." *Journal of Hydraulic Engineering*. 110, 1613-1641, 1984.